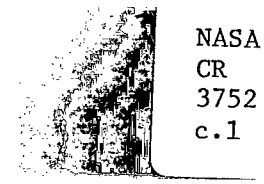

NASA Contractor Report 3752

The Influence of Convective Activity on the Vorticity Budget

Tamara L. Townsend and James R. Scoggins

CONTRACT NAS8-33776
DECEMBER 1983

25th Anniversary
1958-1983

NASA

NASA Contractor Report 3752

The Influence of Convective Activity on the Vorticity Budget

Tamara L. Townsend and James R. Scoggins
Texas A&M University
College Station, Texas

Prepared for
George C. Marshall Space Flight Center
under Contract NAS8-33776

National Aeronautics
and Space Administration

**Scientific and Technical
Information Branch**

1983

TABLE OF CONTENTS

LIST OF TABLES

LIST OF FIGURES

LIST OF FIGURES

LIST OF FIGURES

LIST OF FIGURES

1. INTRODUCTION

Convection is an important mechanism for energy transfer from the boundary layer to the upper troposphere (Palmén and Newton, 1969), thus the need for understanding of the physical processes involved in convective systems. Such processes are important for development of synoptic-scale extratropical cyclones through the release of latent heat. Also, forecasting of such convective activity is important on both the synoptic and local scale. A better understanding of the impact of convective activity on the synoptic-scale flow would be valuable for improvement of numerical prediction methods, especially for prediction of vertical motion fields and precipitation.

Beebe and Bates (1955) described a model of jet structures that aid the release of convective instability by vertical stretching, or lifting. They analyzed configurations of the jet axes and maxima for the regions where low-level (850 mb) convergence occurred in conjuction with upper-level (500 mb) divergence as indicated by the vorticity equation.

McNulty (1978) calculated the synoptic-scale divergence from rawinsonde data and compared it with the position of the upper tropospheric wind maxima (at 300 mb), wave troughs, and severe weather occurrences. It was concluded that upper tropospheric divergence was present when severe weather occurred. Similar conclusions were reached by Endlich and Mancuso (1968) in their objective analysis of atmospheric conditions preceding or accompanying severe weather.

Knowing this relationship between upper-level divergence and severe weather occurrence, the vorticity equation is widely used to determine the sign of the upper-level divergence and, therefore, whether or not convective activity is likely to occur. It is the relationship given by the vorticity equation which is examined here. For this purpose, rawinsonde soundings were taken at 3-hour intervals rather than the routine 12-hour intervals, to provide opportunity for examination of time changes of synoptic-scale features as they are influenced by the mesoscale convective activity.

The primary objective of this research is determination of the influence of convective activity on the synoptic-scale vorticity budget. Also, it is desired to determine whether or not a simplified form of the vorticity equation is appropriate for forecasting purposes. The importance of the

twisting and friction terms of the vorticity budget will be discussed. The last objective involves examining the use of the local time rate-of-change in the expanded equation as a measure of development.

2. PREVIOUS STUDIES

Vorticity budget analyses have been performed over about the past fifteen years for several regions of the world. Most of the studies discussed below deal with tropical oceanic areas, but a few of the analyses are for portions of the troposphere over land. The approaches made by the investigators over the years are somewhat varied, but the conclusions, in general, serve to reinforce the findings of this research effort. Some details of these methods are given below for the purpose of comparsion with the present study.

In a recent examination of the contribution of cloud-cluster scale motions to the vorticity budget of synoptic-scale waves, Esbensen and Tollerud (1982) determined that the cloud-cluster scale vorticity budget is the same order of magnitude as the vorticity changes due to passage of an easterly wave. Compositing (Thompson et al., 1979; Stevens, 1979) was used to isolate the wave and compare the wind, vorticity, and divergence fields of this composite easterly wave with the observed fields during Phase III of GATE. The deviations contributed to the vorticity budget of the composite wave and it was suggested that these contributions were due to the effects of cloud clusters. The analyzed winds were separated into mean flow, wave, and cloud-cluster scale components. Terms of the vorticity budget equation were evaluated using the composited analyzed winds and summed to give a residual, which on the synoptic-scale is usually assumed to be negligible containing only friction effects, perturbations, and computational and measurement error. Mesoscale cloud features were not resolved explicitly, but large cloud-cluster circulations were detected in the data. Cumulus cloud effects and other small-scale motions were separated from cloud-cluster scale motions by evaluating a form of the vorticity equation which defined the apparent source of vorticity due to small-scale motions. The effects of cloud-clusters were then determined by subtracting the effect of small-scale motions from the residual of the vorticity equation for the composite easterly wave. The authors noted the interpretation problems which arose from the fact that the cloud-cluster scale motions included the time-dependent nonlinear part of the wave motion at the cloud-cluster scale as well as the circulations which were primarily the result of cloud clusters. It was also determined that nonlinear contributions of cloud-cluster scale motions to

the average wave structure were small in the lower troposphere, but as large in the middle and upper troposphere as any of the vorticity budget terms involving wave divergence or vertical motion. Also, the value of the residual was less on days of relatively little precipitation convection than on convectively active days.

In addition to budgets of momentum and divergence, Stevens (1979) also analyzed the vorticity budget of synoptic-scale disturbances over the tropical eastern Atlantic with an approach similar to that of Reed and Johnson (1974) and Shapiro (1978) in that synoptic-scale variables were defined as averages over an area larger than a convective element, but small enough to be representative of the synoptic-scale. The terms of the vorticity equation were evaluated using such variables for a composite wave of Phase III, and the sum equalled a residual which was taken to be the apparent source of vorticity for the synoptic-scale vorticity budget. The residual was assumed to be the result of subsynoptic-scale contributions, specifically, cloud effects.

All time and horizontal space deviations were evaluated by the linear/quadratic curve-fitting procedure. So the assumption of a uniformly propagating disturbance was not used and such an assumption may have introduced errors. The alternative procedure which employed centered finite differencing produced essentially identical results so the least squares fit for linear time dependence was consistent with the usual method.

The local time rate-of-change showed the most rapid change in vorticity when η was increasing and decreasing at the level of the low-level easterly jet and its amplitude and structure was similar to that of Shapiro's $11^{o}N$ case. The horizontal vorticity advection was opposite in sign in the mid-troposphere, indicating a large part of $\frac{\partial \eta}{\partial t}$ was due to advection. The sum of terms, however, had a large imbalance at 600 mb for that region just downstream of the trough. The very large negative vorticity advection (NVA) in the region of the ridge was due primarily to strong advection of mean vorticity by the mean zonal wind and advection of wave vorticity by the mean zonal wind.

The vertical advection of vorticity was qualitatively similar to the results of Shapiro (1978) which showed maxima near 800 and 300 mb, and a minimum at 600 mb in the trough region. The divergence term revealed the multi-layered structure of the divergence field.

The low-level vorticity produced by convergence had the largest amplitude of any term in the budget. Divergence at and ahead of the trough at 600 and 300 mb destroyed the vorticity.

The twisting term was found to be less than about one third the magnitude of the others, while the apparent vorticity source, the residual, revealed a complicated structure derived from several of the vorticity equation terms. Above 300 mb the magnitude of the apparent source was attributed mainly to the local time rate-of-change and horizontal terms. At 600 mb between the trough and ridge the value was due to the same terms plus the divergence term and at the trough below 900 mb its magnitude was due to the divergence term. The largest apparent sources and sinks were in the highest and lowest layers, respectively, with the low-level sink being consistent with frictional dissipation.

Stevens (1979) separated the budget of mean vorticity and that for the wave component by decomposing the synoptic fields into time mean and time varying portions. The dominant terms of the mean vorticity budget over the GATE ship array were: 1) the advection of mean vorticity by the three dimensional wind; 2) the advection of planetary vorticity by the mean wind, and; 3) the divergence term for mean motion. The twisting term was of much smaller magnitude. For the mean vorticity balance there was a sink of vorticity below 850 mb to balance the large production by the divergence term. The apparent source in the 350-150-mb layer balanced the advection and divergence terms. A similar distribution was determined by Reed and Johnson (1974). It was concluded that the residual was not negligible, and that cloud effects must be parameterized. The twisting effect was the only term found to be negligible. Also, in the mid-troposphere the vorticity source was only half the magnitude of the local tendency.

In the manner of Yanai et al. (1973), Reed and Johnson (1974), Stevens (1979), and Shapiro (1978) averaged the terms of the expanded vorticity equation over an area and evaluated a residual or apparent vorticity source by adding several terms. And, as in the other investigations, the residual was thought to be associated with cumulus-scale motions. The unique feature of Shapiro's study was that the vorticity budget was determined at a reference latitude of approximately 11^{o}N and the latitudes 4^{o} either side of the reference latitude. At the reference latitude the large-scale twisting terms were found to be very small while the local tendency was much larger than the

value found by Reed and Johnson (1974) and Ruprecht and Gray (1976). As determined by Stevens (1979), the extrema occurred between the trough and ridge. This term was well balanced by the horizontal advection in all portions of the wave, except below 800 mb and above 250 mb. The vertical advection was a maximum near 800 mb and 300 mb. The dominant term in the sum was divergence whose pattern followed that of Reed et al., (1977). Its dominance was consistent with Reed and Johnson's (1974) result for their composite Pacific wave disturbance. In fact, this term had large values in all vorticity budget studies of disturbances with significant convective activity (Reed and Johnson, 1974; Hawkins, 1972). At this latitude (11° N) the apparent source of vorticity exhibited a pattern very similar to the divergence term. The negative residual, or sink, in the lower troposphere and positive residual in the upper troposphere also were found by Reed and Johnson (1974). The large positive residual downstream from the trough in the mid-troposphere corresponds to the divergence maximum found by Reed et al., (1977).

Reed and Johnson (1974) evaluated a form of the vorticity equation which did not include twisting terms and defined the "apparent vorticity source" as the residual resulting from the sum of the terms in the equation. An increase in this residual indicated an increase of the large-scale vorticity by convective processes. Their area mean values of the variables included a weighting of the in-cloud and environmental components according to the fractional area of cumulus convection and that of the environment. To determine the apparent vorticity source they used the change in the difference between the in-cloud and environmental vorticity with pressure and the convective mass flux per unit area, which was inherently positive. Therefore, when there was excess vorticity in the clouds increasing with pressure an apparent source existed and a corresponding sink was thought to occur when excess vorticity increased with height.

Twisting effects were neglected in the equation for vorticity and the single mechanism for generation was assumed to be the effect of horizontal convergence. It was determined that the divergence, or vorticity production term was dominant in the budget for the region of the wave trough. The sum of the remaining terms was much smaller in magnitude. Consequently, a negative residual, or sink, was obtained in the convergent region of the lower troposphere and vice versa. The largest values of the residual

occurred near and west (ahead) of the wave trough in the region of heaviest rainfall and most intense convective activity. These results were very similar to those of Williams (1970) despite the difference in compositing and the different areas and time periods. Both studies indicated that the apparent sources and sinks are greatest in the convectively active regions, and that they act to reduce vorticity changes that are produced by the large-scale motions.

Reeves et al. (1979) used the vorticity budget in areas of suppressed and disturbed convective activity during GATE to examine the effects of convective activity on the large-scale flow. Upper air winds were fit with second-order polynomials for smooth estimates of vorticity, divergence, and vertical motion. The profiles of their residual terms were similar from phase to phase of GATE with maxima of cyclonic (positive) vorticity production in the mid and upper troposphere. The maximum in the upper troposphere was strong in both the suppressed and disturbed states. At the surface, individual residual values were nearly always opposite in sign to the vorticity. The mean budget for the larger array of GATE ship observations showed that the twisting/tilting term had a magnitude comparable to the other terms. Here again the vorticity budget components were the effects described by the terms of the vorticity equation, in which the total derivative had been expanded and the twisting/tilting and friction terms included. Each of these terms was averaged over horizontal areas after all terms had been evaluated from observations, except the friction term and the terms involving products of primed quantities, which were combined as a residual.

Some interesting differences between disturbed and suppressed states were revealed in the vertical profiles of the terms. The profile of the divergence term indicated that the boundary-layer cyclonic vorticity production was four times larger in the disturbed than in the suppressed state. In the upper troposphere the disturbed state underwent anticyclonic vorticity production and the undisturbed state experienced cyclonic vorticity production (a reflection of convergence associated with weak upper tropospheric subsidence). One interesting result was that there was no significant difference in the twisting term between disturbed and suppressed conditions. The residuals for the two states of activity had two significant features. There was a definite tendency for more cyclonic subgrid-scale vorticity production in

the mid-troposphere during the suppressed state. Also, there was an apparent cyclonic vorticity source in the upper troposphere that was equally strong during both states.

Shapiro and Stevens (1980) used a simple one-dimensional model of cloud vorticity which accounted for the net effect of cloud transport and production of vorticity. The effects of twisting did not significantly affect the results. The implication, therefore, was that the net effect of cumulus transport of vorticity on the synoptic-scale may be less dependent on the internal dynamics of the convective system than the net momentum transport and production. Stevens et al. (1977) concluded that cumulus transports in the vorticity budget played a crucial role in determining the dynamic balance in an easterly wave and those in the divergence budget did not. Therefore, adequate parameterization of the vorticity source may be sufficient for proper simulation of these waves.

Chu et al. (1981) re-examined the large-scale vorticity budget over the Marshall Islands in the tropics in an effort to obtain better estimates for the horizontal advection and twisting terms. Their approach was similar to that of Reeves et al. (1979) with comparison of the average vorticity equation terms between disturbed and undisturbed states where "disturbed" refers to significant convective activity and "undisturbed" indicates the presence of little or no convective activity. The mean vertical profile of the residual indicated a large apparent source of positive vorticity in the upper troposphere and an apparent sink near the surface, as with the previously discussed vorticity budget analyses. This profile, however, was more complicated than the earlier results and shows two additional maxima of positive vorticity source in the mid-troposphere. The most important terms for the disturbed cases were horizontal advection and stretching. The twisting term was the same order of magnitude as the vertical advection. In the undisturbed situations the mean local time rate-of-change was compensated by the mean horizontal advection of vorticity.

Cho et al. (1979) also used the large-scale mean vorticity equation and a horizontal area average in a straightforward manner. Next they obtained the cloud vorticity equation by applying the vorticity equation to each cumulus cell. The eddy flux of vorticity due to cumulus activity was primarily in the vertical direction. Thus, the mean horizontal eddy flux of

vorticity was equal to zero, and cumulus clouds contributed to the apparent source by eddy vertical advection and the eddy twisting of vorticity.

For the large-scale vorticity budget the local tendency, vertical advection, twisting term, and horizontal divergence were approximately equal in magnitude and, therefore, contributed about equally to the large-scale budget. The residual vertical profile revealed a strong apparent source below 600 mb with an apparent sink of comparable magnitude between 350 and 250 mb and small fluctuation between 650 and 350 mb. Thus, despite the smallness of the horizontal scale of the cumulus clouds, the vertical component of cloud vorticity averaged over a cross-section of a cloud is the same order of magnitude as the large-scale mean vorticity. The cloud effects on the large-scale field were represented by 1) the vertical advection of vorticity by the vertical mass flux of cumulus clouds, and 2) the twisting of horizontal components of large-scale mean vorticity into the vertical due to the uneven large-scale distribution of the cloud mass flux. The authors state that proper understanding of large-scale disturbances requires insight into the dynamic interactions between the cumulus and large-scale circulations.

Holton and Colton (1972) employed the linearized vorticity equation in their investigation of the 200-mb vorticity balance in the tropics in which they hypothesized that vertical transport of vorticity by convection, and the subsequent increase of vorticity at 200 mb, leads to rapid decay of the vorticity field at 200 mb. Their results confirmed this hypothesis as they concluded that the observed mean vorticity and divergence fields at 200 mb were mutually consistent only if the vorticity was dissipated in less than one day. A possible mechanism for this rapid dissipation was determined to be vertical transport of vorticity by cumulus convection.

In addition to vertical motion and divergence, Lateef (1967) examined the tropospheric vorticity over the Caribbean for a three day period in August of 1963. He found the local time rate-of-change term to be the largest in the vorticity equation with the horizontal advection of vorticity and divergence terms being an order of magnitude smaller. The vertical advection of vorticity and twisting terms was relatively small. Averaging of the terms over a "sizeable" area improved the estimates of expected changes of vorticity since correlations between the observed and expected vorticity changes based on the terms of the vorticity equation were not reliable on a point-by-point basis.

Hodur and Fein (1977) performed a vorticity budget analysis for the spring and summer months over the Marshall Islands by evaluating the average monthly values of the terms of the expanded large-scale vorticity equation. Large imbalances in the budget were correlated with the ITCZ and, therefore, related to intense convection. Parameterization of effects of subgrid-scale processes was the purpose of the study with interpretation of the synoptic-scale residual being the objective. Based on four months of data, the average synoptic fields of motion were used to determine these effects.

The same expanded form of the vorticity equation employed in the present study was used except for the inclusion of the twisting and friction terms. The subgrid-scale phenomena was included in the residual, which also contained errors due to data analysis and computational procedures. The largest portions of this residual, however, were thought to be due to cumulus convection in which strong upward motion may account for the transport of vorticity. Additional discussion of this approach also is presented in Yanai and Nitta (1967), Riehl and Pearce (1968), and Williams and Gray (1973). Ruprecht and Gray (1976) combined both conventional rawinsonde and satellite data.

In their study relating synoptic-scale vorticity imbalance to convection during AVE IV, Read and Scoggins (1977) examined the time changes of vorticity in areas of convective storms. They observed significant variation in the magnitudes of terms in the synoptic-scale vorticity equation at different stages of squall-line development. Average vorticity budgets were computed for all convective areas and a systematic imbalance in the terms indicated an imbalance that was primarily the result of subgrid-scale processes.

These previous investigations of the effects of convective activity on synoptic-scale circulations (by way of a feedback mechanism) reveal that large imbalances result when the terms in the vorticity equation are evaluated using synoptic-scale variables. This suggests there is some smaller-scale process that is important to the understanding of the synoptic-scale vorticity budget.

3. DATA AND SYNOPTIC CONDITIONS

3.1. Data

Upper air soundings taken during NASA's seventh Atmospheric Variablility Experiment (AVE VII) and first Atmospheric Variability Experiment-Severe Environmental Storms and Mesoscale Experiment (AVE-SESAME I) comprised the basic data used in this analysis. The AVE VII period extended from 0000 GMT 2 May 1978 to 1200 GMT 3 May 1978 with soundings taken at 22 National Weather Service (NWS) upper air stations in the central U.S. at 0000, 1200, 1500, 1800, and 2100 GMT on 2 May 1978, and 0000, 0300, and 1200 GMT on 3 May 1978. Table 1 lists the stations involved and Fig. 1 shows their locations. The AVE-SESAME I period extended from 1200 GMT 10 April 1979 to 1200 GMT 11 April 1979 with soundings taken every three hours at 23 NWS stations and sixteen special rawinsonde sites. These stations are listed in Table 2 and their locations are shown in Fig. 2.

The pressure contact and wind data were reduced to 25-mb intervals using the procedure described by Fuelberg (1974). The data for AVE VII were presented by Davis et al. (1978), and for AVE-SESAME I by Gerhard et al. (1979). The 25-mb interval data provide more detailed profiles of the atmosphere than the standard National Weather Service (NWS) upper air data. Pressure, temperature, and relative humidity were computed for each contact and winds were computed using 30- or 60-second interval angle data.

The AVE VII sounding data (temperature, dewpoint temperature, and wind components) were gridded by the Barnes (1964) technique at 50-mb intervals from 900 mb to 100 mb for the grid points shown in Fig. 3. The only difference between the grid used for AVE VII and that for AVE-SESAME I was a two-grid distance westward displacement for AVE-SESAME I. The grid spacing is approximately 158 km. Vertical motion for the same gridded field and 50 mb intervals was computed using the kinematic method and modified by the O'Brien (1970) technique. The values were adjusted to vertical motion computed at 100 mb by the adiabatic method. Other data used in the analysis were primarily the facsimile synoptic charts and NWS radar summaries for the AVE VII and AVE-SESAME I periods.

3.2. Synoptic Conditions

AVE VII. Surface and upper air charts for 1200 and 2100 GMT 2 May 1978, and 0300 GMT 3 May 1978 are presented in Figs. 4, 5, and 6. These maps

Table 1. List of rawinsonde stations participating in the AVE VII experiment.

Station Number	Location
220 (AQQ)	Apalachicola, Florida
229 (CKL)	Centerville, Alabama
232 (BVE)	Boothville, Louisiana
235 (JAN)	Jackson, Mississippi
240 (LCH)	Lake Charles, Louisiana
247 (GGG)	Longview, Texas
255 (VCT)	Victoria, Texas
260 (SEP)	Stephenville, Texas
261 (DRT)	Del Rio, Texas
265 (MAF)	Midland, Texas
327 (BNA)	Nashville, Tennessee
340 (LIT)	Little Rock, Arkansas
349 (UMN)	Monett, Missouri
353 (OKC)	Oklahoma City, Oklahoma
363 (AMA)	Amarillo, Texas
429 (DAY)	Dayton, Ohio
433 (SLO)	Salem, Illinois
451 (DDC)	Dodge City, Kansas
456 (TOP)	Topeka, Kansas
532 (PIA)	Peoria,Illinois
553 (OMA)	Omaha, Nebraska
562 (LBF)	North Platte, Nebraska
11001	Marshall Space Flight Center, Alabama
33001	Texas A&M University, College Station, Texas

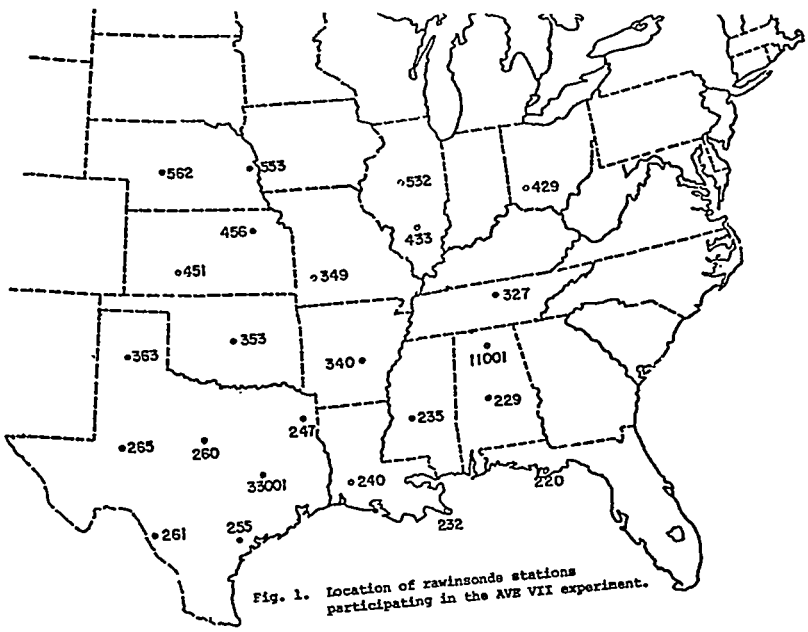

Fig. 1. Location of rawinsonde stations participating in the AVE VII experiment.

Table 2. Rawinsonde stations participating in the AVE-SESAME I experiment.

Station Number	Location
NWS Stations	
229 (CKL)	Centerville, AL.
232 (BVE)	Boothville, LA.
235 (JAN)	Jackson, MS.
240 (LCH)	Lake Charles, LA.
247 (GGG)	Longview, TX.
255 (VCT)	Victoria, TX.
259 (SEP)	Stephenville, TX.
261 (DRT)	Del Rio, TX.
265 (MAF)	Midland, TX.
270 (ELP)	El Paso, TX.
327 (BNA)	Nashville, TN.
340 (LIT)	Little Rock, AR.
349 (UMN)	Monett, MO.
354 (OCK)	Oklahoma City, OK.
363 (AMA)	Amarillo, TX.
365 (ABQ)	Albuquerque, NM.
433 (SLO)	Salem, IL.
451 (DDC)	Dodge City, KS.
456 (TOP)	Topeka, KS.
469 (DEN)	Denver, CO.
532 (PIA)	Peoria, IL.
553 (OMA)	Omaha, NE.
562 (LBF)	North Platte, NE.
Special Stations	
001 (ABI)	Abilene, TX.
002 (BVO)	Bartlesville, OK.
003 (COU)	Columbis, MO.
004 (CDS)	Childress, TX.
005 (CLL)	College Station, TX.
006 (CNK)	Concordia, KS.
007 (DUA)	Durant, OK.
008 (FSM)	Fort Smith, AR.
009 (GAG)	Gage, OK.
010 (GLD)	Goodland, KS.
011 (ICT)	Wichita, KS.
012 (JCT)	Junction, TX.
013 (MLU)	Monroe, LA.
014 (MRF)	Marfa, TX.
015 (MTX)	Morton, TX.
016 (OTM)	Ottumwa, IA.
017 (POF)	Poplar Bluff, MO.
018 (RTN)	Raton, NM.
019 (UOX)	Oxford, MS.

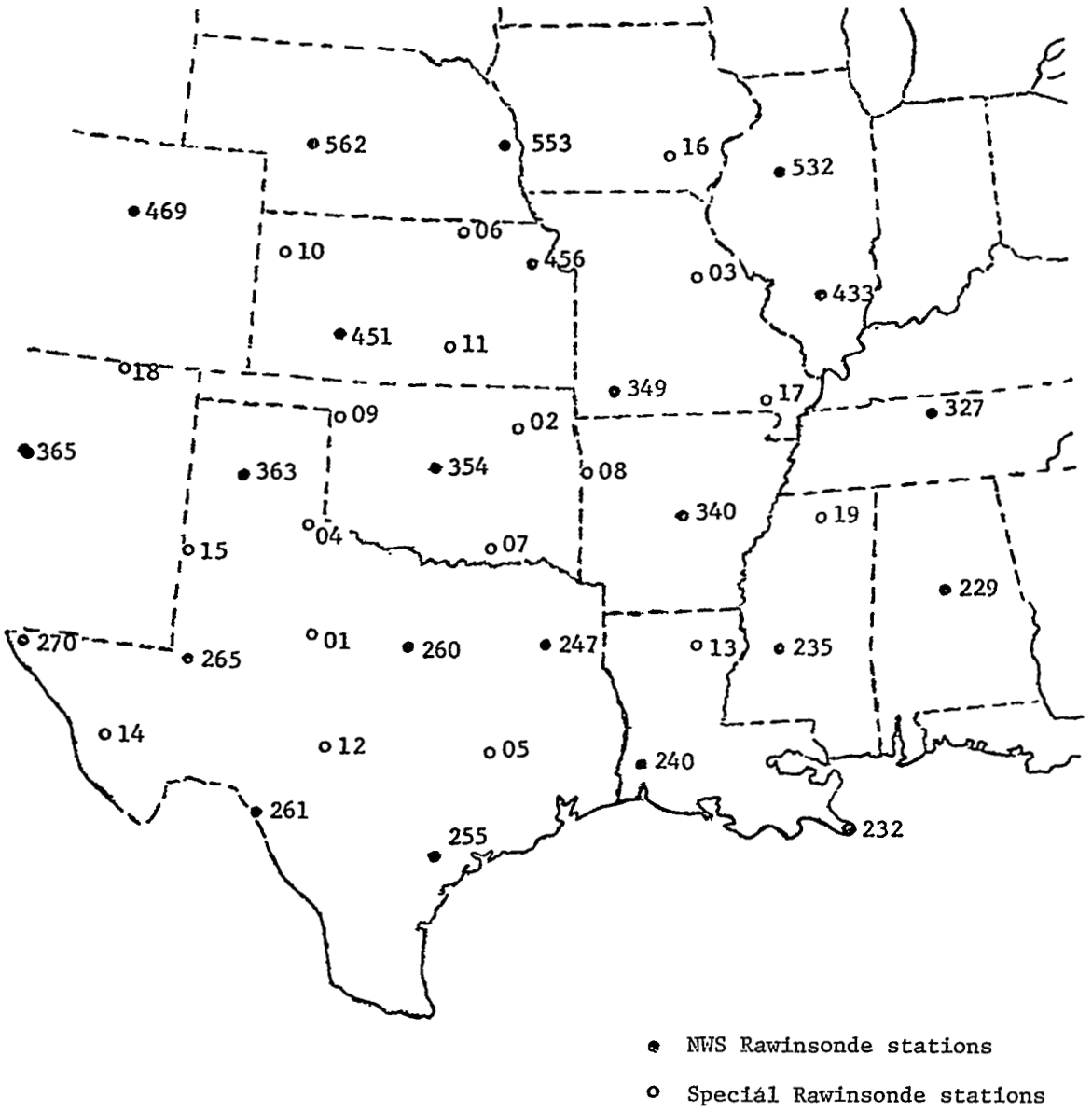

Fig. 2. Location of rawinsonde stations participating in the AVE-SESAME I experiment.

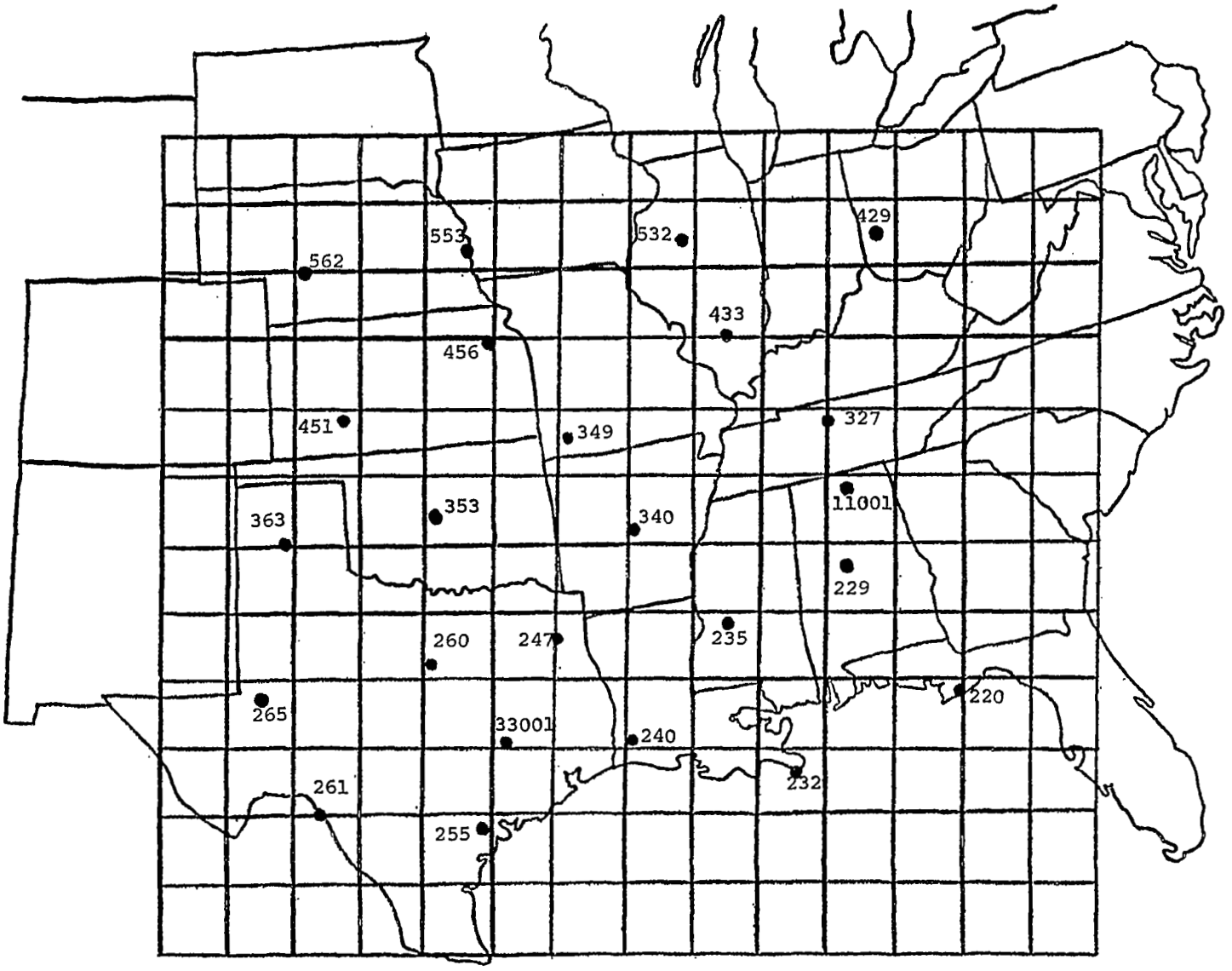

Fig. 3. Grid for AVE VII.

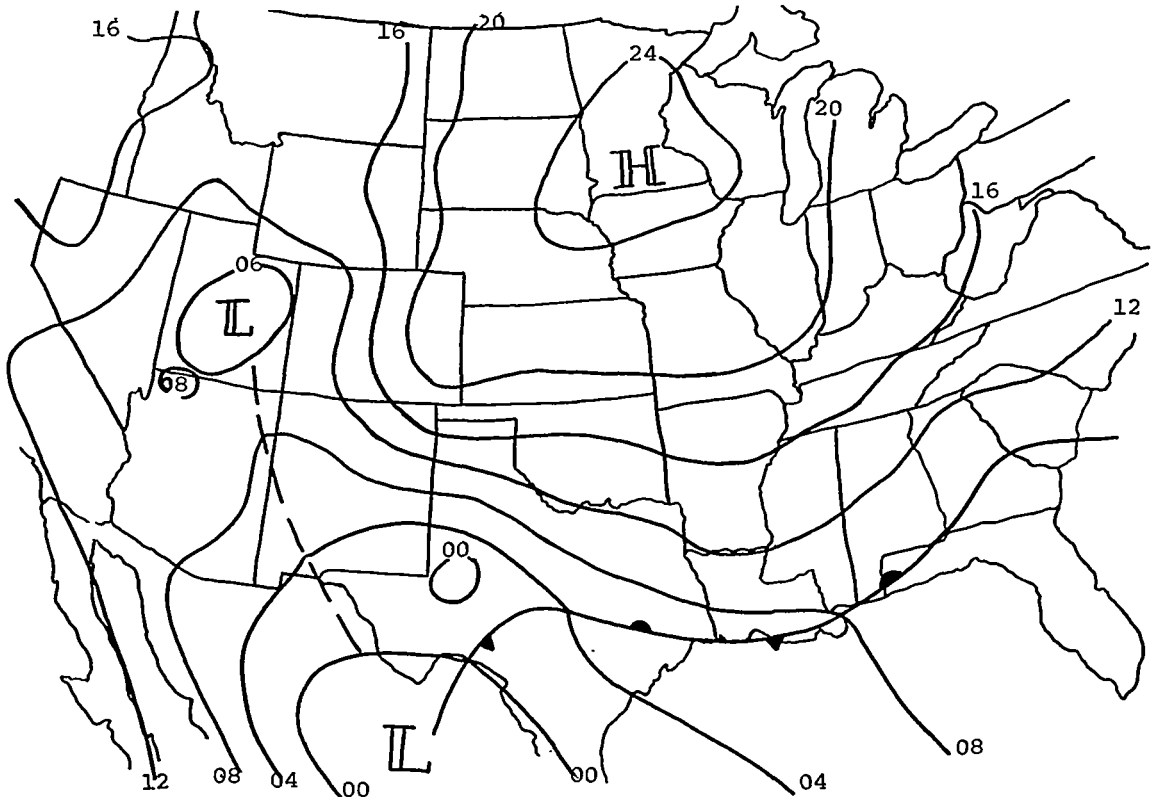

(a) Surface

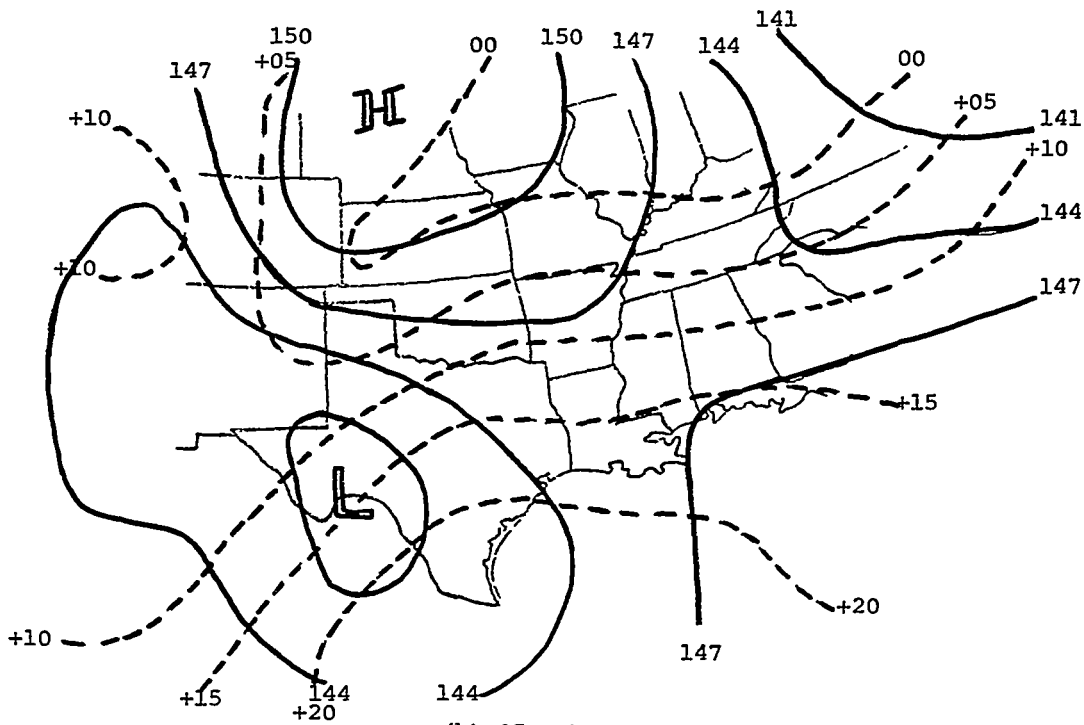

(b) 850 mb

Fig. 4. Synoptic charts for 1200 GMT 2 May 1978.

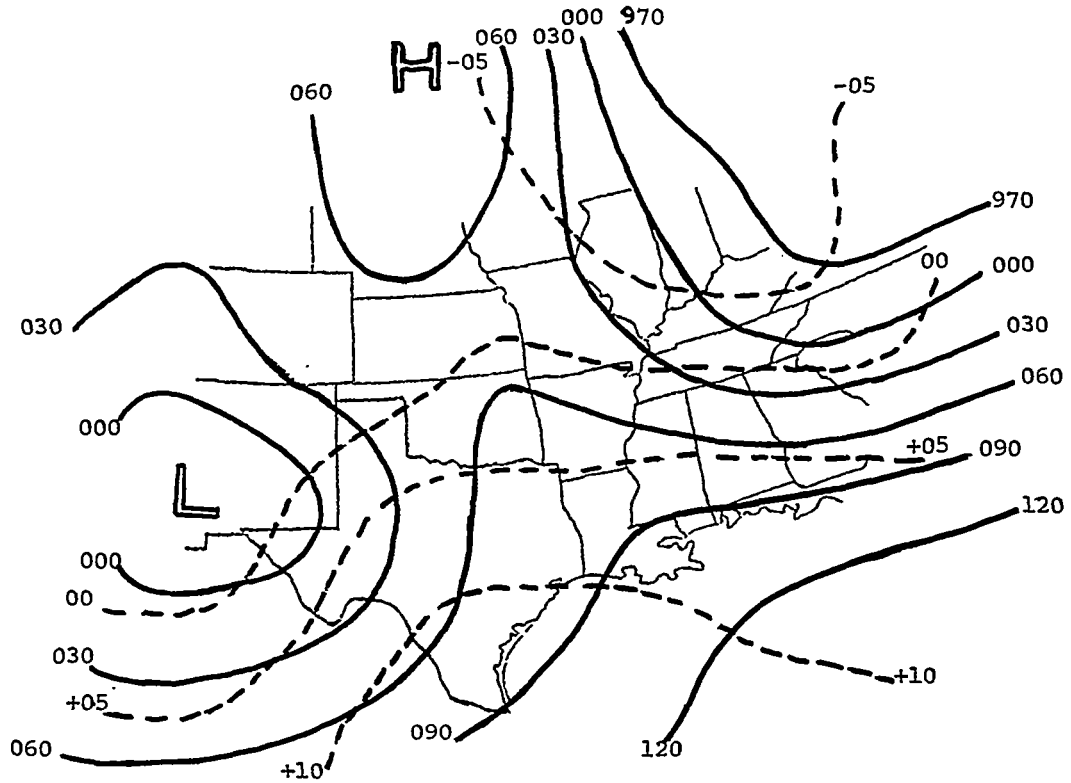

(c) 700 mb

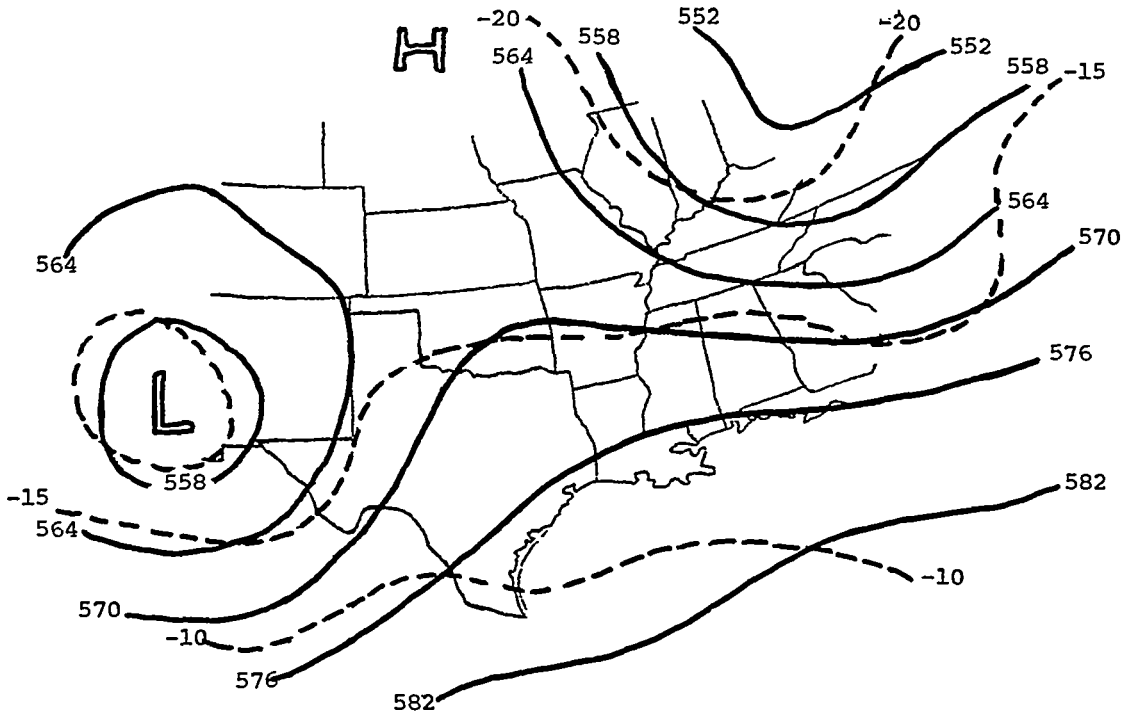

(d) 500 mb

Fig. 4. Continued.

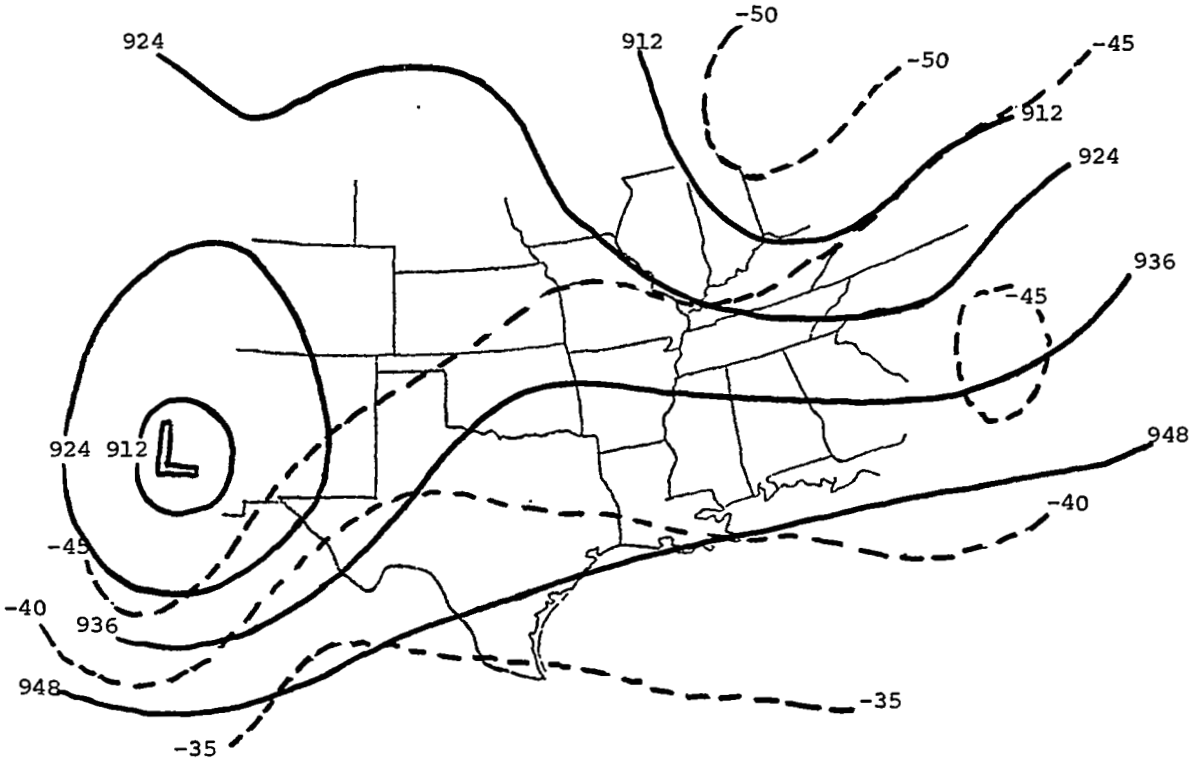

(e) 300 mb
Fig. 4. Continued.

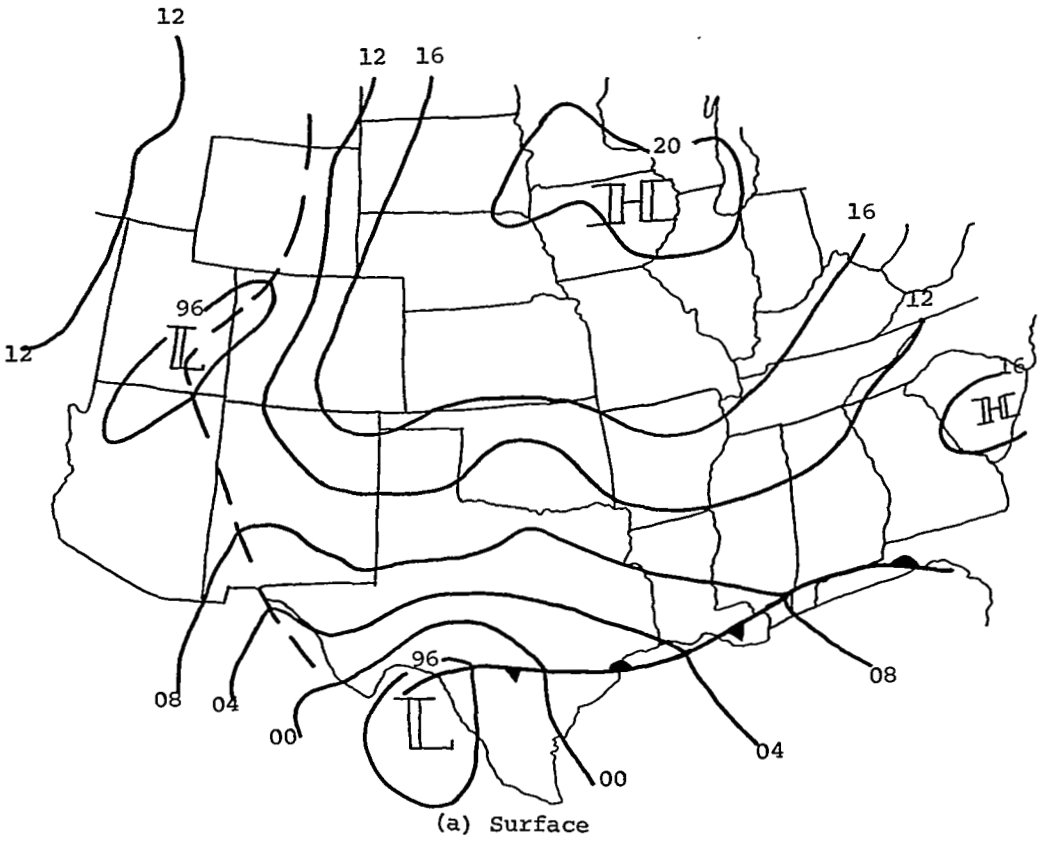

(a) Surface

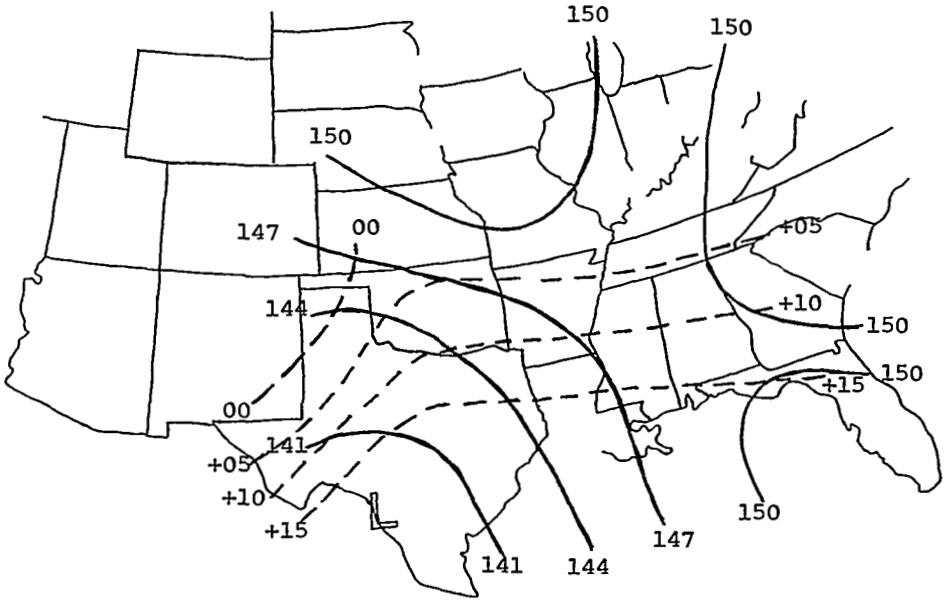

(b) 850 mb

Fig. 5. Synoptic charts for 2100 GMT 2 May 1978.

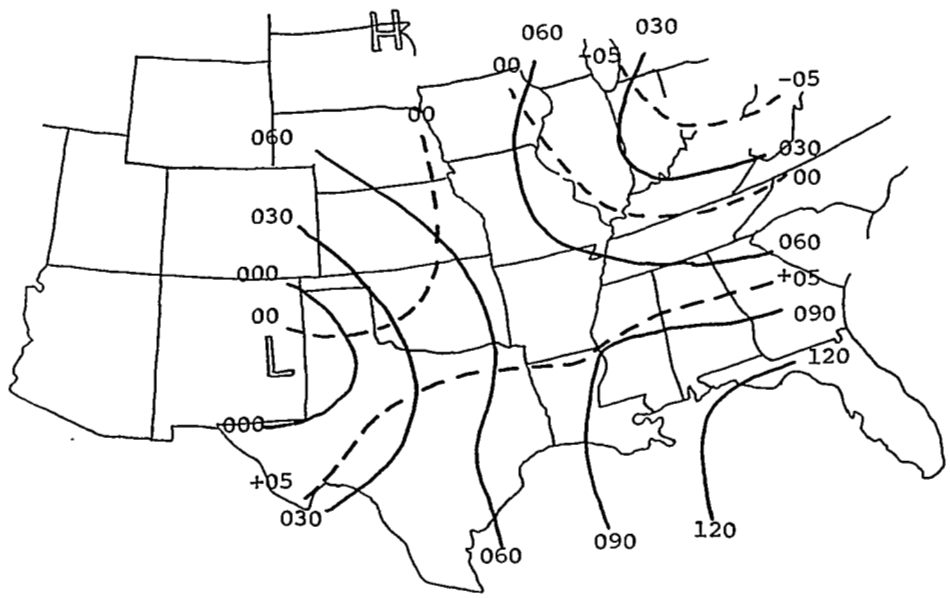

(c) 700 mb

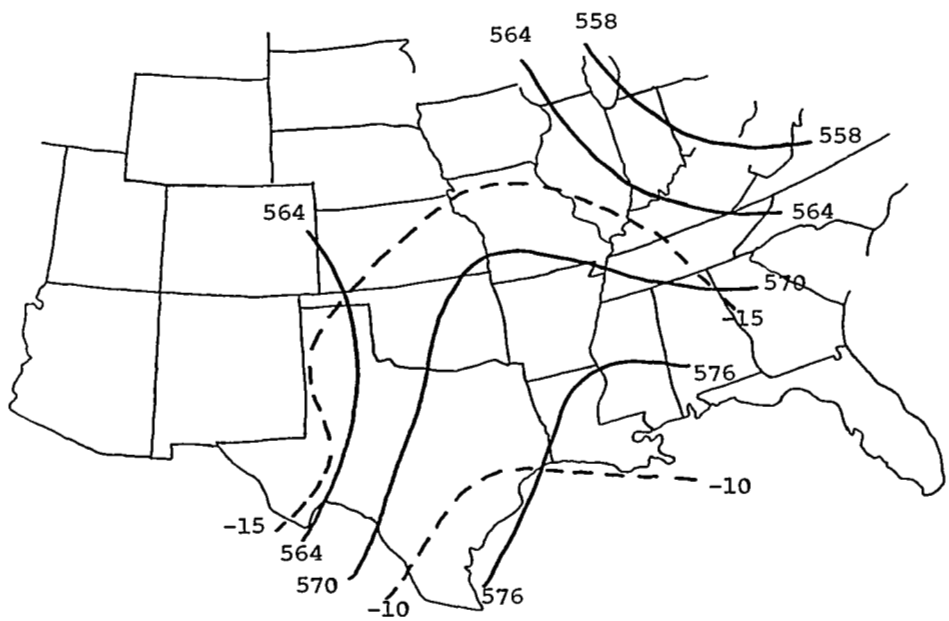

(d) 500 mb

Fig. 5. Continued.

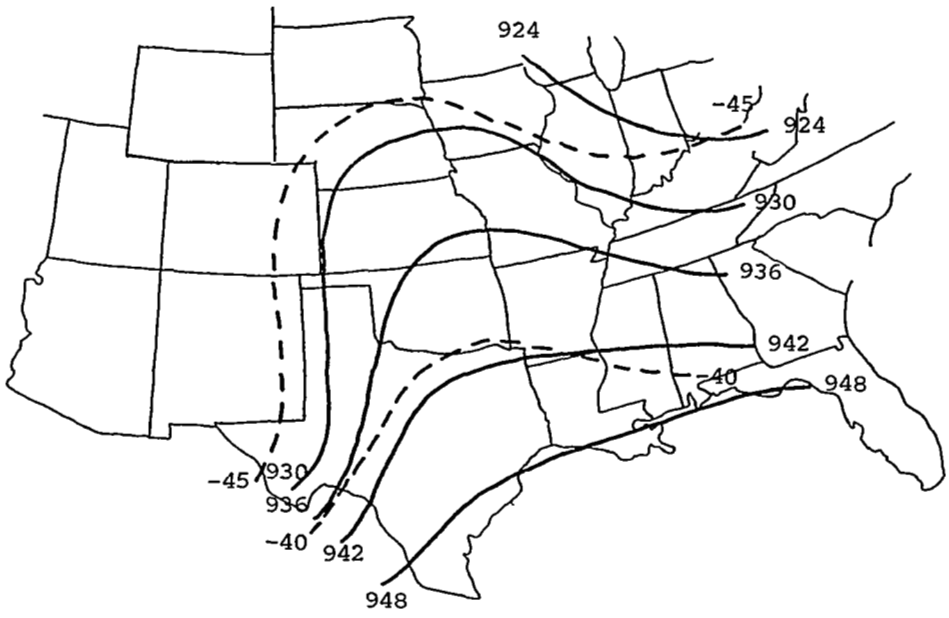

(e) 300 mb

Fig. 5. Continued.

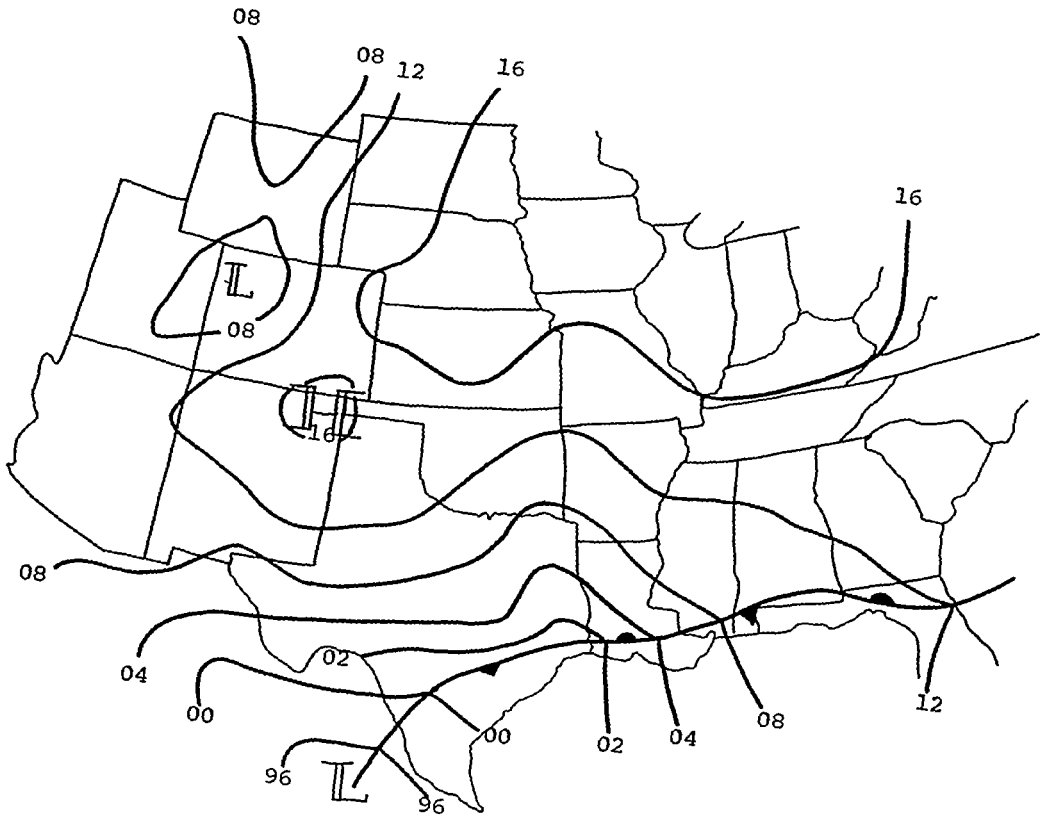

(a) Surface

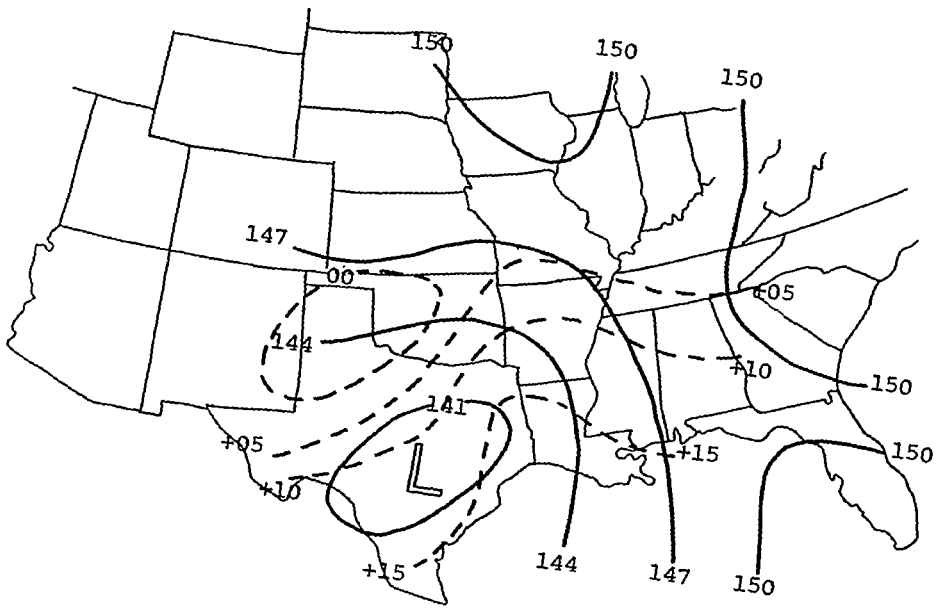

(b) 850 mb

Fig. 6. Synoptic charts for 0300 GMT 3 May 1978.

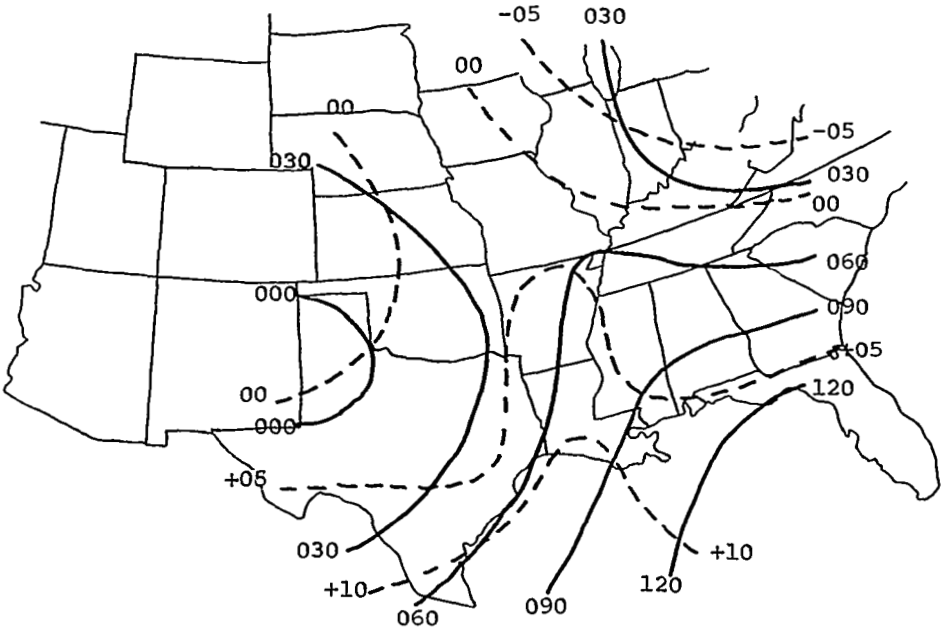

(c) 700 mb

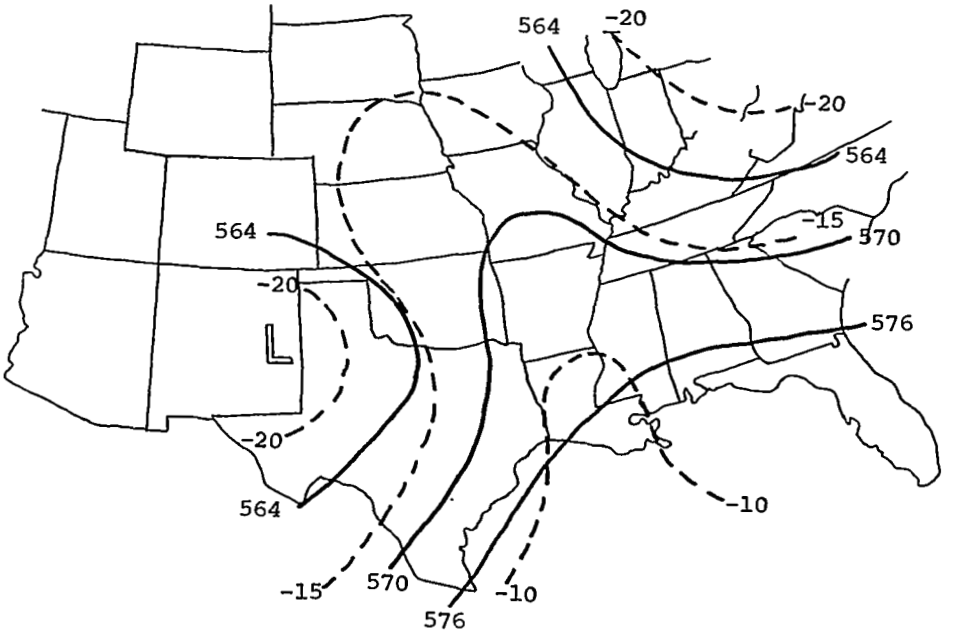

(d) 500 mb

Fig. 6. Continued.

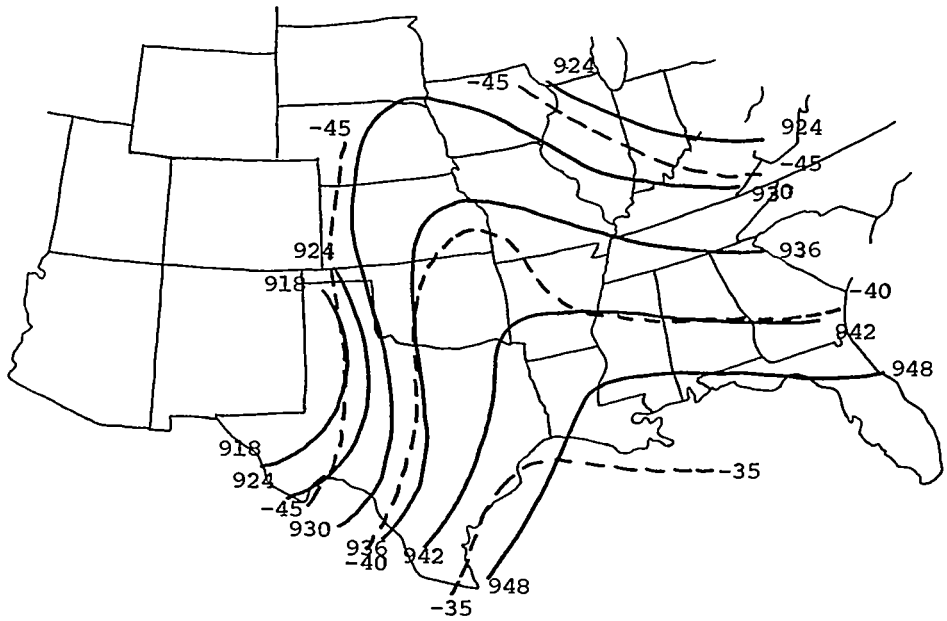

(e) 300 mb

Fig. 6. Continued.

depict only the general synoptic situation at each given time. Radar summary charts near the chart times are shown in Figs. 7, 8, and 9. These charts show the areas of convective development and precipitation.

At 1200 GMT, Fig. 4(a), a stationary front in the southeastern and south central United States extended from central Georgia, south of Alabama and Mississippi, through southeast Louisiana into Texas then curved southwestward into a low pressure center located in Mexico south of the Big Bend area of Texas. The surface high pressure area north of the front was centered over southern Minnesota. Also at the surface, a trough extended northwestward through southwest New Mexico from the low in northern Mexico.

Aloft, as seen in Figs. 4(b)-4(e), a cold-core low located over Arizona and New Mexico intensified with height. Cold air extended well to the south into the low while a warm tongue extended northward into the central states. A high pressure ridge tilted westward with height over the central region. At 200 mb the jet stream extended from west to east along the Gulf Coast with speeds of about 150 kt. Precipitation in the form of showers and thundershowers occurred in west Texas and New Mexico in association with the front and advancing low.

By 2100 GMT, Fig. 5(a), the surface synoptic situation had changed only slightly. The low center in northern Mexico moved toward the east a little and a slight trough of low pressure formed in central Texas and Oklahoma in association with the system. At 850 mb, Fig. 5(b), the flow was strong from the Gulf of Mexico over Texas. A wide area of moisture encompassed southern Mississippi and Arkansas, Louisiana, most of Texas, western Oklahoma, and southwest Kansas.

The same general upper level features also persisted with the low center located over New Mexico, Fig. 5(b-e). The ridge in the central region, however, increased in intensity as a tongue of warm air pushed further northward. At 200 mb the position of the jet stream remained the same as that at the previous observation time. Two lines of thunderstorms had developed in south-central Texas while over southeast Louisiana and southern Mississippi an intense convective cell also formed.

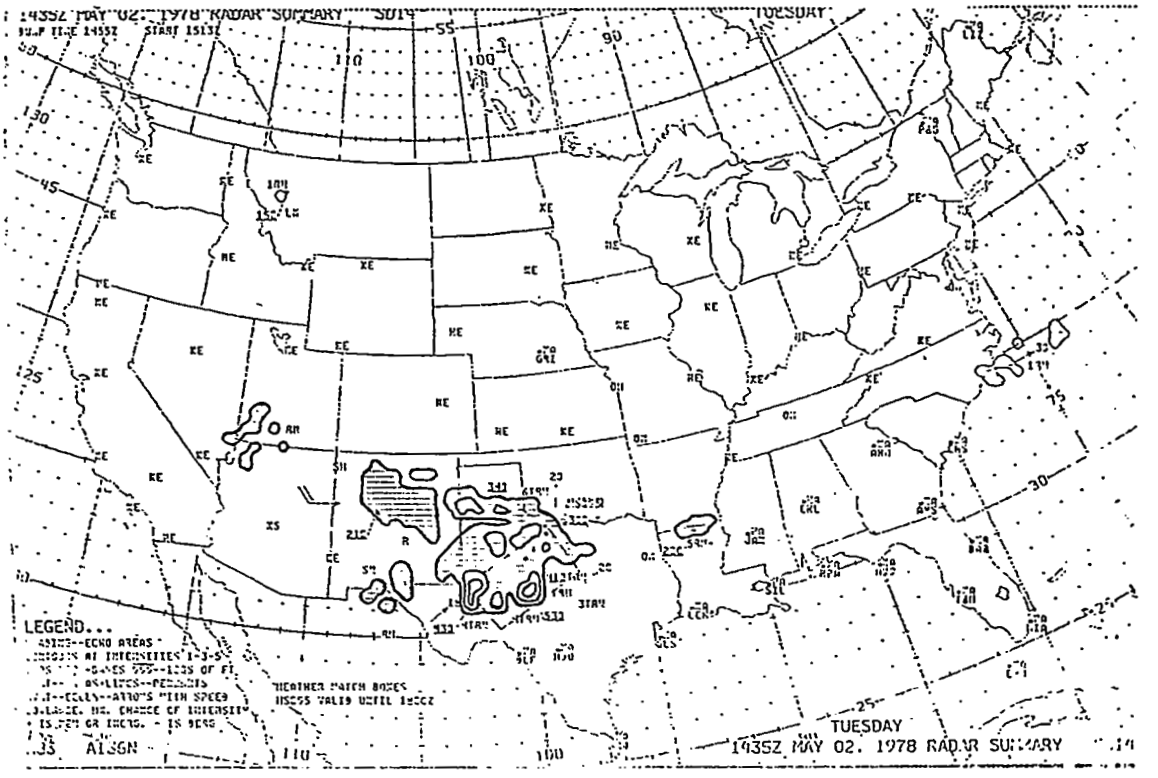

Fig. 7. Radar summary for 1435 GMT 2 May 1978.

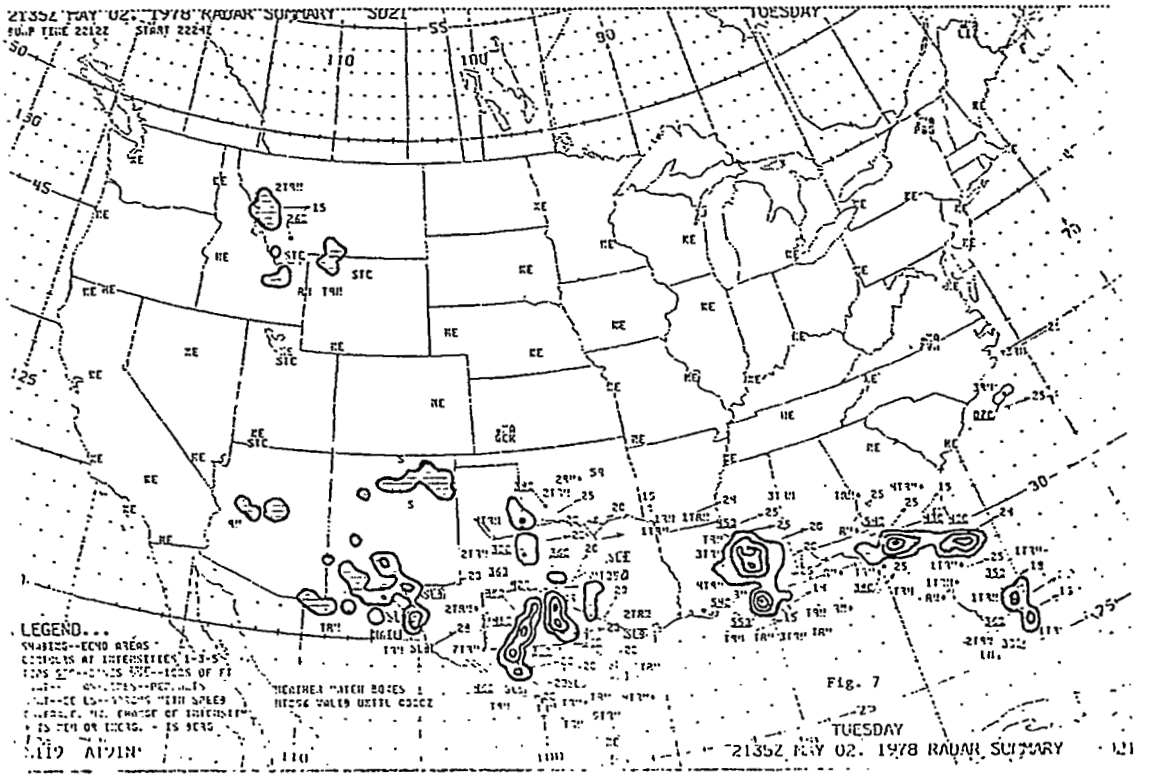

Fig. 8. Radar summary for 2135 GMT 2 May 1978.

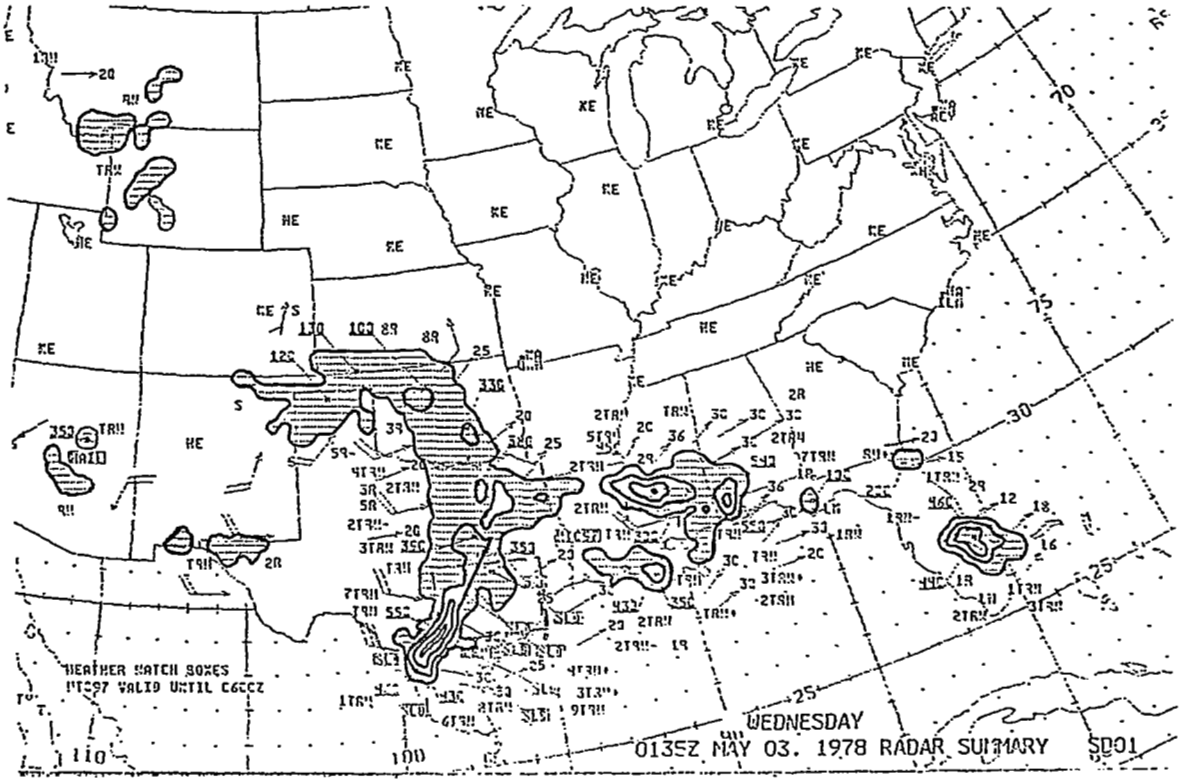

Fig. 9. Radar summary for 0135 GMT 3 May 1978.

By 0300 GMT 3 May 1978, Fig. 6(a), the surface low pressure center had shifted southeastward while the surface front maintained its position along the Gulf of Mexico coastal region of the AVE VII area. High surface pressure encompassed the area north of the front except east Texas and Oklahoma where a trough extended northward from its intersection with the front in southeast Texas. The 850-mb low center was located in south-central Texas, and downstream the onshore flow from the Gulf of Mexico was strong. Also, a warm tongue of air extended northward over Louisiana and Arkansas. The upper air synoptic situation did not change much during the three-hour period since the previous observation except that the centrally located high pressure ridge strengthened and the stacking of the low became more nearly vertical. Rain fell over southeast Louisiana and Mississippi and southwest Alabama. The line in south-central Texas persisted as the large area of precipitation increased to cover northeast Texas, most of Oklahoma, the extreme northern Texas panhandle, and southern Kansas.

The overall synoptic situation during AVE VII presented conditions favorable for the development of convective activity throughout the observation period. The conditions present were low-level advection of moisture from the Gulf of Mexico, lifting of moisture-laden Gulf air over the front and into the low pressure system, and upper level intrusion of dry air around the low over the low level moist air.

AVE-SESAME I. Figures 10, 11, and 12 show surface and upper air charts for 1200 GMT 10 April 1979, and 0000 and 1200 GMT 11 April 1979, respectively, while the corresponding radar summary charts are presented in Figs. 13, 14, and 15.

At 1200 GMT, Fig. 10(a), a surface cold front extended from a low pressure center on the Colorado-Wyoming border southward through Colorado, eastern New Mexico, and far west Texas then curved into northern Mexico. There was a high pressure center in the midwestern United States while an approaching front was located to the south along the Gulf of Mexico coastal region. The 850-mb synoptic picture shows the same low pressure center with its associated front located a little farther north due to slope of the front toward the colder air.

Stacking of the low pressure center was such that the 700-mb position, Fig. 10(c), was over northwest Colorado. To the east, a high pressure

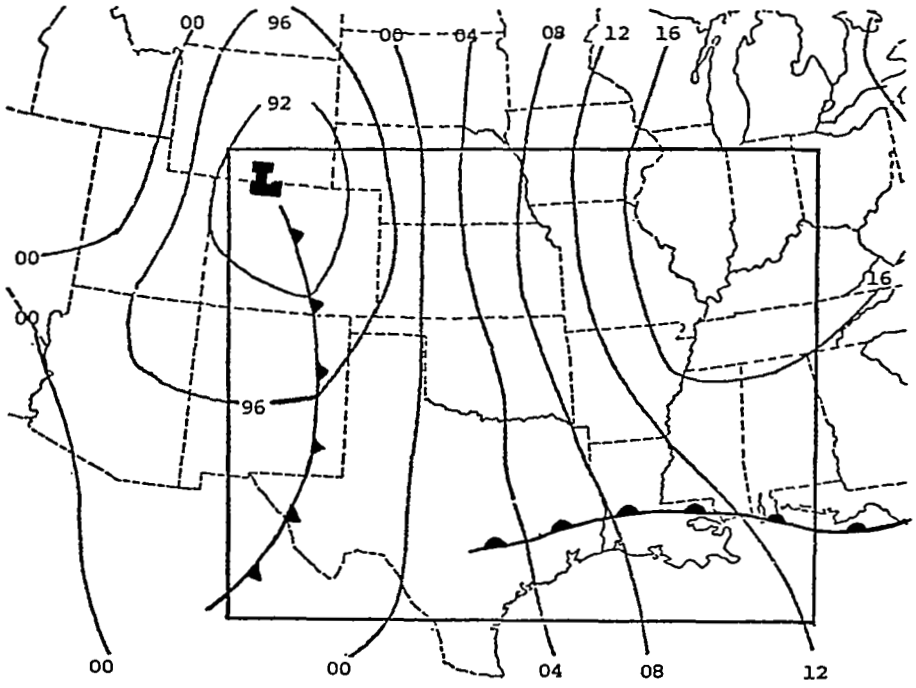

(a) Surface

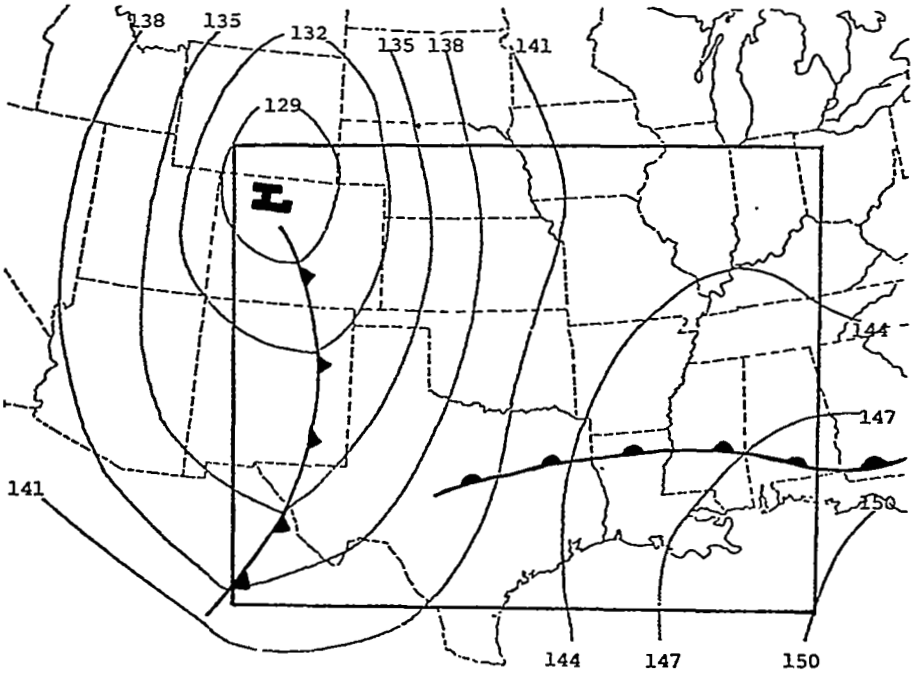

(b) 850 mb

Fig. 10. Synoptic charts for 1200 GMT 10 April 1979. (after Williams et al., 1980). The box outlines the study area.

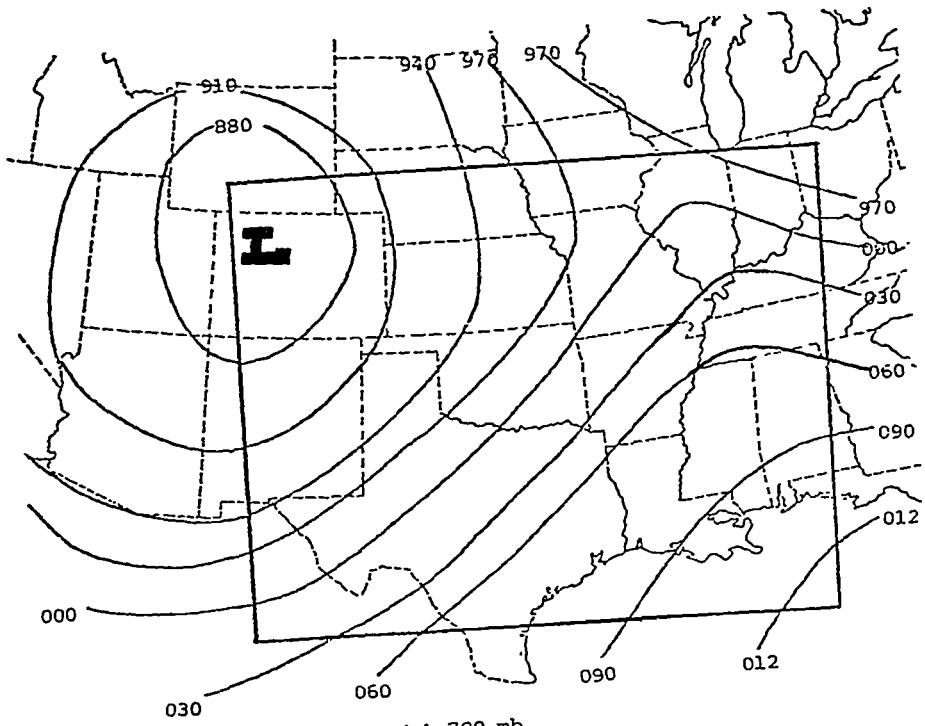

(c) 700 mb

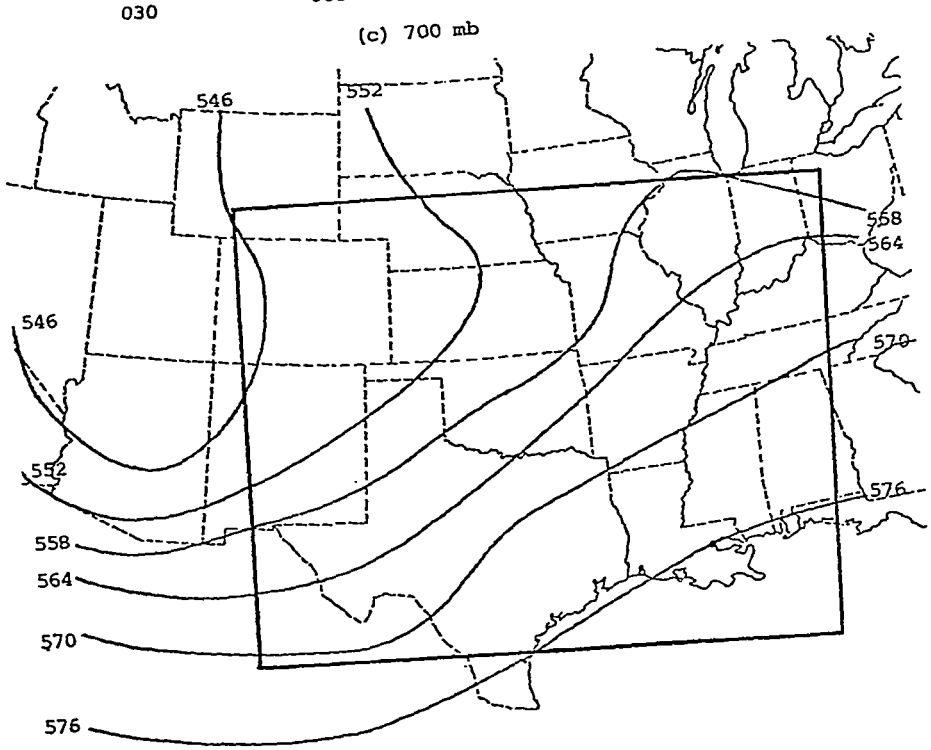

(d) 500 mb

Fig. 10. Continued.

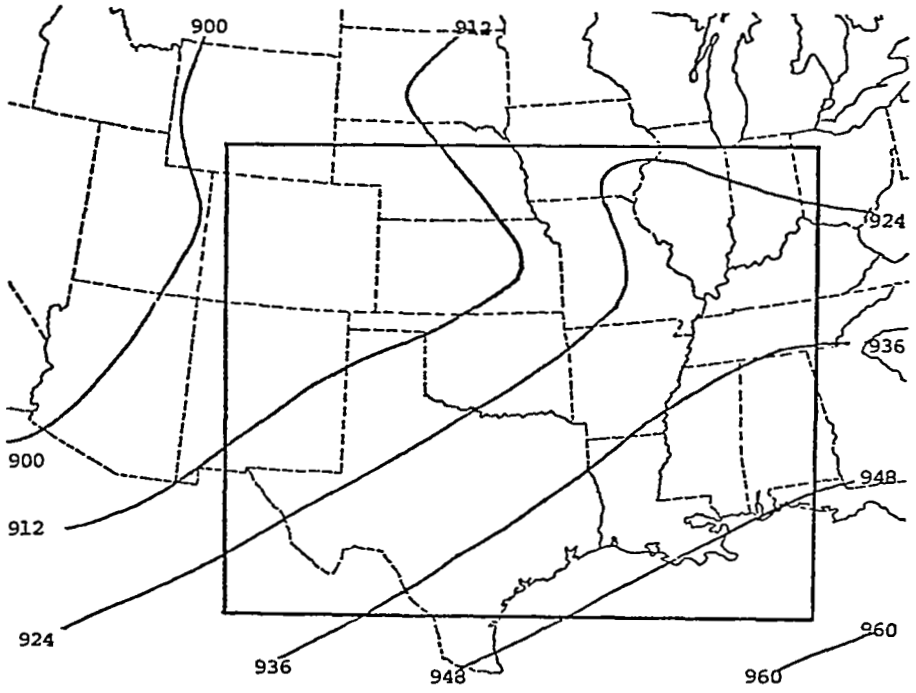

(e) 300 mb

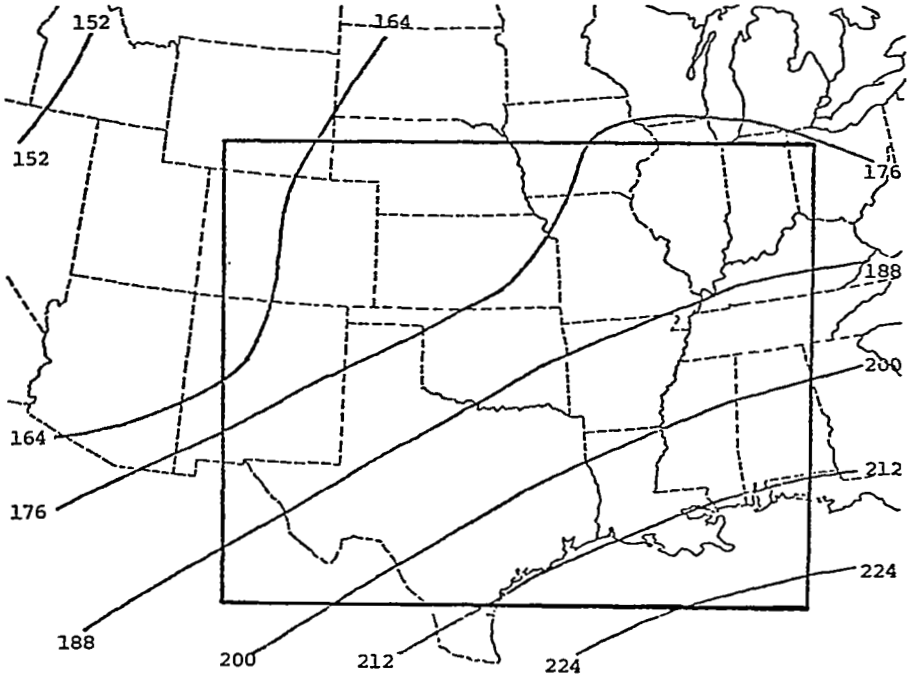

(f) 200 mb

Fig. 10. Continued.

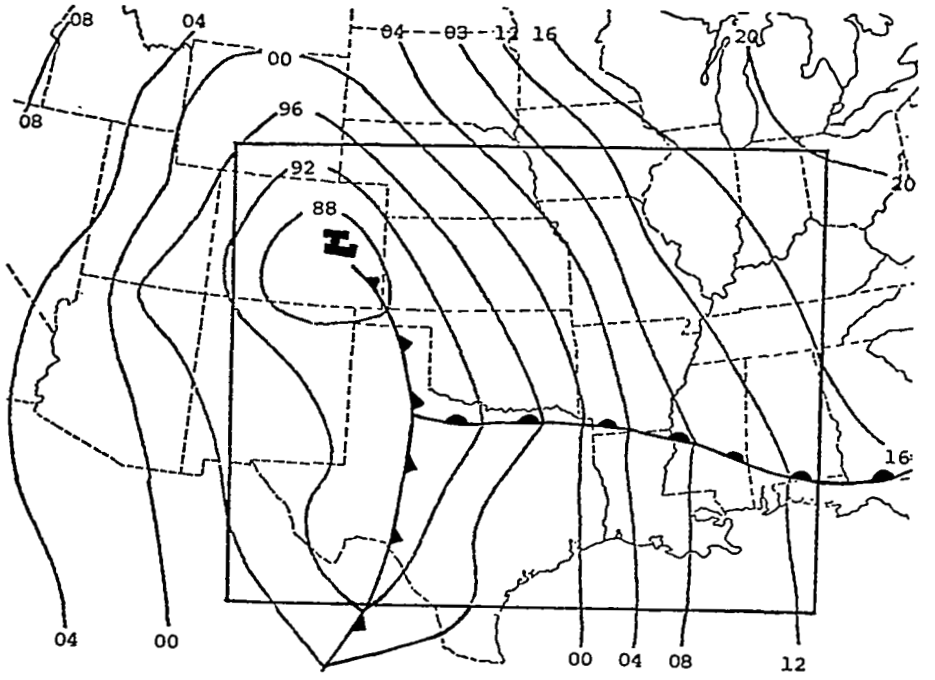

(a) Surface

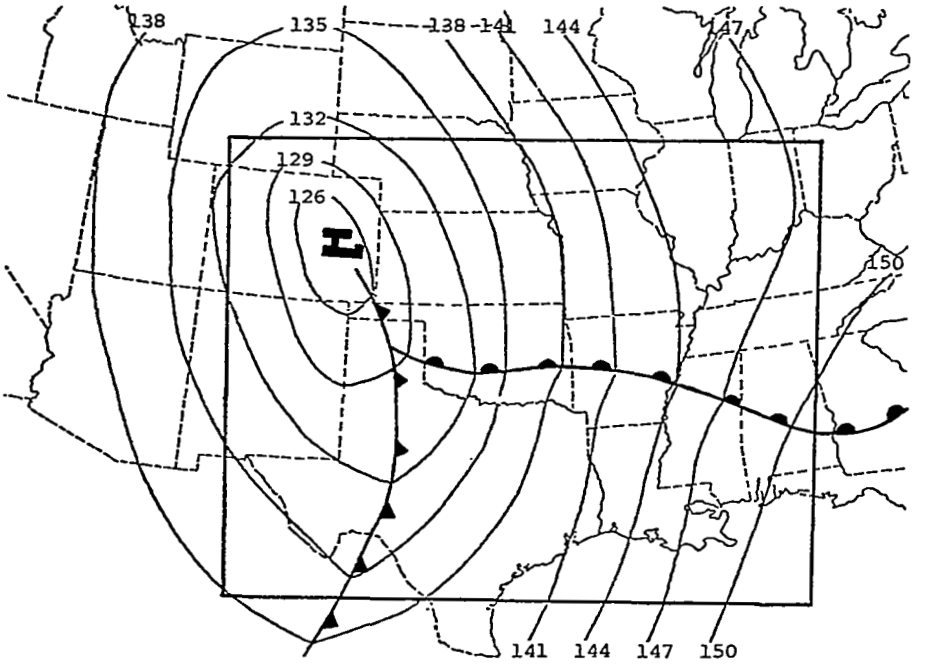

(b) 850 mb

Fig. 11. Synoptic charts for 0000 GMT 11 April 1979. (after Williams et al., 1980). The box outlines the study area.

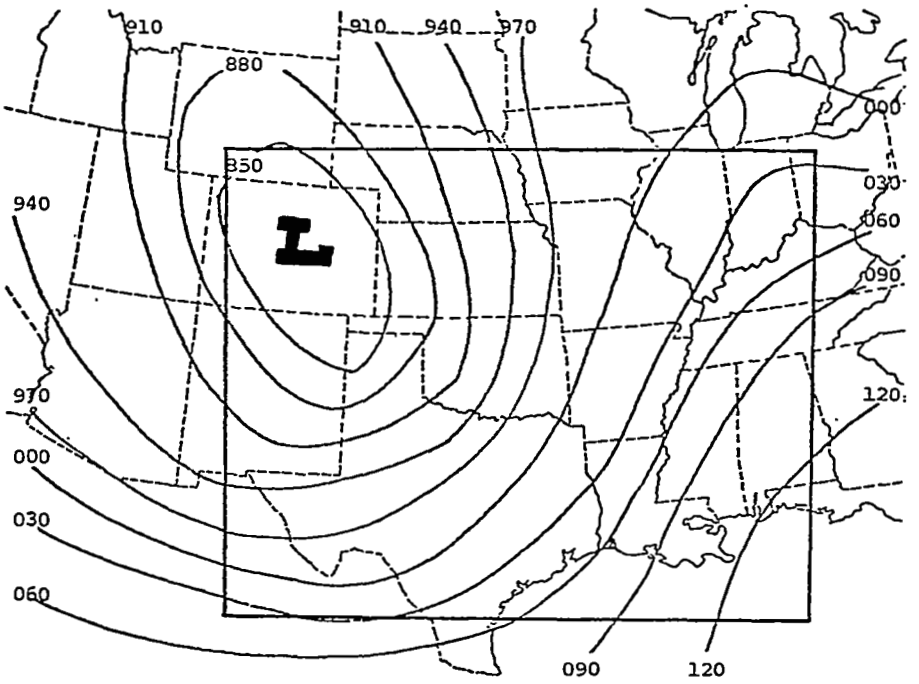

(c) 700 mb

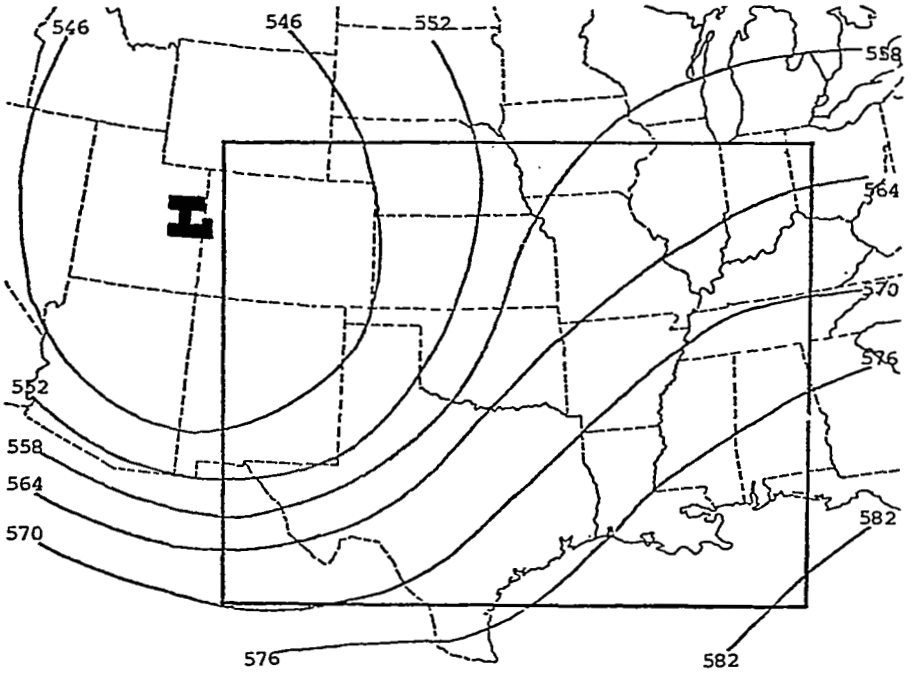

(d) 500 mb

Fig. 11. Continued.

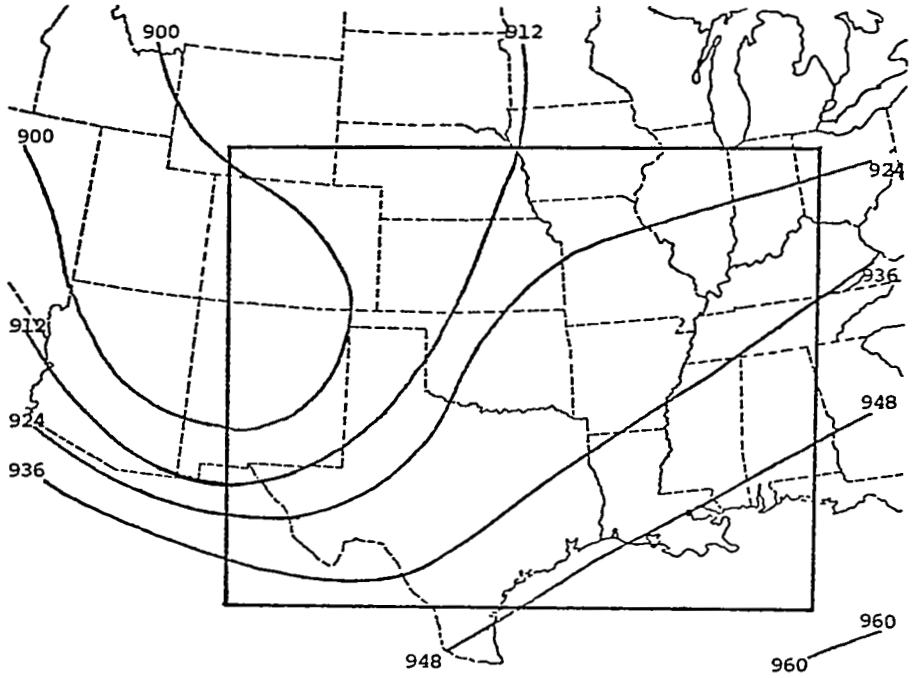

(e) 300 mb

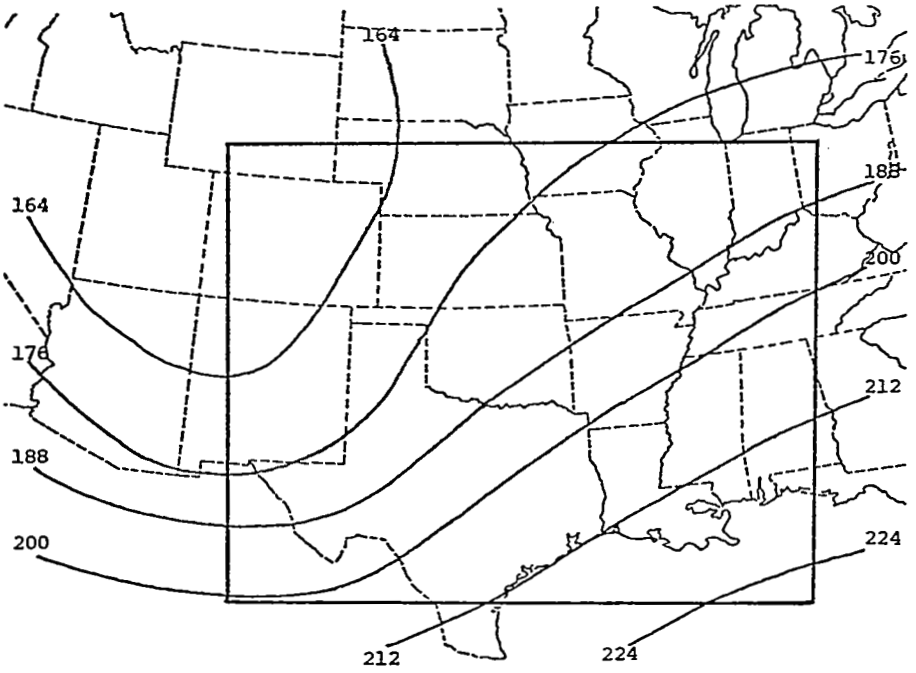

(f) 200 mb

Fig. 11. Continued.

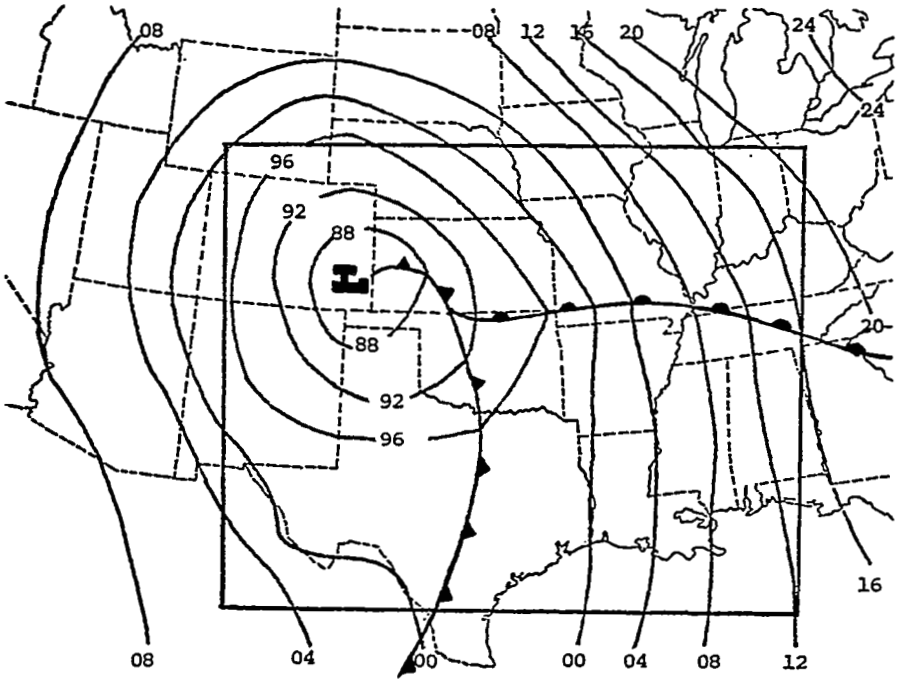

(a) Surface

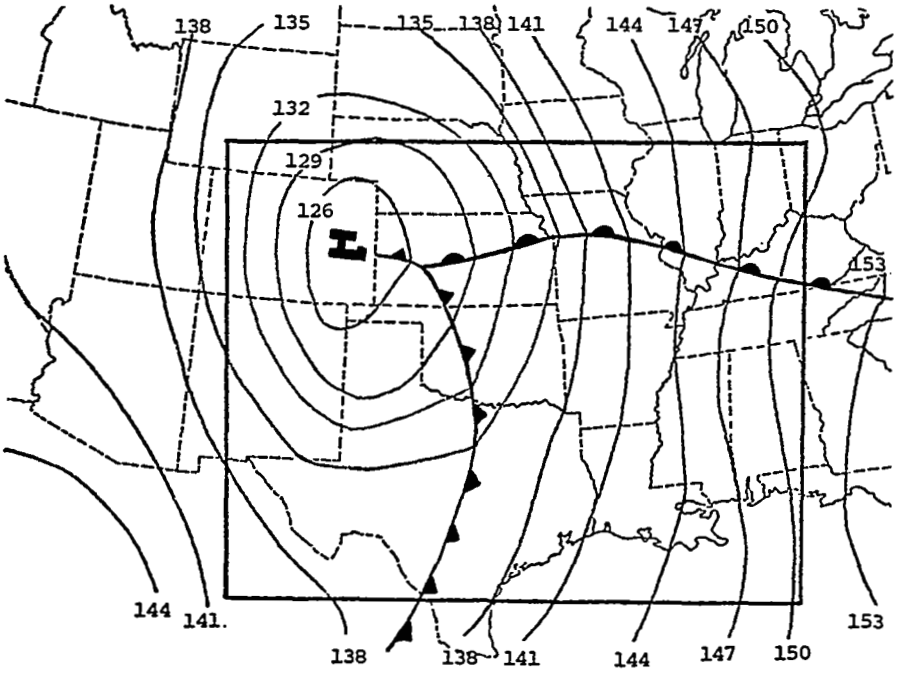

(b) 850 mb

Fig. 12. Synoptic charts for 1200 GMT 11 April 1979. (after Williams et al., 1980). The box outlines the study area.

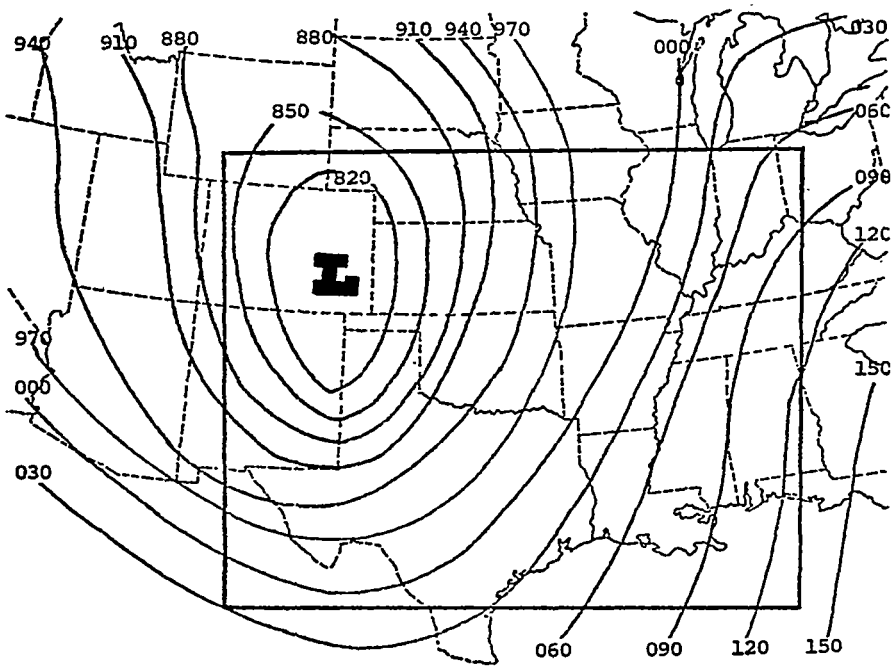

(c) 700 mb

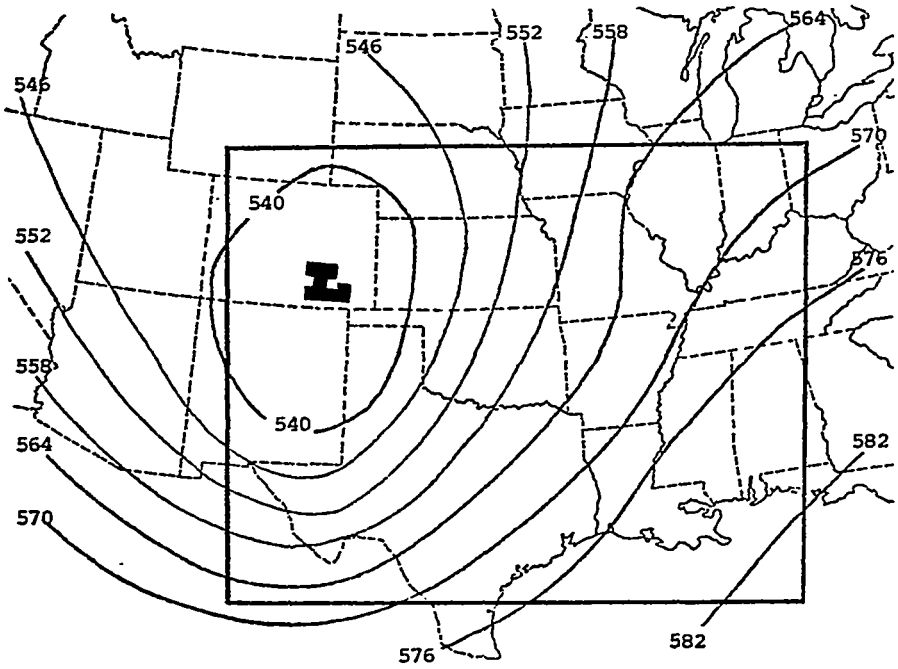

(d) 500 mb

Fig. 12. Continued.

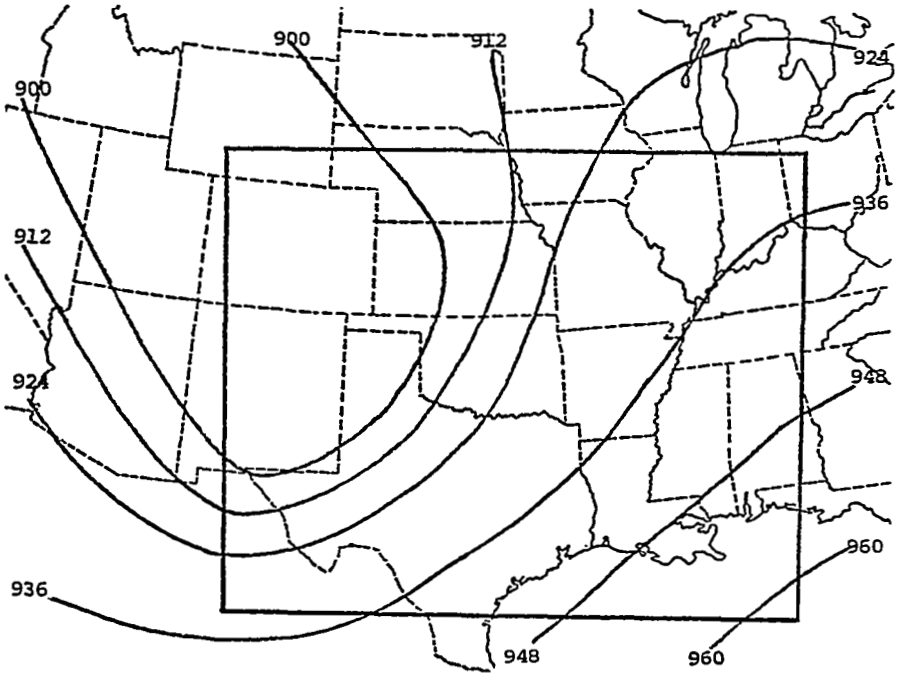

(e) 300 mb

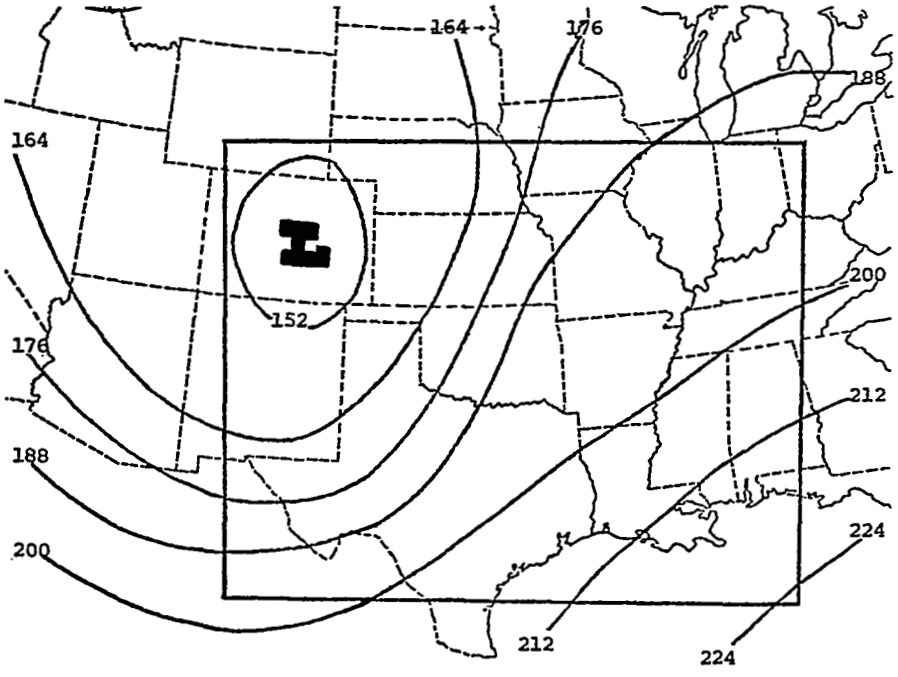

(f) 200 mb
Fig. 12. Continued.

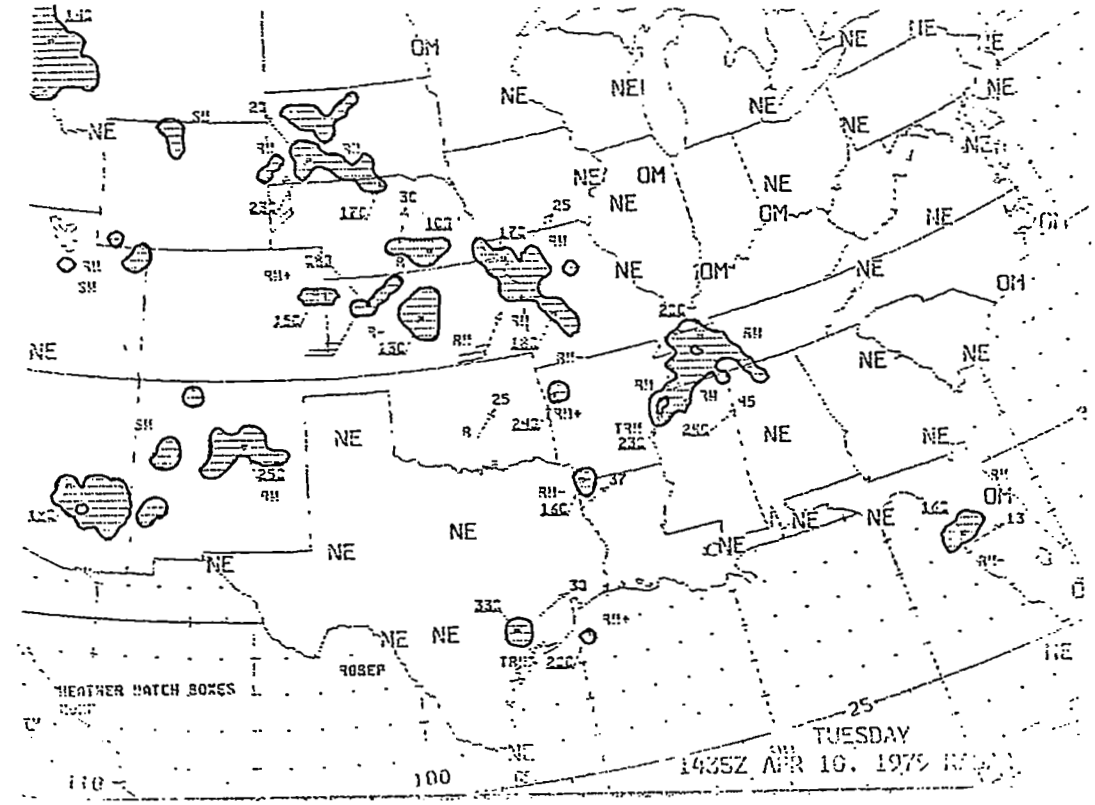

Fig. 13. Radar summary for 1435 GMT 10 April 1979.

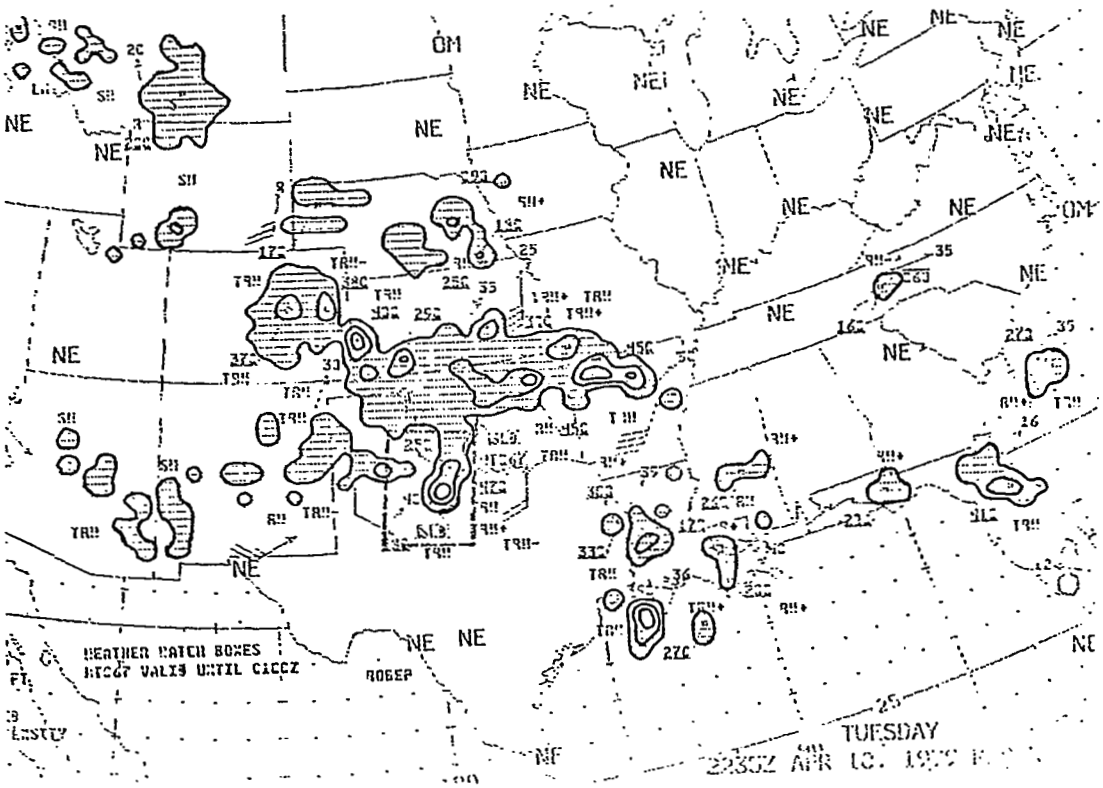

Fig. 14. Radar summary for 2235 GMT 10 April 1979.

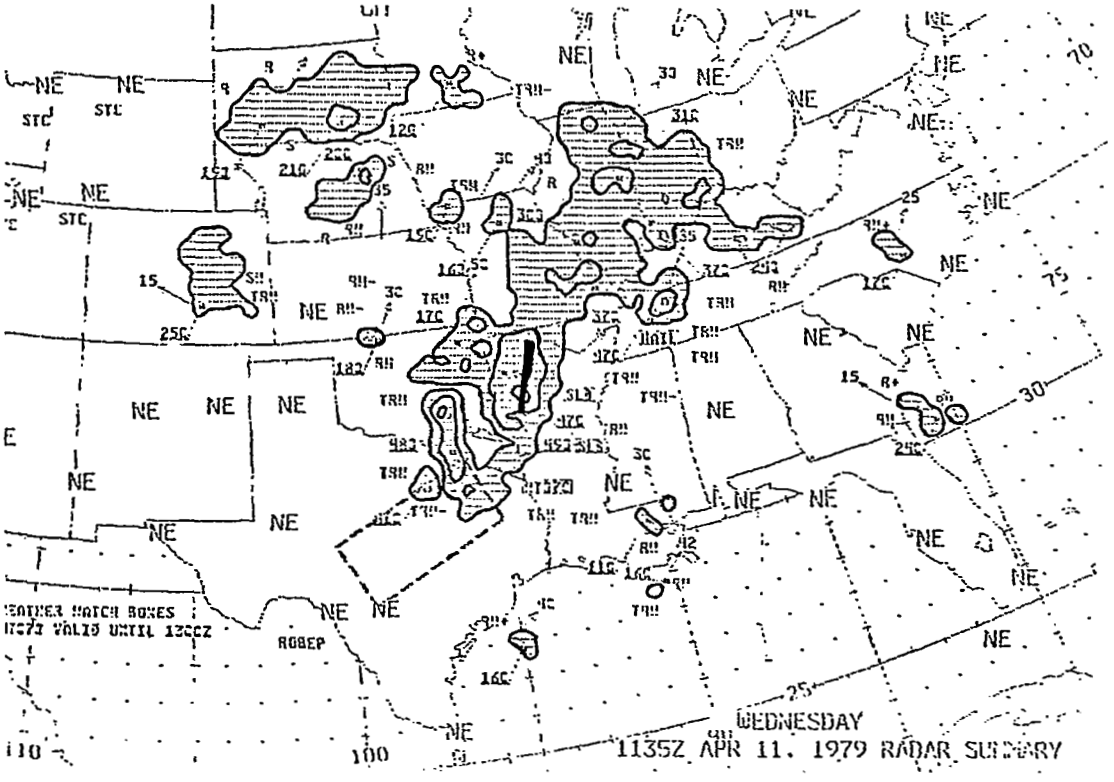

Fig. 15. Radar summary for 1135 GMT 11 April 1979.

ridge extended from Indiana southward to Alabama. At 500 mb, Fig. 10(d), the low pressure center was outside the region of study in Utah and the ridge position was about the same. There was a trough over Nebraska and western Missouri. This trough was rather sharp at the 300-mb level, Fig. 10(e), and still noticeable at 200 mb.

By 0000 GMT, Fig. 11(a), the surface cold front had advanced eastward into the Texas panhandle and extended southward into northeast Mexico and northwestward to the low center in eastern Colorado. This low pressure center had intensified since 1200 GMT. The portion of the warm front nearest this cold front advanced the most to a position just south of the Texas-Oklahoma border and intersecting the cold front as shown in Fig. 11(a). Figure 11(b) shows that the 850-mb low pressure center had moved to eastern Colorado and deepened with the associated cold and warm frontal system.

The NWS radar summary for 2235 GMT 10 April 1979, Fig. 14, shows that the convective areas had become better organized. The main area of convection occurred either side of a line extending southeastward from eastern Colorado to Oklahoma and eastward along the Nebraska-Oklahoma border into northern Arkansas. From this area, a solid line of thunderstorms extended through southwestern Oklahoma into north central Texas.

Extensive deepening of the low occurred at 700 mb between 1200 and 0000 GMT as the center progressed to central Colorado. The ridge also progressed eastward. The 500-mb low was now positioned over far eastern Utah and the short wave over Nebraska and Missouri was no longer noticeable. This trough had also disappeared from the 300-mb level where before it was so pronounced. In its place was a small ridge over northeast Oklahoma and southern Missouri. At 300 mb, the flow pattern was quite smooth with a low in the northwest and an accompanying trough extending through the southwest. Over the eastern two-thirds of the area, the flow was northeasterly on the upstream side of a high pressure ridge.

The surface cold front curved in western Nebraska into the low pressure center in the southeast corner of Colorado by 1200 GMT 11 April 1979, Fig. 12(a). The warm front was located along the Kansas-Oklahoma border through southern Missouri and curved through Tennessee into Georgia and South Carolina. The cold front had progressed into central Oklahoma and extended southward through central Texas. Precipitation was

spread out from northeast Texas to Illinois and Indiana with a solid line of thunderstorms in western Arkansas.

At 850 mb, Fig. 12(b), the frontal system had progressed such that the cold front curved from the low in eastern Colorado through western Nebraska and Oklahoma and central Texas. The warm front extended eastward to Missouri and curved into Kentucky. The 700-mb low pressure center continued to deepen over eastern Colorado as it did at 500 mb, Fig. 12(c). Fig. 12(e) shows that the 300-mb trough progressed a little northeastward and extended from southwest Wyoming through northeast New Mexico into west Texas, while at 200 mb a closed low formed over central Colorado with a ridge to the east of the area.

4. THEORETICAL CONSIDERATIONS

4.1. The Vorticity Equation

Panofsky (1956) describes three methods for deriving the equation of the component of vorticity about a vertical axis. The simplest of these involves differentiating the first equation of motion with respect to y and subtracting it from the second equation of motion differentiated with repect to x. Upon combining and rearranging certain terms, the following equation results:

$$\frac{d\zeta_a}{dt} = -\zeta_a \vec{\nabla}_p \cdot \vec{V}_p + \frac{\partial\omega\partial u}{\partial y\partial p} - \frac{\partial\omega\partial v}{\partial x\partial p} + \vec{k} \cdot \vec{\nabla}x\vec{F}. \qquad (1)$$

This equation illustrates the different effects that can change the absolute vorticity, $\zeta_a = \zeta + f$, of a parcel of air. This change is equal to the sum of 1) vorticity production by horizontal velocity divergence, 2) production of vorticity by tilting of horizontal components of vorticity where there are large horizontal gradients of vertical motion and large vertical gradients of horizontal wind, and 3) generation of vorticity by frictional effects.

The expanded form of Eq. (1), i.e.,

$$\underset{1}{\frac{\partial\zeta}{\partial t}} + \underset{2}{\vec{V}_p \cdot \vec{\nabla}_p \zeta} + \underset{3}{\omega\frac{\partial\zeta}{\partial p}} + \underset{4}{\beta v} = \underset{5}{-(\zeta+f)\vec{\nabla}_p \cdot \vec{V}_p} + \overbrace{\frac{\partial\omega\partial u}{\partial y\partial p} - \frac{\partial\omega\partial v}{\partial x\partial p} + \vec{k}\cdot\vec{\nabla}x\vec{F}}^{6} \qquad (2)$$

was used to examine the synoptic scale vorticity budget and to determine the influence of convective activity on the vorticity budget. Term 1 represents the local time rate-of-change of relative vorticity, term 2 the advection of relative vorticity on isobaric surfaces, term 3 the vertical advection of vorticity, term 4 the change in the vorticity of the ground due to north-south motion, term 5 the concentration or dilution of absolute vorticity through divergence, and terms 6 a combination of the twisting terms and vorticity production by friction. Terms 1-4 reflect the change of vorticity following the motion due to the production of vorticity by terms 5 and 6.

The vorticity equation in the form of Eqs. (1) or (2) is not normally used when dealing with the synoptic scale. Instead, the terms that are

usually considered to be smaller by an order of magnitude are neglected so that when determining development the equation is used in the form

$$\frac{d\zeta}{dt}_a = -\zeta_a \vec{\nabla}\cdot\vec{V}.$$

Also, several assumptions are usually made which lead to use of the vorticity equation in the form

$$\vec{V}_p \cdot \vec{\nabla}_p \zeta \simeq -(\zeta+f)\vec{\nabla}_p \cdot \vec{V}_p. \qquad (3)$$

If the sign of the advection term in Eq. (3) can be determined, then it can be implied whether or not a level is experiencing divergence or convergence since $(\zeta+f)$ is almost always positive. When this equation is applied at some level above the level of nondivergence (LND) this approximation states that if positive vorticity advection $(\vec{V}_p \cdot \vec{\nabla}_p \zeta<0)$ is occurring then the level is experiencing velocity divergence. By Dine's compensation principle, velocity divergence in the upper layers implies convergence in the lower troposphere and upward motion in the mid-troposphere. This approximation is usually applied at the 500-mb level, which is assumed to be above the LND, to delineate areas of upward vertical motion which may coincide with areas of convective activity.

Equation 2 may be written in the form

$$\frac{\partial \eta}{\partial t} + \vec{V}\cdot\vec{\nabla}\eta + \omega\frac{\partial \eta}{\partial p} + \eta\vec{\nabla}\cdot\vec{V} = \frac{\partial \omega}{\partial y}\frac{\partial u}{\partial p} - \frac{\partial \omega}{\partial x}\frac{\partial v}{\partial p} + F_r \qquad (4)$$

where $\eta = \zeta+f$. If we apply Reynolds' decomposition rule to this equation and average, neglecting perturbations in $\vec{V}$ and $\vec{F}$, the result is:

$$\frac{\partial \bar{\eta}}{\partial t} + \bar{\eta}\vec{\nabla}\cdot\vec{V} + \vec{V}\cdot\vec{\nabla}\bar{\eta} + \bar{\omega}\frac{\partial \bar{\eta}}{\partial p} = \overline{\omega'\frac{\partial \eta'}{\partial p}} + \frac{\partial \bar{\omega}}{\partial y}\frac{\partial \bar{u}}{\partial p} + \overline{\frac{\partial \omega'}{\partial y}\frac{\partial u'}{\partial p}} - \frac{\partial \bar{\omega}}{\partial x}\frac{\partial \bar{v}}{\partial p}$$

$$- \overline{\frac{\partial \omega'}{\partial x}\frac{\partial v'}{\partial p}} + \bar{F}. \qquad (5)$$

The left-hand side of this equation ($\frac{d\bar{\eta}}{dt} + \eta\vec{\nabla} \cdot \vec{v}$) is called by Reed and Johnson (1974) the "apparent vorticity source" which they equated to the first term on the right-hand side of the equation. They neglected the twisting and tilting and friction terms in their theoretical development although in their computed vorticity budget it appears that the left-hand side of Eq. 5 was equated to a residual representing all terms on the right-hand side of the equation as we have done.

If the three perturbation-product terms on the right-hand side of Eq. 5 are neglected, as is customarily done, Eq. 5 with bars omitted is identical to Eq. 2. Equation 2 is evaluated in the present research over an area, but the bars have been omitted for convienence.

4.2. Vertical Motion

The kinematic method of estimating vertical motion involves the continuity equation in the form

$$-\frac{\partial\omega}{\partial p} = \vec{\nabla}_p \cdot \vec{v}_p + \frac{1}{\rho}\frac{d\rho}{dt}$$

where $\frac{1}{\rho}\frac{d\rho}{dt}$ is much smaller than the other terms. Thus,

$$-\frac{\partial\omega}{\partial p} = \vec{\nabla}_p \cdot \vec{v}_p$$

is a good approximation.

Integration of this equation from the surface to some arbitrary pressure level yields the following equation for vertical motion (μbar s^{-1}) on constant-pressure surfaces:

$$\omega_p = \omega_s - \int_{p_s}^{p} \vec{\nabla}_p \cdot \vec{v}_p dp.$$

If vertical velocity at the surface (ω_s) is neglected, it can be seen that the vertical motion will be downward ($\omega>0$) in the middle troposphere if the lowest layers experience velocity divergence. The converse is also true.

A similar relationship can be established by integrating from an arbitrary pressure surface, p, to the top of the atmosphere where the

vertical velocity vanishes. The result is

$$\omega_p = \int_p^{p=0} \vec{\nabla}_p \cdot \vec{V}_p \, dp.$$

Thus, if there is velocity divergence in the upper layers, the mid-tropospheric vertical motion will be upward ($\omega<0$) and vice versa.

One objective of this research was to use the vorticity equation and this relationship between vertical motion and divergence to determine the sign of the mid-tropospheric vertical motion.

4.3. Computational Procedures

The gridded fields of the u and v wind components and vertical motion were used to compute the vorticity budget for the 850-, 700-, 500-, and 300-mb levels. Equation (2) was approximated by

$$\underset{1}{\frac{\Delta\zeta}{\Delta t}} + \underset{2}{u_p\left(\frac{\Delta\zeta}{\Delta x}\right)_p} + \underset{3}{v_p\left(\frac{\Delta\zeta}{\Delta y}\right)_p} + \underset{4}{\omega\frac{\Delta\zeta}{\Delta p}} + \underset{5}{\beta v} = \underset{6}{-(\zeta+f)\left[\left(\frac{\Delta u}{\Delta x}\right)_p + \left(\frac{\Delta v}{\Delta y}\right)_p\right] + R} \quad (6)$$

where term 6 represents the residual, R, which is the vorticity production term that includes the tilting effect, friction effect, and measurement and computational errors.

Term 1, the local change term, was computed using centered finite differences, except for the first and last observation times when forward and backward differences were used, respectively. The centered finite difference form of Term 1 is

$$\left(\frac{\Delta\zeta}{\Delta t}\right)_t = \frac{\zeta_{t+1} - \zeta_{t-1}}{t_{t+1} - t_{t-1}}.$$

In terms 2, 3, and 5 of Eq. (6) the horizontal and vertical spatial derivatives were approximated by centered finite differences. Term 2, the horizontal vorticity advection term, was approximated in the following manner at grid point i, j:

$$(\vec{V}_p \cdot \vec{\nabla}_p\zeta)_{i,j} = u_{i,j}\left[\frac{\zeta_{i+1,j} - \zeta_{i-1,j}}{2\Delta x}\right]_p + v_{i,j}\left[\frac{\zeta_{i,j+1} - \zeta_{i,j-1}}{2\Delta y}\right]_p$$

where $2\Delta x = 2\Delta y = 316$ km. The vertical vorticity advection, Term 3, was

evaluated at each grid point on a constant pressure surface, p, using the following equation:

$$\left(\omega\frac{\Delta\zeta}{\Delta p}\right)_{i,j} = \omega_{i,j}\left[\frac{\zeta_{p+\delta p} - \zeta_{p-\delta p}}{\Delta p}\right]_{i,j}$$

where $\Delta p = 100$ mb and $\delta p = 50$ mb.

The finite difference form of Term 5, the divergence term, at the grid point i,j is:

$$\left[-(\zeta+f)\vec{\nabla}_p \cdot \vec{V}_p\right]_{i,j} = -(\zeta_{i,j} + f_{i,j})\left[\left(\frac{u_{i+1,j} - u_{i-1,j}}{2\Delta x}\right) + \left(\frac{v_{i,j+1} - v_{i,j-1}}{2\Delta y}\right)\right].$$

In Term 4, which is a measure of the latitudinal effect, β was evaluated by

$$\beta = \frac{2\Omega\cos\Phi}{E}$$

where Ω is the angular velocity of the earth, E is the radius (in m) of the earth, and Φ is the latitude at the grid point.

The residual, Term 6, is the sum of the terms on the left-hand side of (6) minus Term 5, the divergence term (another production term). This definition of the residual is consistent with that used by other authors.

5. RESULTS

5.1. Fields of Terms in the Vorticity Equation

The terms of the vorticity equation were computed and the resultant gridded fields contoured for three consecutive observation times during both AVE VII and AVE-SESAME I. The initial time for AVE VII was 2100 GMT 2 May 1978, and for AVE-SESAME I it was 1800 GMT 10 April 1979. The 850-mb contoured field of vertical vorticity advection contains shaded areas which represent the areas of convective activity at that time. These fields will be discussed in chronological order, beginning with the AVE VII results, with the features and changes thereof being related to synoptic conditions. The boxes within certain plots will be referred to in the following section.

The average values of terms in the vorticity equation associated with the convective areas were estimated at each level in hopes of establishing the relationship among the terms within an area of convective activity. Specifically under consideration was the relationship between positive vorticity advection at 500 mb and the mid-tropospheric vertical motion and the usual assumption concerning this relationship, i.e., that all terms are negligible except the horizontal advection and divergence terms. Unfortunately, only a qualitative analysis could be made using the contoured fields.

The approximation

$$\vec{V}_p \cdot \vec{\nabla}_p \zeta \simeq -\zeta_a \vec{\nabla}_p \cdot \vec{V}_p$$

could not be examined at the 500-mb level because it was determined from the contoured fields of velocity divergence that the level of nondivergence occurred above this level. The 300-mb level was chosen instead to examine the use of the approximation in the convective area. (Refer to the figures of the fields of terms in the vorticity equation at 300-mb for the respective times.) At this level the PVA areas were delineated by the outline of the convective activity and there was a fairly good correspondence with the positive centers of the divergence term. Thus, the PVA in the areas of convective activity indicates positive (upward) vertical motion in the mid-troposphere. As stated before, this was not

an accurate analysis, but rather it was only a general, qualitative examination using the contoured fields.

5.1.1. AVE VII

2100 GMT 2 May 1978

At 850 mb, as seen in Fig. 16, the divergence and residual terms appear to be the largest. They are nearly the same magnitude but opposite in sign near MAF. The sign of the divergence term indicates whether or not convergence or divergence is occurring. Since (ζ+f) is almost always positive, the level is experiencing divergence if the sign of the divergence term is negative and convergence if it is positive. The centers of divergence and residual terms near MAF roughly correspond to the NWS radar echoes which occurred between DRT and CLL. The outer contour of the radar echo has been superimposed on the contoured field of vertical advection. Such low level convergence, determined from the divergence term, is to be expected in an area of convective activity. In the case of R, the relationship stems from the increased horizontal gradients of vertical motion, Fig. 17(a), in the area of convection. Large horizontal gradients of ω suggest that R is primarily composed of twisting/tilting. A less intense R center occurred near JAN in conjunction with convective activity.

The situation is not much different at 700 mb, Fig. 18, except there is a center of positive vertical advection coinciding with the area of convection near MAF and SEP. Examination of the field of vertical motion, Fig. 17(b), reveals that there is rising vertical motion ($\omega<0$) in this area, so larger relative vorticity is being lifted.

At 500 mb, Fig. 19, the local time rate-of-change and horizontal advection terms are of increased importance in the vorticity budget. The local change was substantially larger in an area which included the northern Texas panhandle, western Oklahoma, and southwestern Kansas. It was also larger in the area between SEP and CLL and southward. This may be an indication of development of convective activity since the following observation shows activity in this same area that was not observed prior to that time (See Fig. 26). It can be seen in Fig. 19 that the areas of positive vorticity advection at 500 mb generally occurred in the areas of convective activity (recall that negative values indicate positive vorticity advection). This supports the use of the approximate vorticity equation, Eq. (3), as a method of delineating

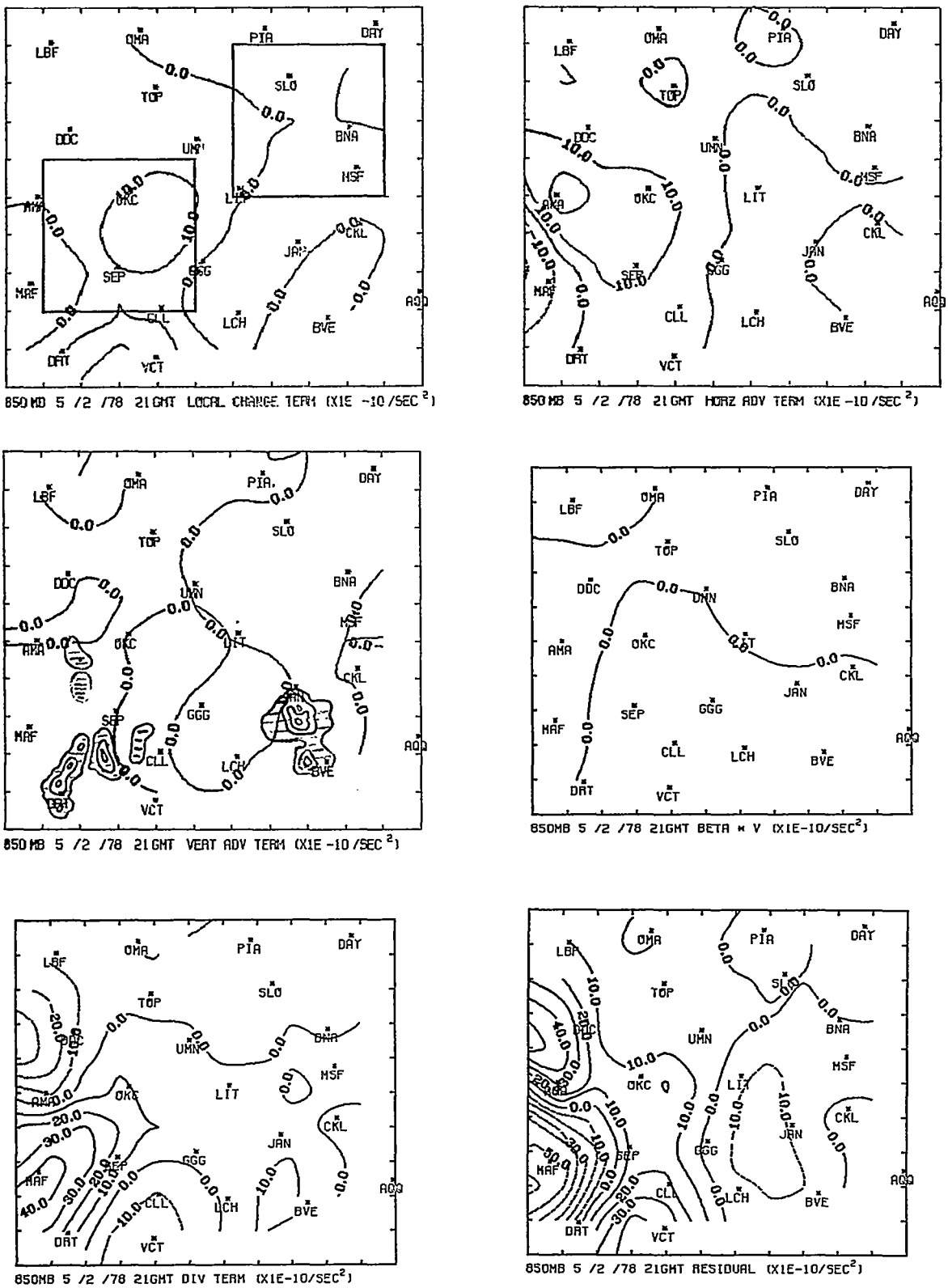

Fig. 16. Fields of terms in the vorticity equation at 850 mb for 2100 GMT 2 May 1978.

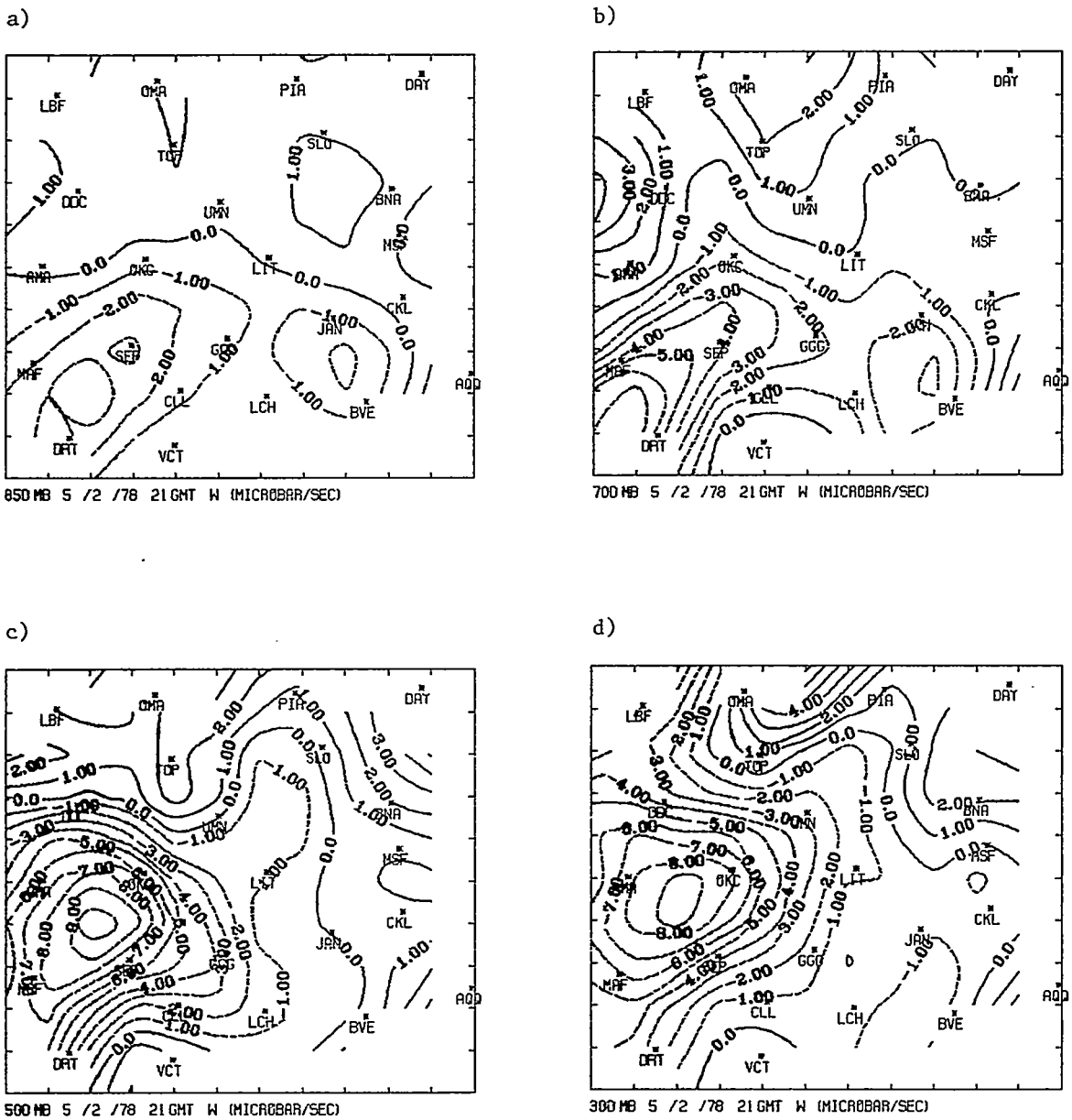

Fig. 17. Vertical motion, ω (μbars s^{-1}), for 2100 GMT 2 May 1978.

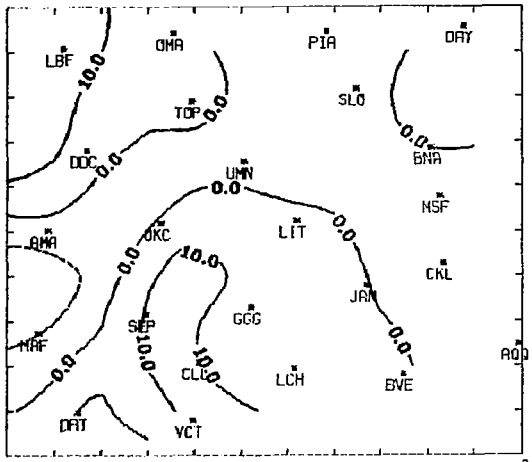

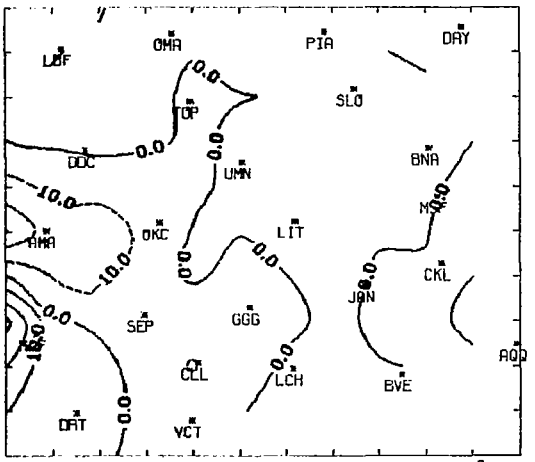

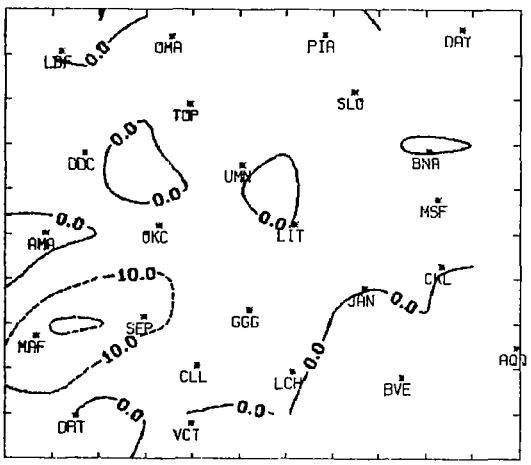

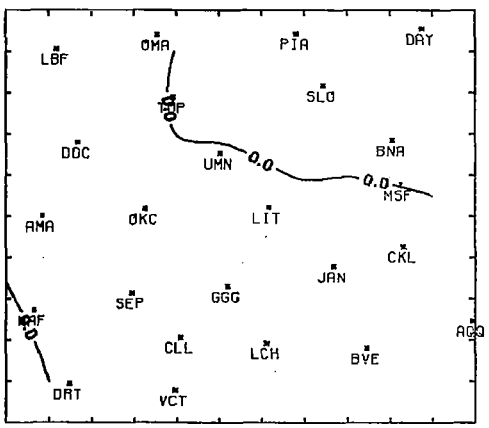

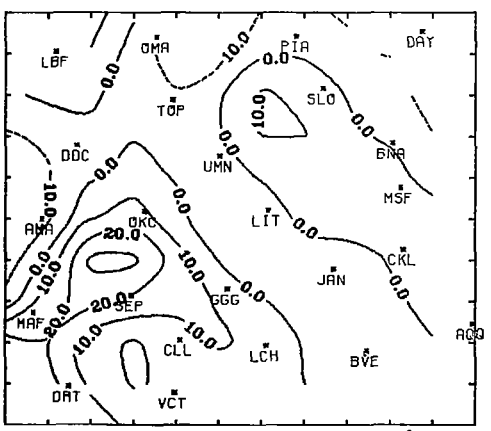

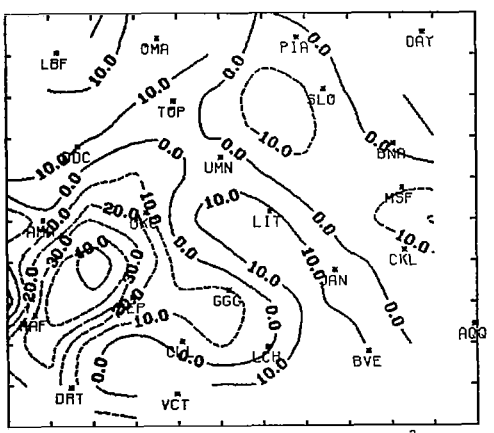

Fig. 18. Fields of terms in the vorticity equation at 700 mb for 2100 GMT 2 May 1978.

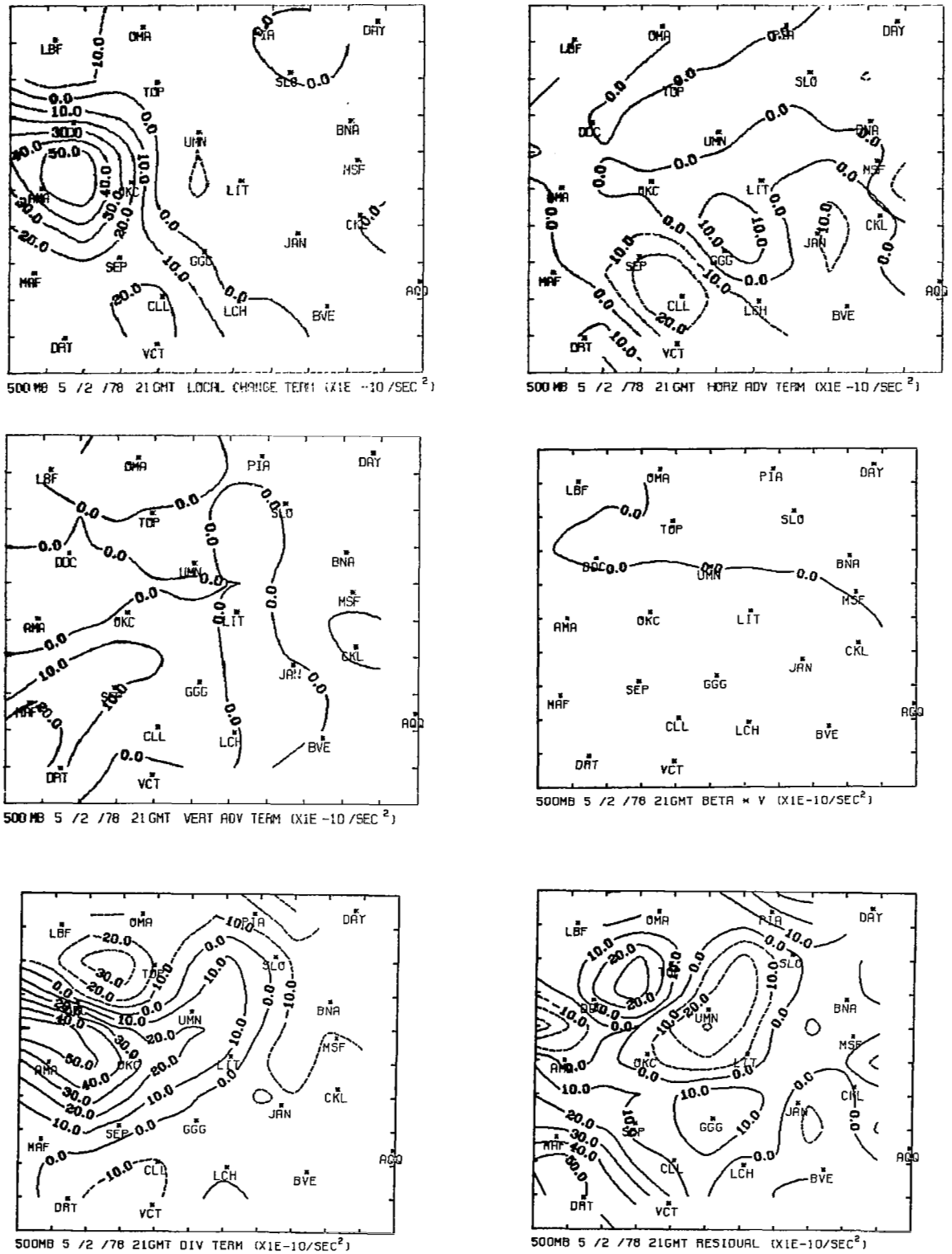

Fig. 19. Fields of terms in the vorticity equation at 500 mb for 2100 GMT 2 May 1978.

probable areas of convective activity. Comparison of this contoured field of horizontal relative vorticity advection with the corresponding 500-mb wind chart, Fig. 20(a), and contoured field of relative vorticity, Fig. 20(b), shows that higher values of vorticity in the region of the trough in west Texas were being advected toward the northeast.

The vertical advection term was small throughout the region at 500 mb, Fig. 19, except in southwest Texas. This small area of relatively large negative vertical advection (indicated by positive values) corresponds to an area of strong positive vertical motion at this level, Fig. 17(c), in which smaller values of relative vorticity were being advected upward. The $\frac{df}{dy}$, or βv, term was an order of magnitude smaller than the other terms and, therefore, contributed little to the overall budget of vorticity.

The wind flow at 300 mb, Fig. 21(a), shows that the trough and ridge pattern was more pronounced as was the horizontal advection of relative vorticity due to large gradients of vorticity, Fig. 21(b), and strong winds from high to low values of vorticity. This level was determined to be above the level of nondivergence by examination of the contoured fields of velocity divergence, Fig. 22. The widespread positive vorticity advection, Fig. 23, was over the area where convective activity developed by 0000 GMT. The divergence term field shows a large negative center over part of this same area indicating that divergence was occurring. Therefore, this is a case in which the approximate vorticity equation, Eq. (3), at least gives the proper sign of the horizontal vorticity advection for the purpose of delineating areas of convective activity.

The problem with the use of Eq. (3), however, is the assumption that all terms in the vorticity equation, Eq. (1), except the horizontal advection and divergence terms are negligible. In this case, as with the two subsequent observation times, the residual term is not negligible. As previously mentioned, this large magnitude is believed to be due to large horizontal gradients of vertical motion associated with large vertical gradients of horizontal wind in the area of the developing convective activity. Also, the magnitude of the local time rate-of-change is larger than is usually assumed. There are two positive centers of $\frac{\partial \zeta}{\partial t}$ and a large area of significant negative values, which seems to correspond to increased anticyclonic relative vorticity around the ridge whose axis lies N-S through the north central United States. The

a)

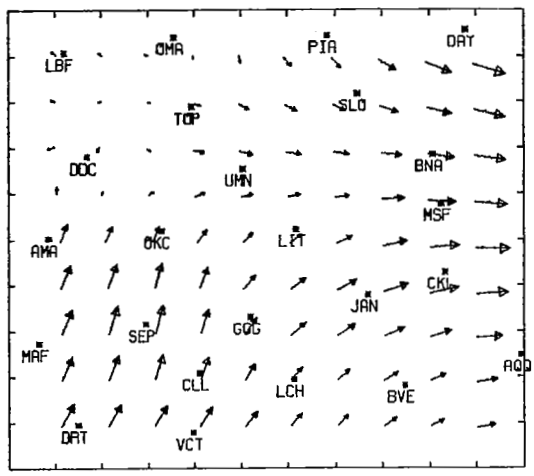

500 MB 5 /2 /78 21 GMT WIND

b)

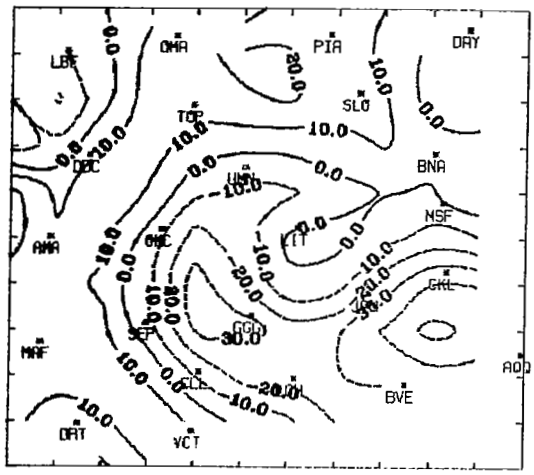

500 MB 5 /2 /78 21 GMT ZETA (X1E-6/SEC)

Fig. 20. Fields of wind and relative vorticity at 500 mb for 2100 GMT 2 May 1978.

a)

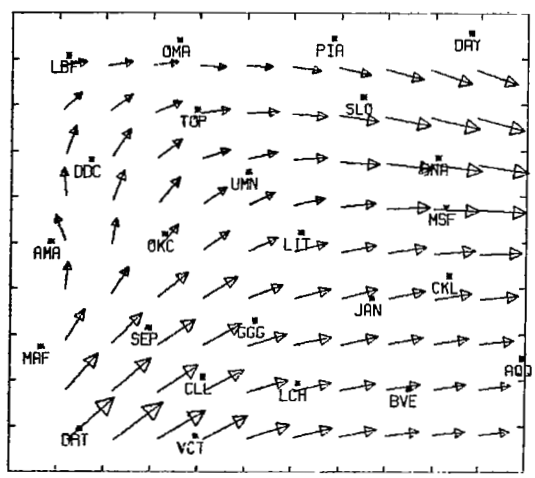

300 MB 5 /2 /78 21 GMT WIND

b)

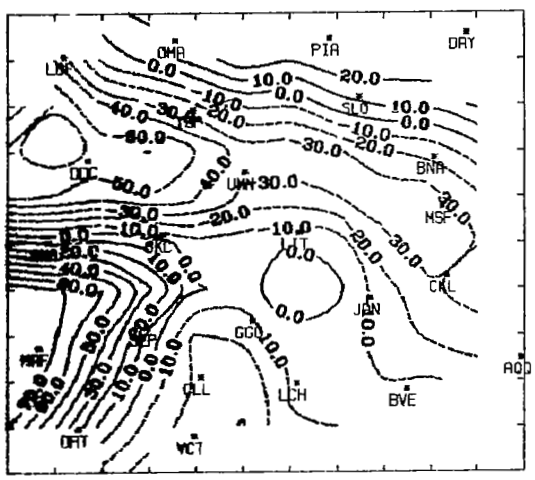

300 MB 5 /2 /78 21 GMT ZETA (X1E-6/SEC)

Fig. 21. Fields of wind and relative vorticity at 300 mb for 2100 GMT 2 May 1978.

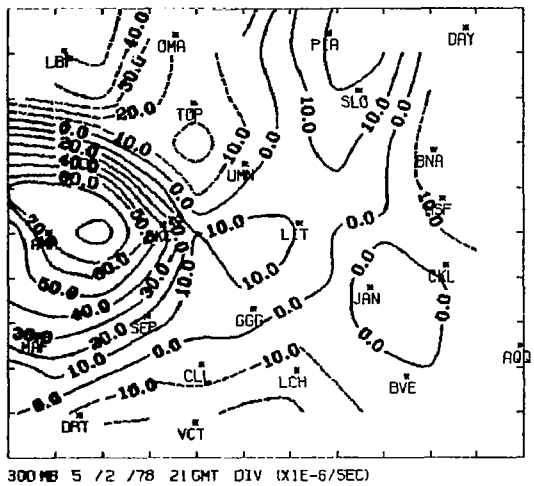

Fig. 22. Field of velocity divergence at 300 mb for 2100 GMT 2 May 1978.

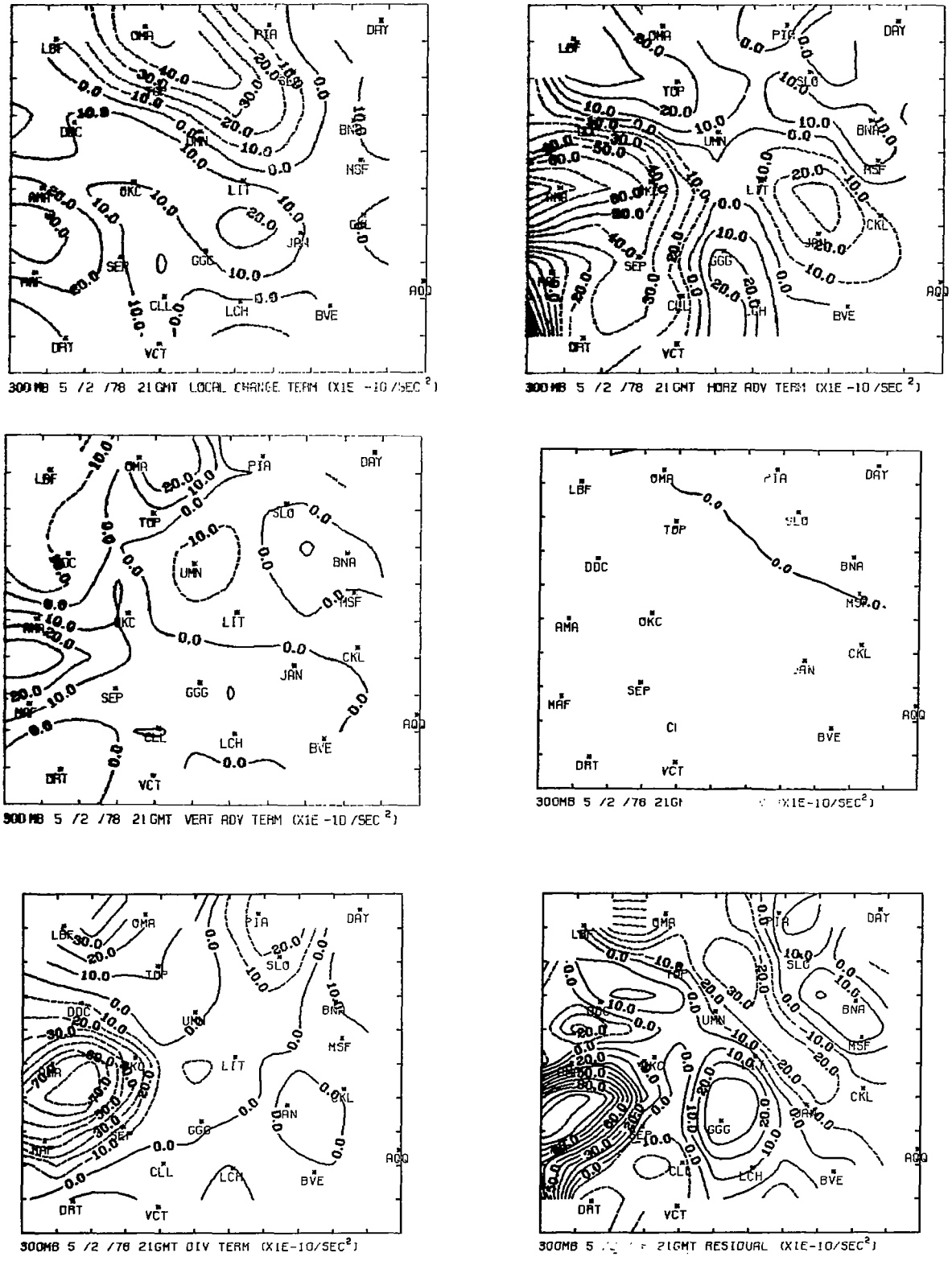

Fig. 23. Fields of terms in the vorticity equation at 300 mb for 2100 GMT 2 May 1978.

magnitude of the vertical advection of vorticity also is large enough in certain areas not to be considered negligible. The primary center of negative vertical advection occurred in conjunction with a center of large positive vertical motion, Fig. 17(d), in which smaller values of relative vorticity at a lower level were being advected upward. Lastly, the βv term is negligibly small, as would be expected due to little north-south motion in the flow field.

The large residual term is of interest because it contributes to the production or destruction of vorticity and is of the same order of magnitude as the divergence term, which is also a production term.

0000 GMT 3 May 1978

By 0000 GMT, the local time rate-of-change term at 850 mb, Fig. 24, had increased roughly three-fold in the region where convection developed between 2100 and 0300 GMT. The central axis of maximum $\frac{\partial \zeta}{\partial t}$ was along that of the convective activity observed at 0300 GMT, Fig. 28. Thus, it may be possible to use the local change term as a measure of development. The field of horizontal vorticity advection remained positive (indicating negative vorticity advection) in the region where development was occurring or toward which the activity was moving.

The vertical advection and βv terms remained small at the 850-mb level, while the production terms were large. The center of positive divergence, which advanced northeastward and intensified in the three hours since 2100 GMT, indicates a maximum of low-level convergence north of SEP. This entire region of convergence corresponds to the more intense westernmost area of activity (See the outlined radar echoes on the vertical advection field.). The contours of the residual term, although its magnitude remained large, did not change much, except to propagate eastward and intensify slightly as was expected in a region where the horizontal gradients of vertical motion increased with the developing convective activity.

The positive center of the local change term continued in the upper layers, Figs. 25 and 26, except at 300 mb, Fig. 27, where it became negative. The horizontal advection was small at 700 mb, Fig. 25, as is usually the case while the vertical advection term definitely became significant in magnitude in the western portion of the region. The βv term was negligible at this level as well as the 500- and 300-mb levels.

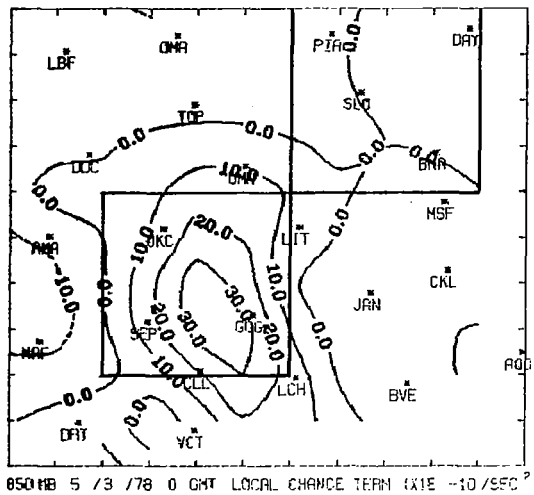

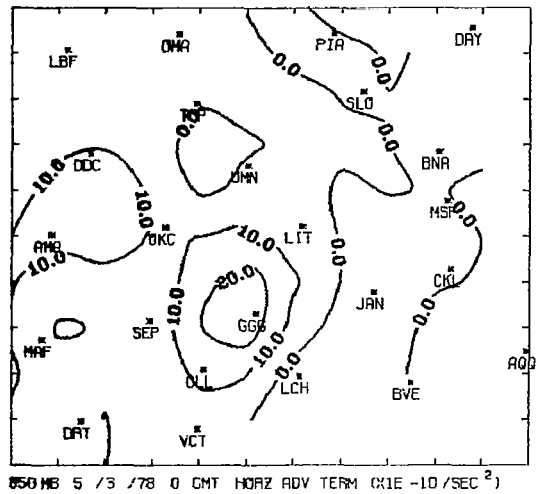

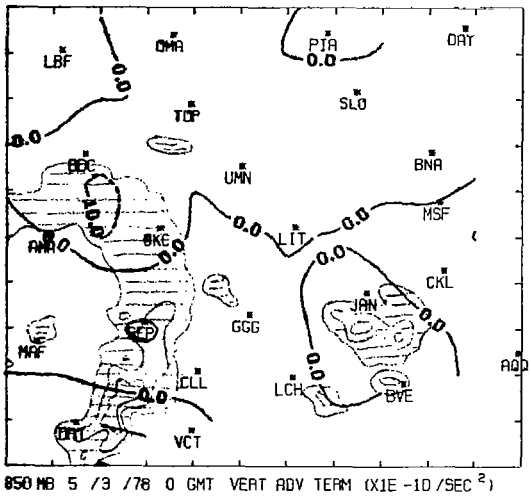

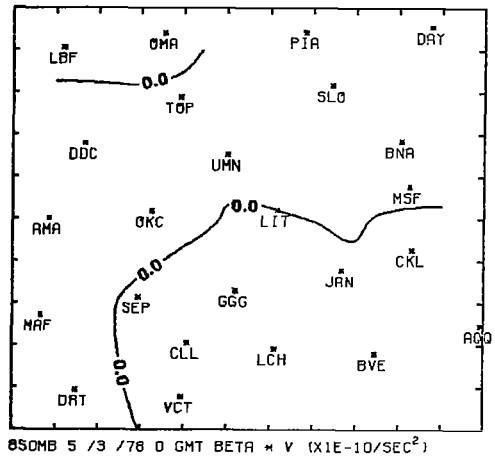

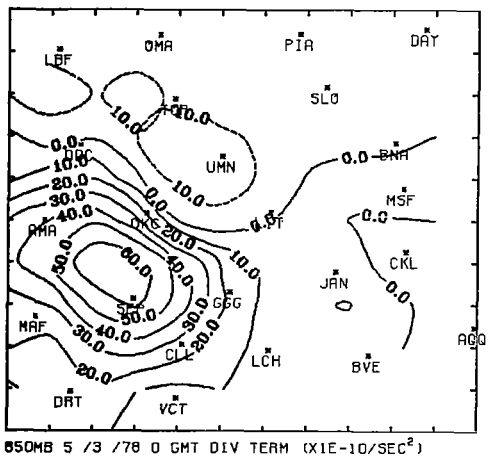

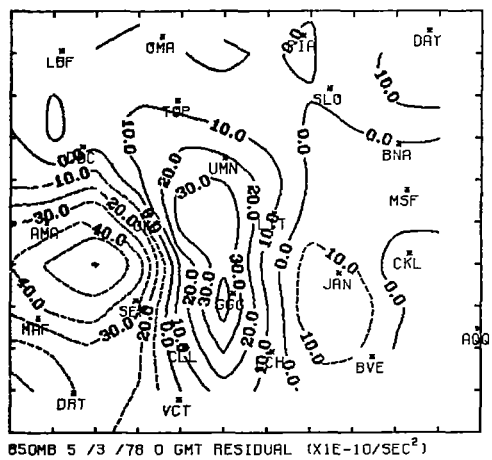

Fig. 24. Fields of terms in the vorticity equation at 850 mb for 0000 GMT 3 May 1978.

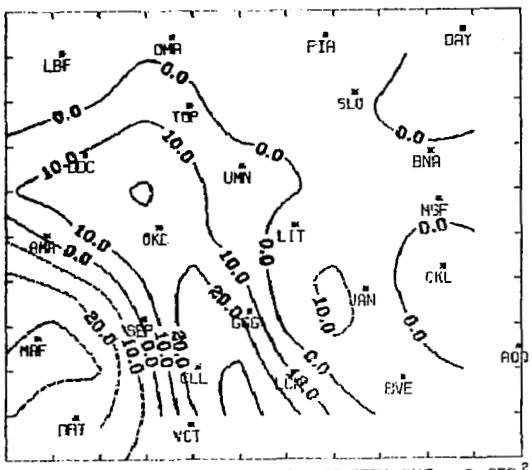

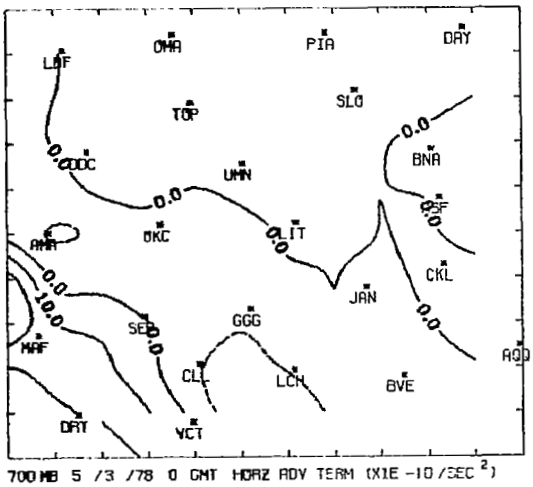

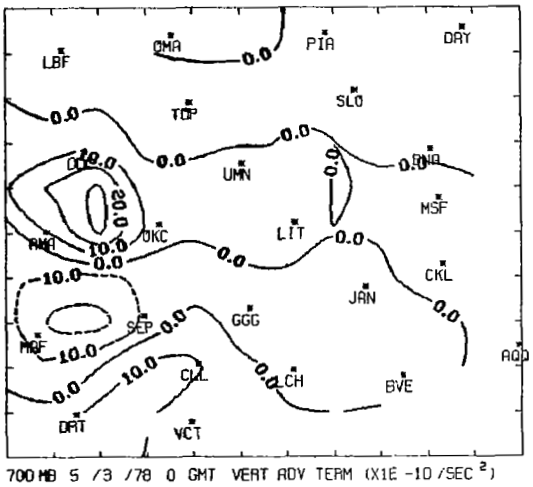

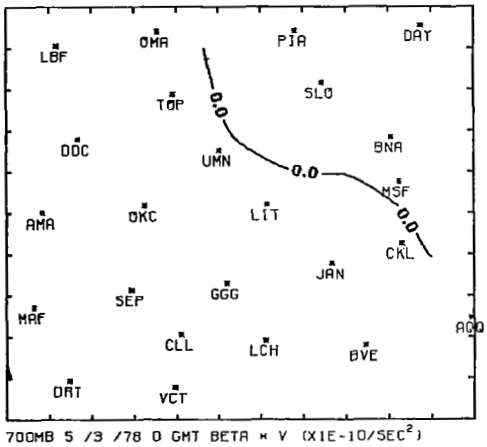

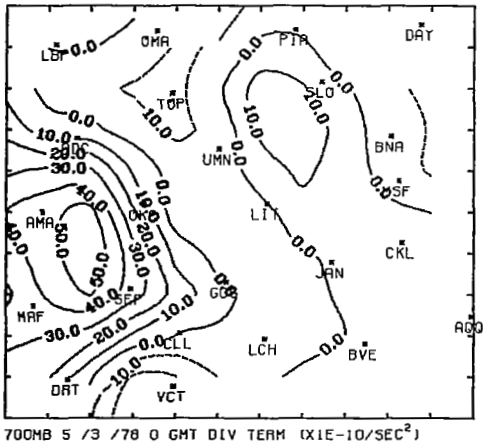

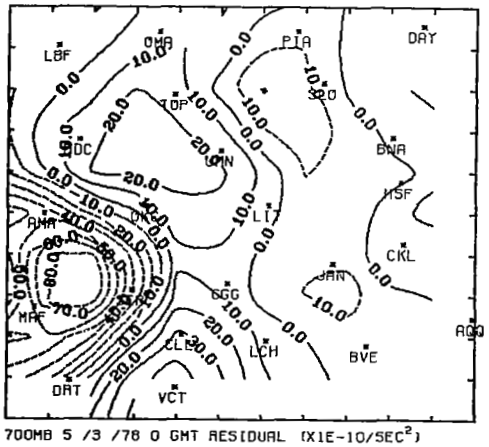

Fig. 25. Fields of terms in the vorticity equation at 700 mb for 0000 GMT 3 May 1978.

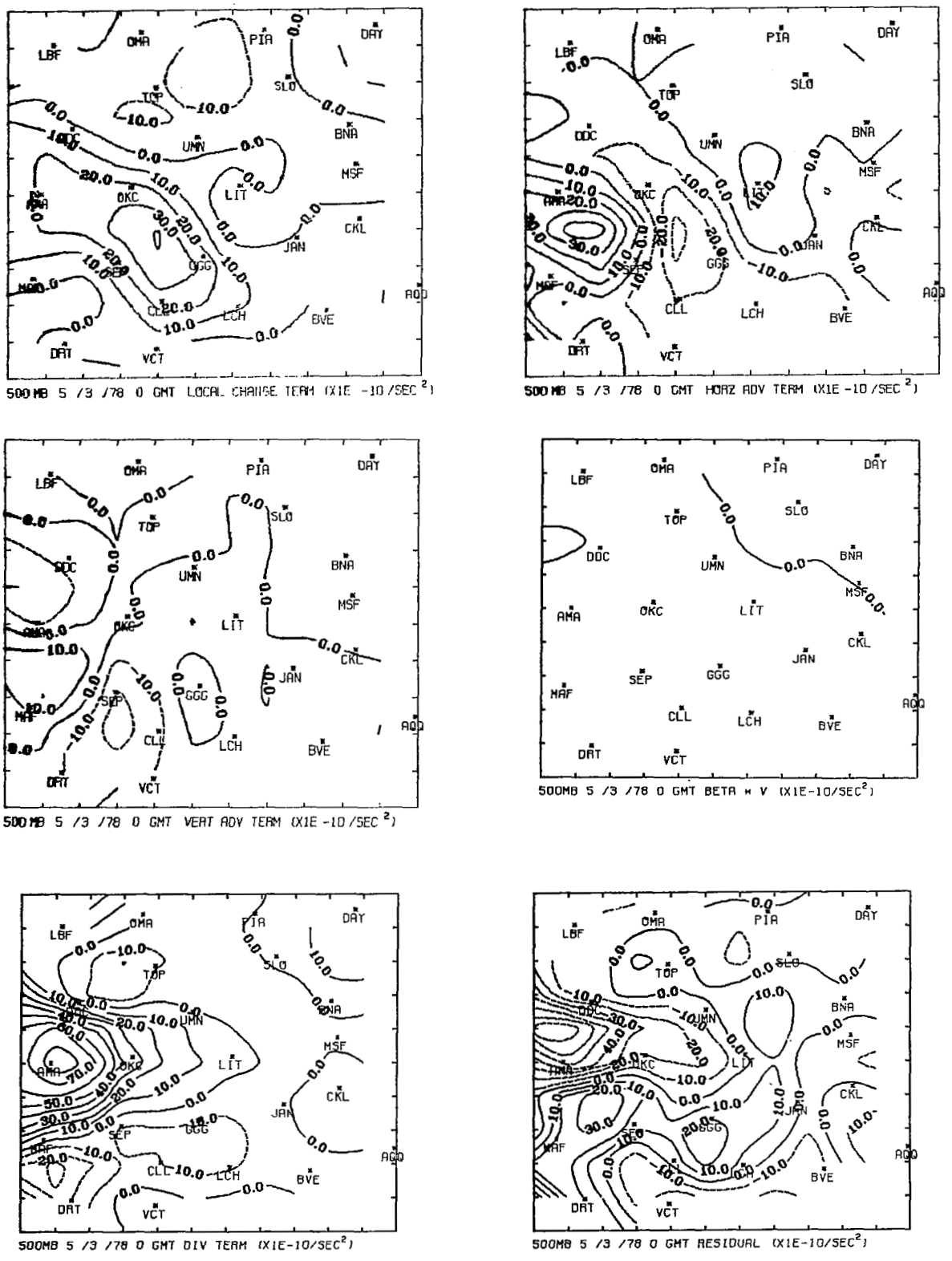

Fig. 26. Fields of terms in the vorticity equation at 500 mb for 0000 GMT 3 May 1978.

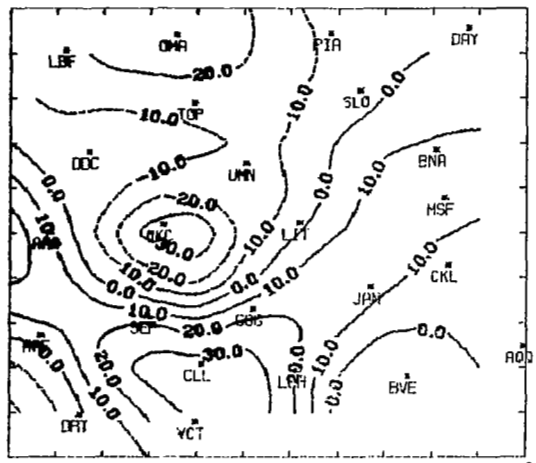

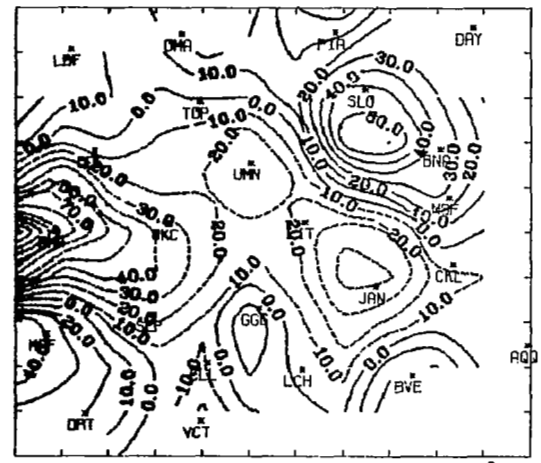

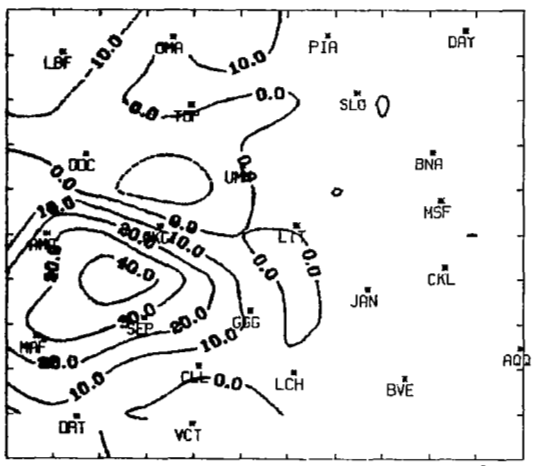

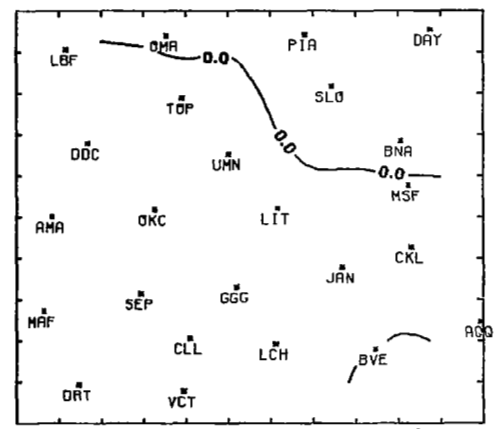

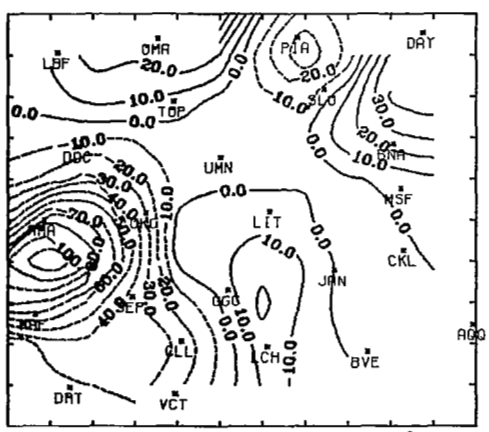

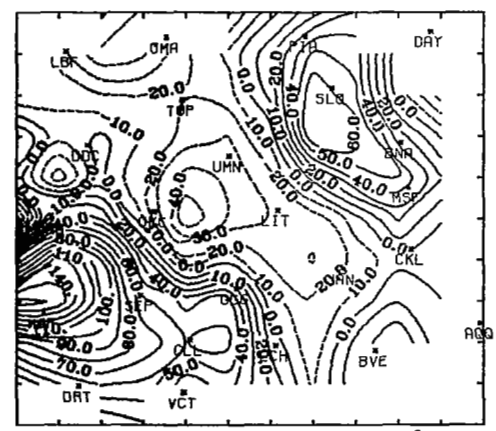

Fig. 27. Fields of terms in the vorticity equation at 300 mb for 0000 GMT 3 May 1978.

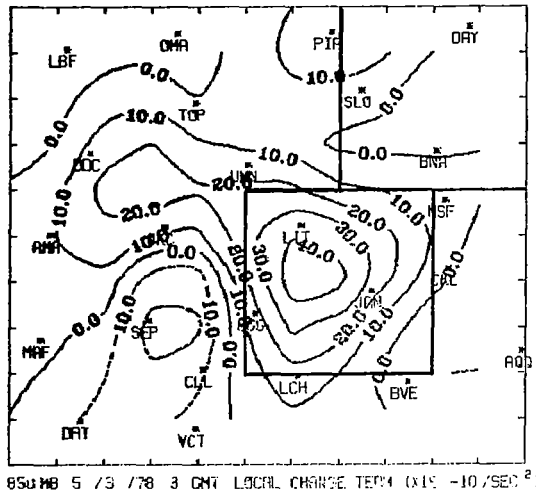

850 MB 5 /3 /78 3 GMT LOCAL CHANGE TERM (X1E -10/SEC ^{2})

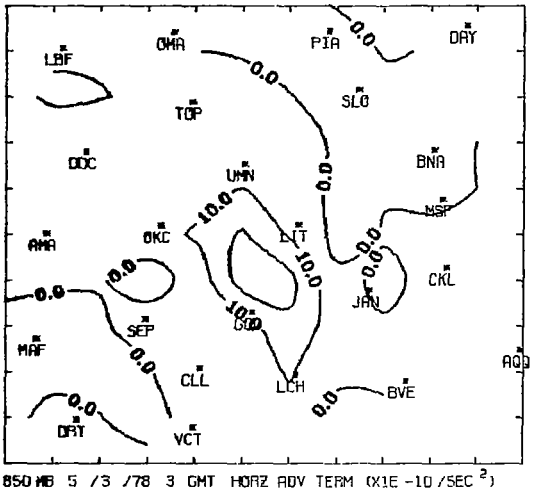

850 MB 5 /3 /78 3 GMT HORZ ADV TERM (X1E -10/SEC ^{2})

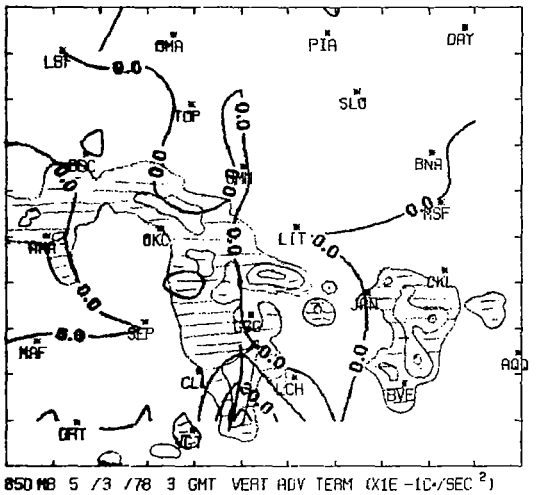

850 MB 5 /3 /78 3 GMT VERT ADV TERM (X1E -10/SEC ^{2})

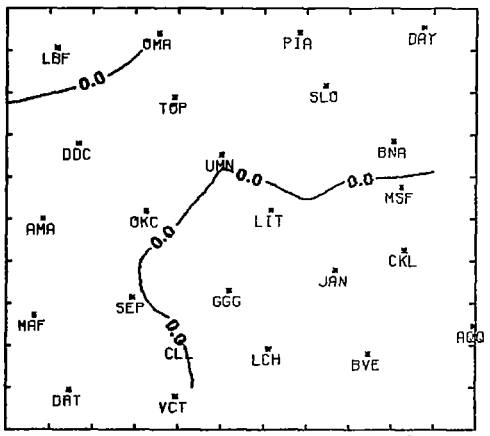

850MB 5 /3 /78 3 GMT BETA * V (X1E-10/SEC^2)

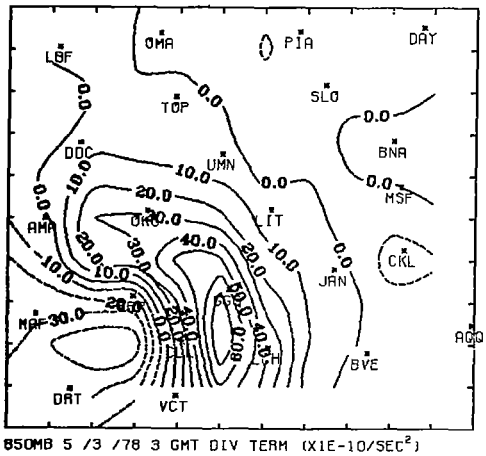

850MB 5 /3 /78 3 GMT DIV TERM (X1E-10/SEC^2)

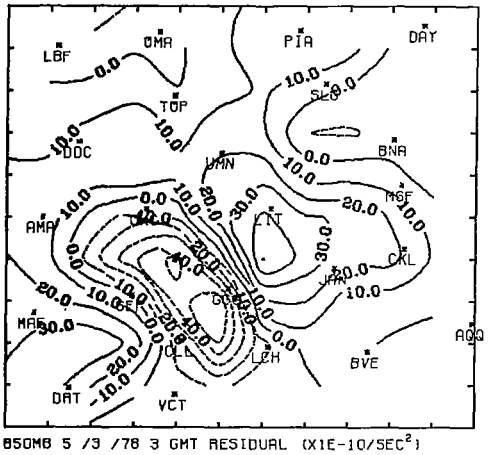

850MB 5 /3 /78 3 GMT RESIDUAL (X1E-10/SEC^2)

Fig. 28. Fields of terms in the vorticity equation at 850 mb for 0300 GMT 3 May 1978.

The divergence term continues to indicate convergence at 700 and 500 mb in the vicinity of the convective activity while above the LND divergence is indicated. This corresponds to the negative vorticity advection below the LND, and positive vorticity advection above the LND in this region. The sign of the divergence term once again gives the sign of the horizontal advection term as in the approximate vorticity equation. Unlike in the approximate vorticity equation, Eq. (3), however, the residual at all levels was the same order of magnitude as the horizontal advection and divergence terms.

0300 GMT 3 May 1978

By this time, the main area of convective activity had progressed to the east with the most intense activity propagating southward within the convective region. The local time rate-of-change term was large at all four levels.

The vertical advection and βv terms were negligibly small at 850 mb, Fig. 28, and the βv term remained small at the other levels as well. The vertical advection term, however, became more important in the upper levels. At 700 mb, Fig. 29, largely negative (meaning positive advection) values occurred in the region and since there is a large corresponding center of upward ($\omega<0$) vertical motion, Fig. 30, the gradient of vorticity with height at this level must have been negative (i.e., larger values of relative vorticity were being advected upward toward lower vorticity values). Examination of the remaining production fields at all four levels, Figs. 28, 29, 31, and 32, reveals conditions similar to those of the two previous observation times.

5.1.2. AVE-SESAME I

1800 GMT 10 April 1979

At 850 mb some terms in the vorticity equation are small, Fig. 33, but the production terms are large and of the same magnitude but opposite in sign. The large positive divergence term in the west near ABQ is due to large convergence associated with the frontal system. This is verified in Fig. 34, which shows a zone of convergence in that area. Examination of this area in Fig. 35 reveals a horizontal gradient of vertical motion and, thereby, the tilting of relative vorticity in the vertical.

At 700 mb, the vertical advection and βv terms were still neglibibly small while the $\frac{\partial \zeta}{\partial t}$ and R terms were of the same order of magnitude as

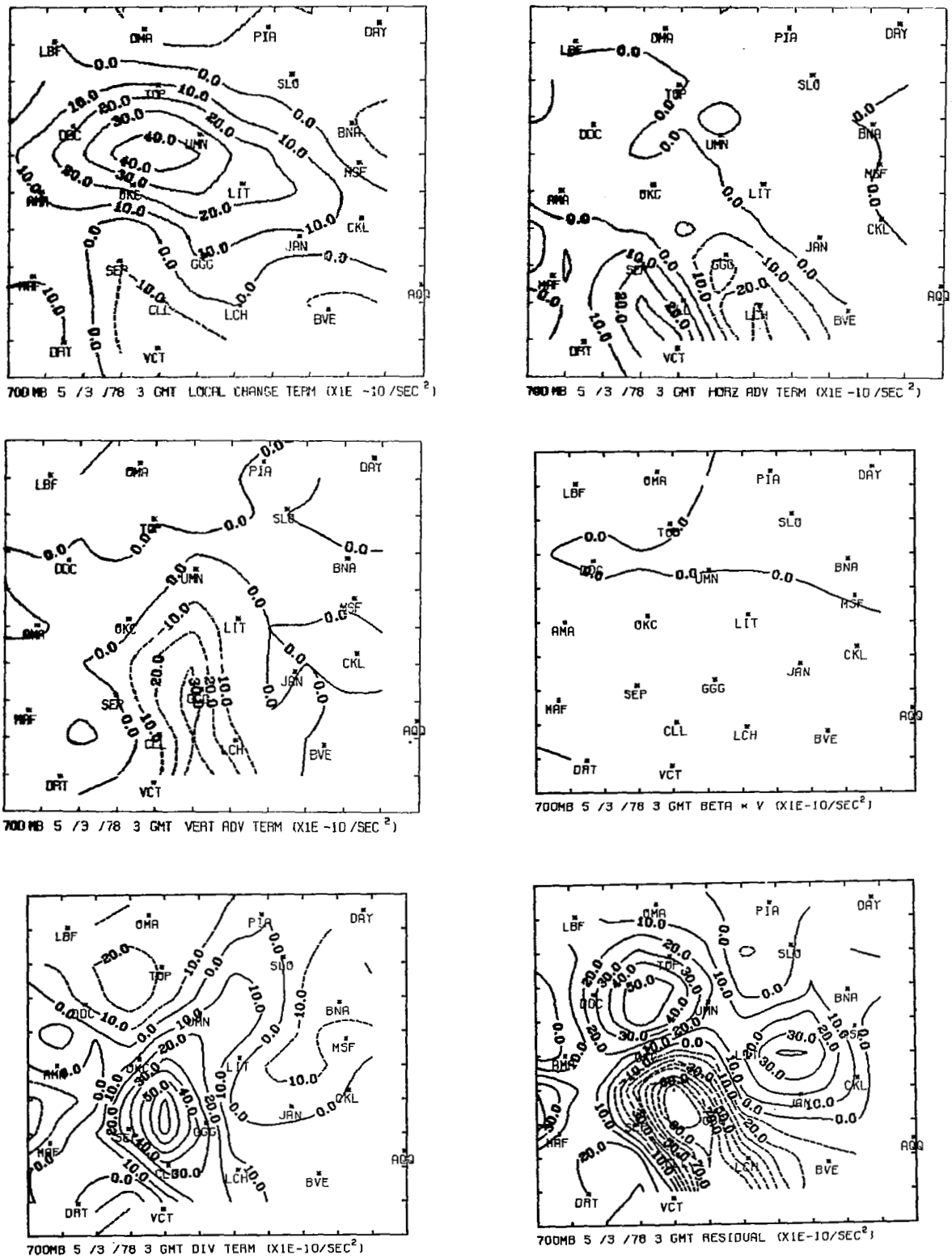

Fig. 29. Fields of terms in the vorticity equation at 700 mb for 0300 GMT 3 May 1978.

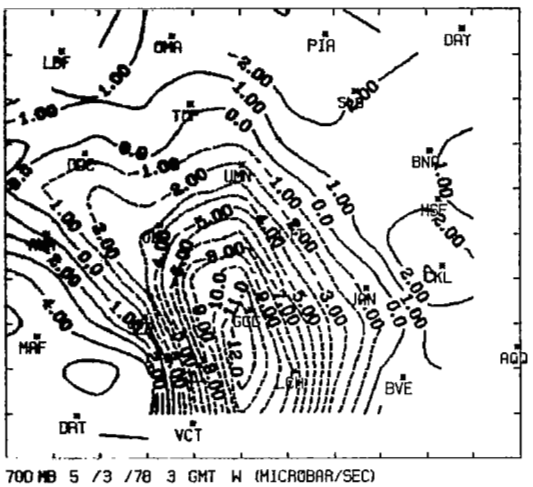

Fig. 30. Vertical motion, ω (μbars s^{-1}), at 700 mb for 0300 GMT 3 May 1978.

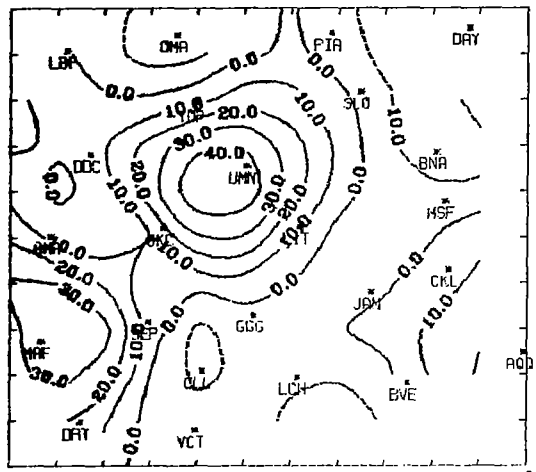

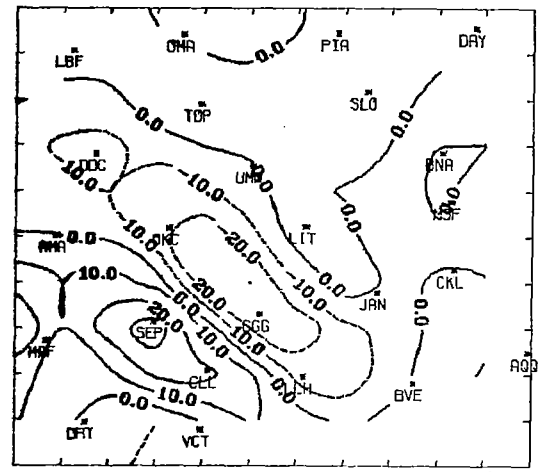

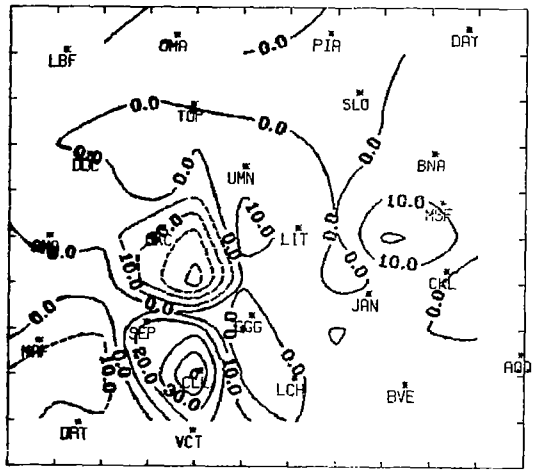

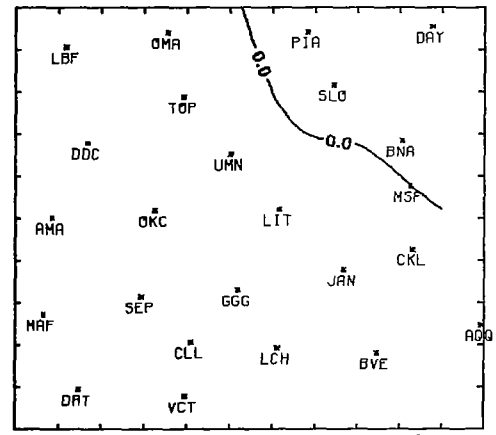

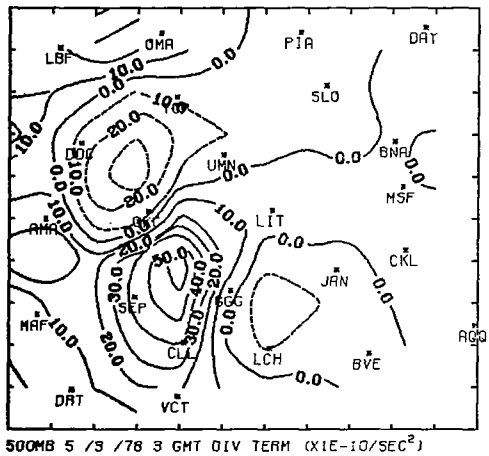

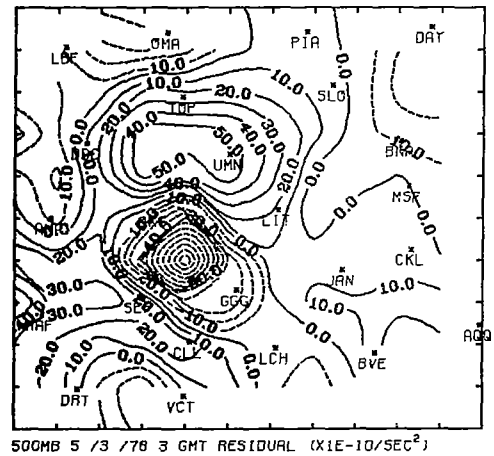

Fig. 31. Fields of terms in the vorticity equation at 500 mb for 0300 GMT 3 May 1978.

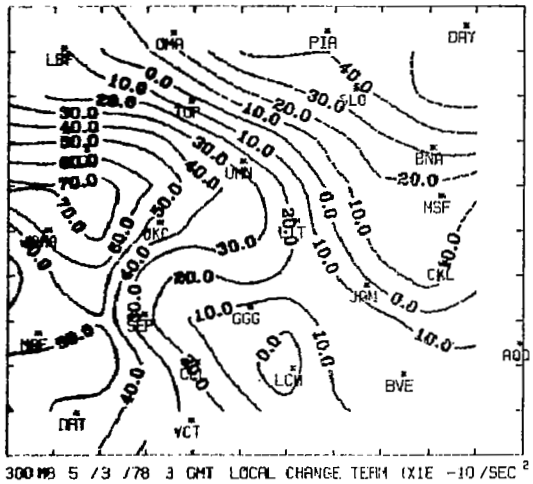

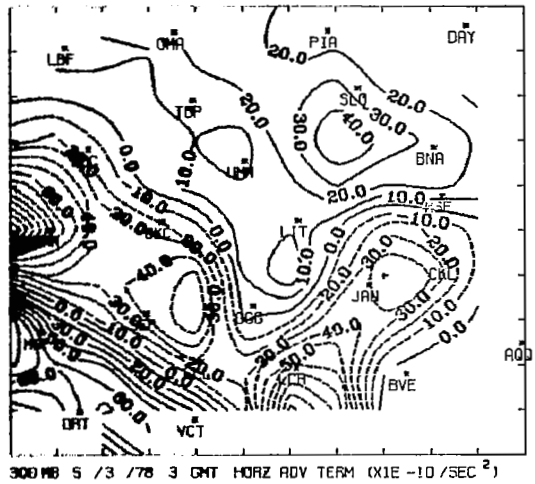

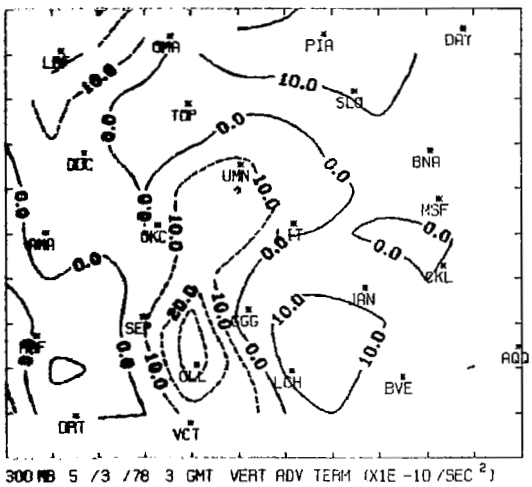

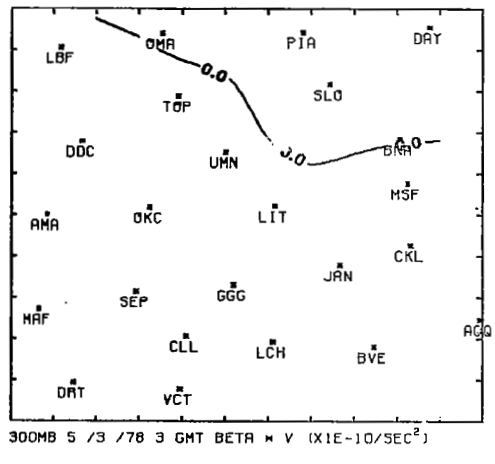

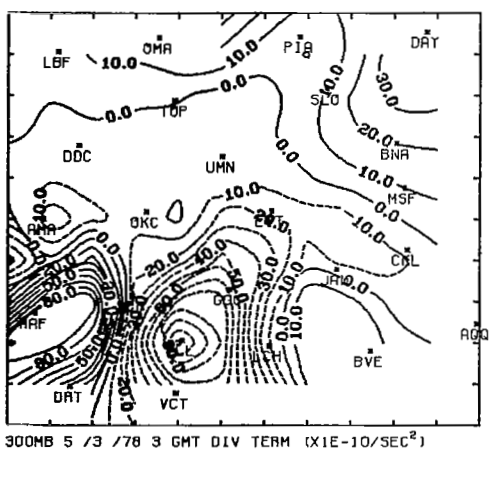

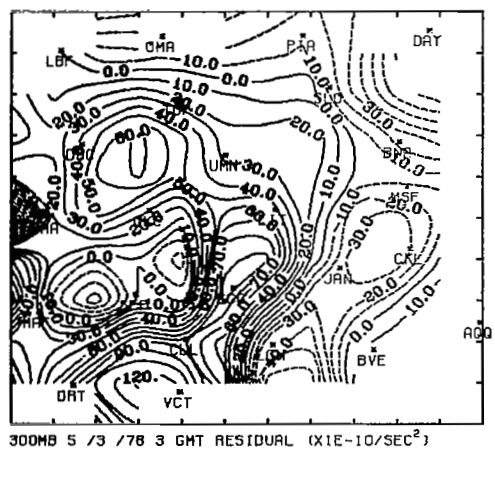

Fig. 32. Fields of terms in the vorticity equation at 300 mb for 0300 GMT 3 May 1978.

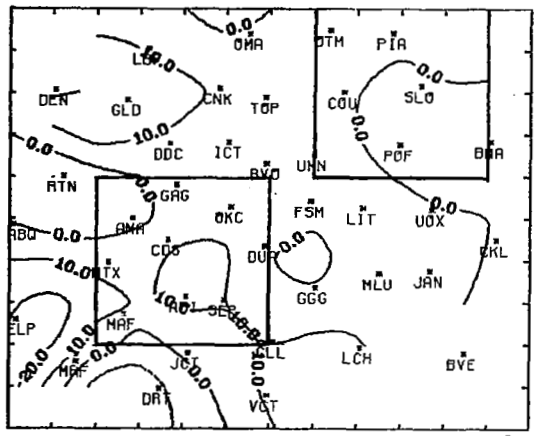

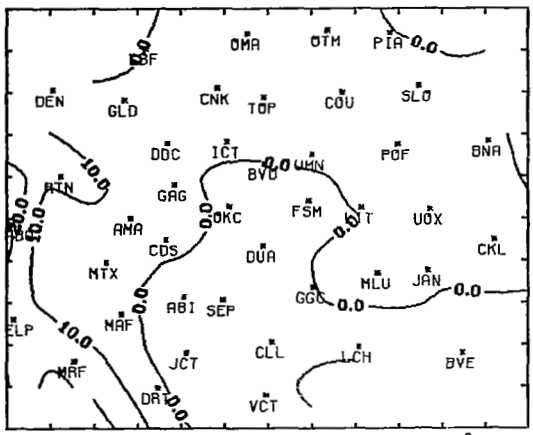

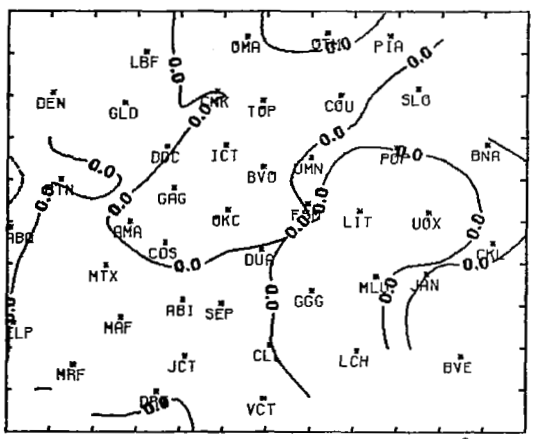

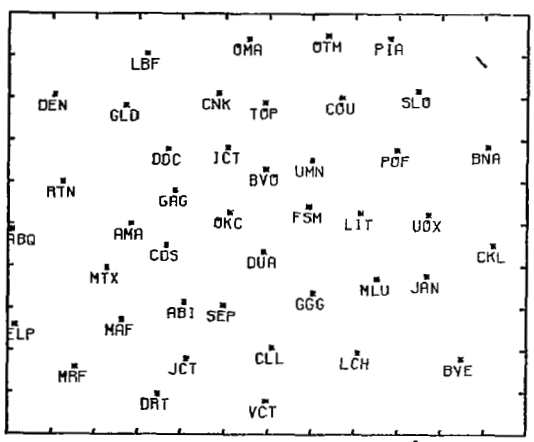

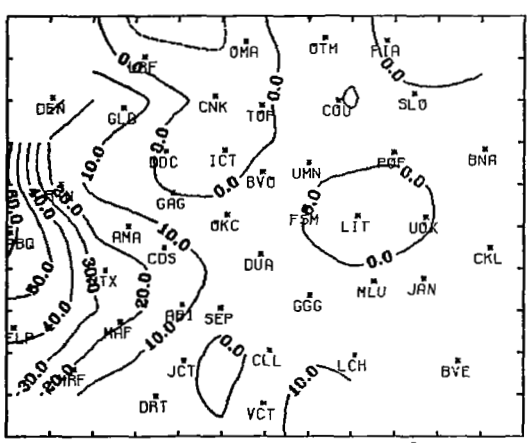

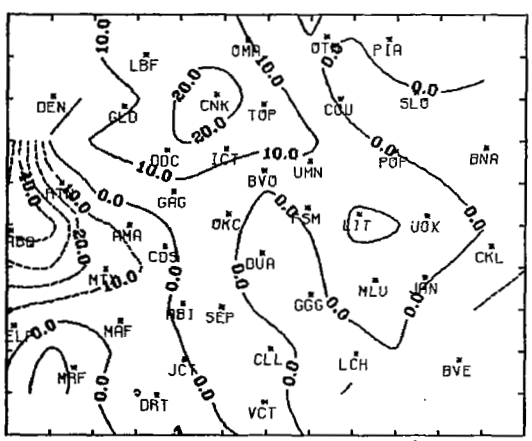

Fig. 33. Fields of terms in the vorticity equation at 850 mb for 1800 GMT 10 April 1979.

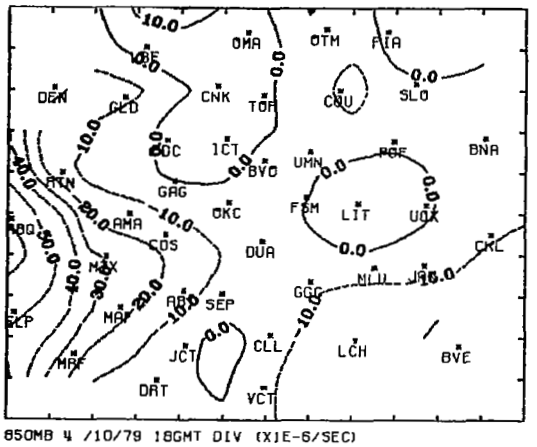

Fig. 34. Velocity divergence at 850 mb for 1800 GMT 10 April 1979.

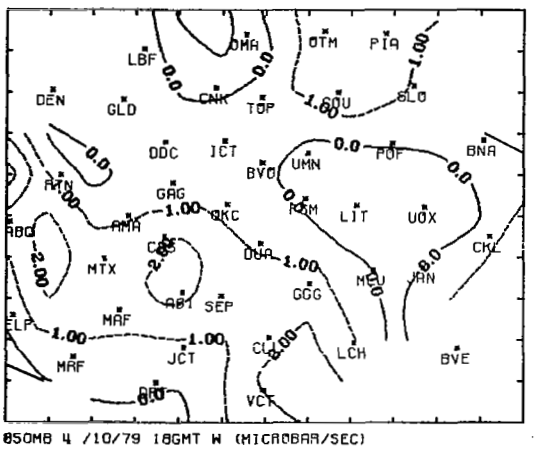

Fig. 35. Vertical motion, ω (μbars s^{-1}), at 850 mb for 1800 GMT 10 April 1979.

the horizontal advection and divergence terms, Fig. 36. The center of maximum $\frac{\partial \zeta}{\partial t}$ over RTN appears to be a measurement of increased vorticity near the low-pressure center at upper levels. Examination of the 700-mb wind fields in Fig. 37 shows anticyclonic turning of the flow from 1800 GMT to 2100 GMT in the northeast half of the region. The flow in this portion of the region at 1500 GMT (not shown) was less anticyclonic than the subsequent observations. This shift of the flow toward more anticyclonic curvature resulted in the widespread area of negative $\frac{\partial \zeta}{\partial t}$ over the same region.

The contoured field of divergence at this level exhibits a pattern similar to that of the velocity divergence, Fig. 38, with the center of convergence (positive values) near the upper level low and additional convergence in the warm sector ahead of the surface cold front approaching from the west as discussed regarding Fig. 10. There was an area of positive vorticity advection centered over CDS and ABI. This center of PVA corresponds to the position of strong vertical development which occurred by 2100 GMT and there was a small corresponding center of vorticity production by divergence which indicates development of convection. These two terms, however, are not related in this area by the approximate vorticity equation, Eq. (3), since the sign of the divergence term does not give the sign of the horizontal vorticity advection. Therefore, use of Eq. (3) would not have been appropriate in this case. The local change and residual terms were too large for Eq. (3) to be valid; they must be included in the vorticity budget.

At 500 mb, Fig. 39, the area of positive vorticity advection corresponds to divergence, which is manifested by the negative sign of the divergence term and this area delineates the area of convective development. This level was above the LND and Eq. (3) is applicable in order to determine the sign of the mid-tropospheric vertical motion. The relationship in this equation does not, however, accurately describe the budget of vorticity in this situation since the local change and residual terms cannot be neglected. The significant increase in relative vorticity over time at this level is a measure of the progression of the synoptic-scale cyclone. This maximum of $\frac{\partial \zeta}{\partial t}$ shows up as a maximum in R as a result of cancellation of the horizontal advection and divergence terms and the fact that $\omega\frac{\partial \zeta}{\partial p}$ and βv were negligibly small. The negative R centers near ABQ and MLU are due to the twisting/tilting effect.

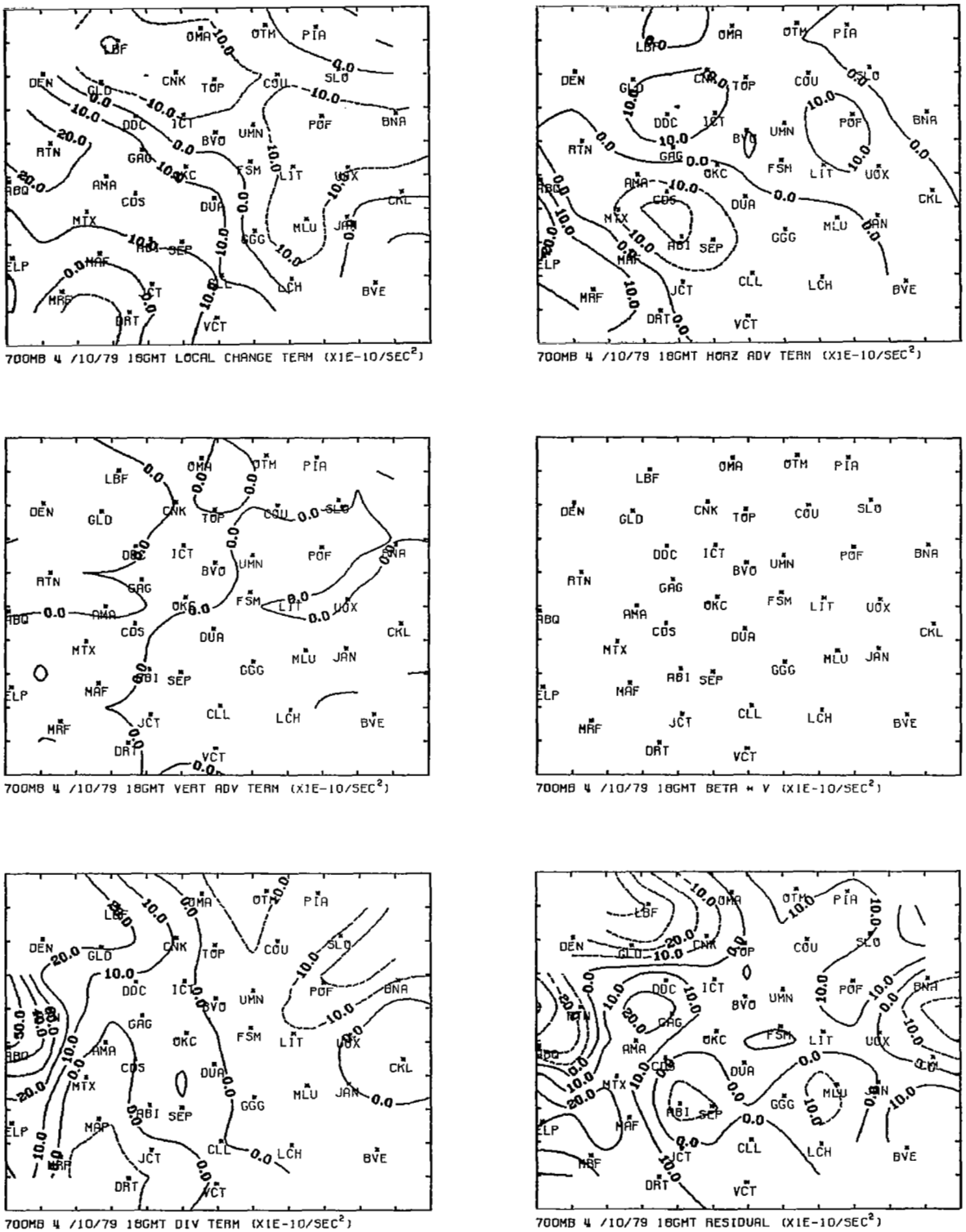

Fig. 36. Fields of terms in the vorticity equation at 700 mb for 1800 GMT 10 April 1979.

a)

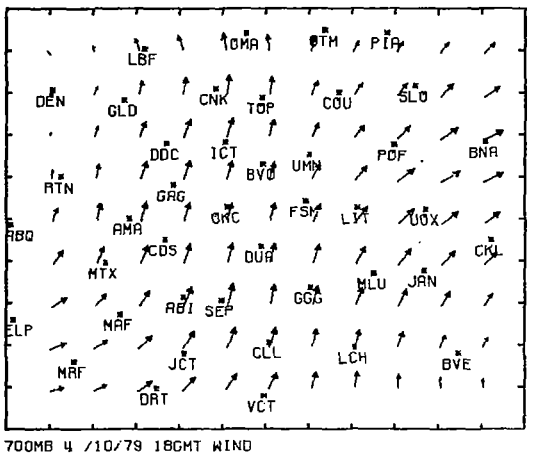

b)

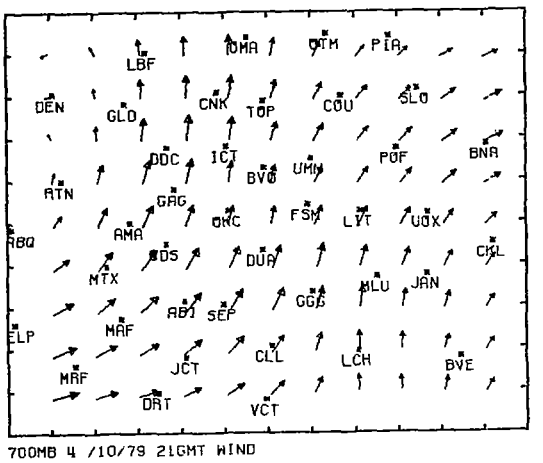

Fig. 37. Wind fields at 700 mb for a) 1800 GMT and b) 2100 GMT 10 April 1979.

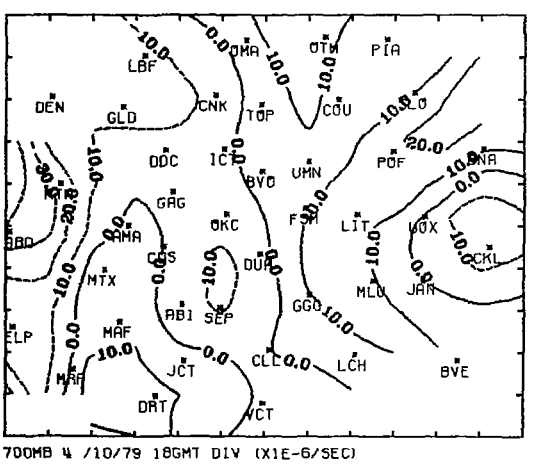

Fig. 38. Velocity divergence at 700 mb for 1800 GMT 10 April 1979.

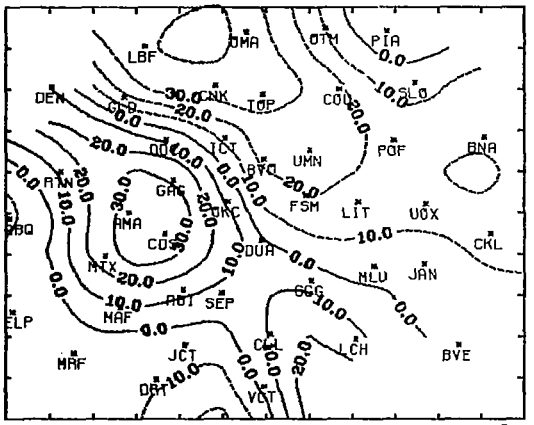

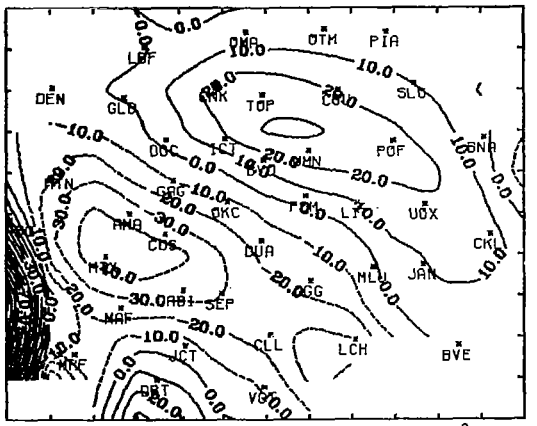

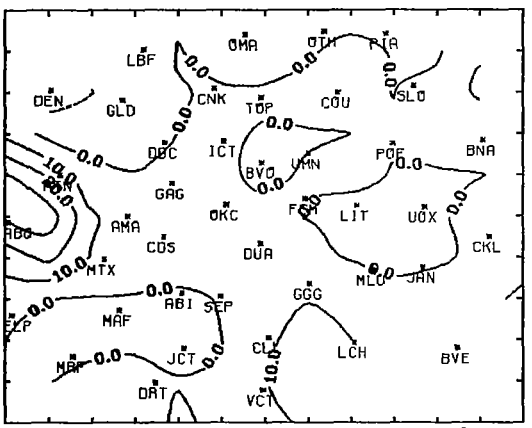

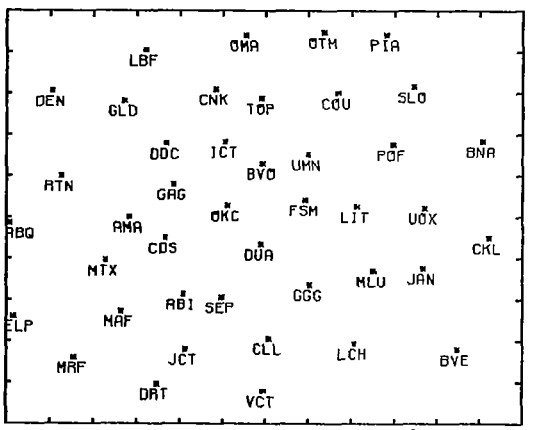

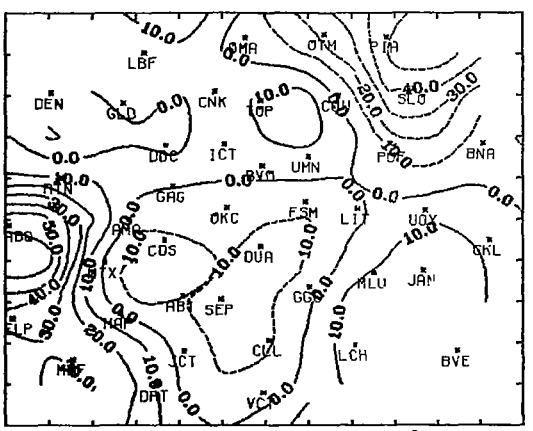

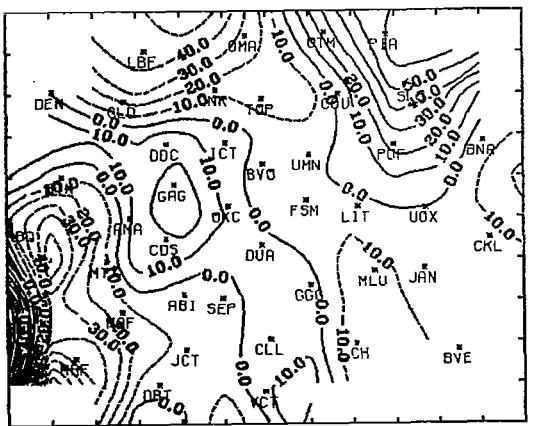

Fig. 39. Fields of terms in the vorticity equation at 500 mb for 1800 GMT 10 April 1979.

The situation at 300 mb, Fig. 40, was similar with regard to the comparable configuration of the horizontal advection and divergence terms with regions of positive vorticity advection corresponding to divergence and indicating positive vertical motion, Fig. 41, in the area of most intense convective activity. The $\omega\frac{\partial\zeta}{\partial p}$ and βv terms remained negligible while the $\frac{\partial\zeta}{\partial t}$ field was nearly the same except for an increase in the vicinity of GAG and CDS. Also, the residual, R, was significantly large as before.

2100 GMT 10 April 1979

At 850 mb, Fig. 42, the local change term increased since the previous observation over GAG where intensification and development of the convection continued. The horizontal and vertical advection and βv terms were as small as usual, with the exception of an area of negative vertical advection of relative vorticity by upward vertical motion. The divergence term indicates that convergence occurred in a region feeding into the convection and the residual is too large in magnitude to be considered negligible.

Figure 43 shows the same large center of $\frac{\partial\zeta}{\partial t}$ over GAG at 700 mb and the horizontal advection term had a moderate center of positive vorticity advection. The divergence term, however, did not reveal corresponding divergence, as in the approximate vorticity equation, Eq. (3), but rather convergence is to be expected at this level in an area of convective activity since the LND is assumed to be well above this level, which it is in this case. The βv term was once again small and remained so at the 500- and 300-mb levels. The vertical advection also remained small, except for a noticeable center of negative vertical advection over GAG, the position of the intense activity, where lower values of relative vorticity were advected upward by the positive vertical motion. The residual was a little more organized at this level with a large positive center in the vicinity of the activity. The vertical motion associated with the activity created a large gradient of vertical motion in the horizontal which contributed to a larger than usual R due to non-negligible twisting and tilting effects.

There was also a widespread area of large positive $\frac{\partial\zeta}{\partial t}$ with a negative area in the northeast at 500 mb, Fig.44. There was a large band of positive vorticity advection oriented from north-northwest to south-southeast and centered between OKC and DDC. As a result of the strong convective activity there was a center of negative divergence near CDS which indicates the occurrence of upper-level divergence.

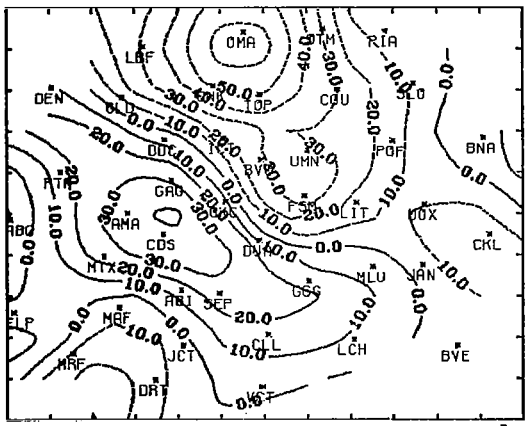

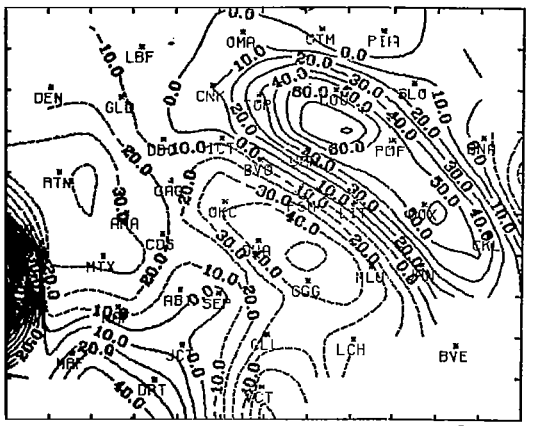

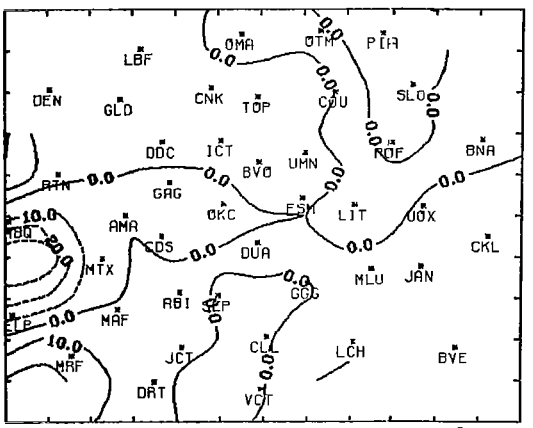

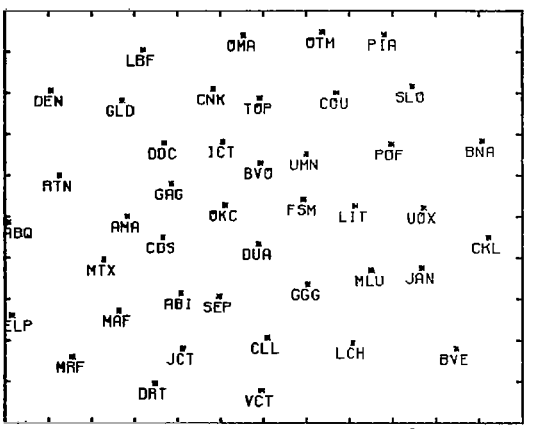

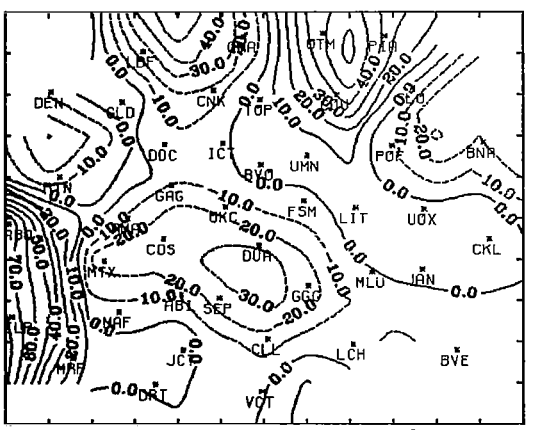

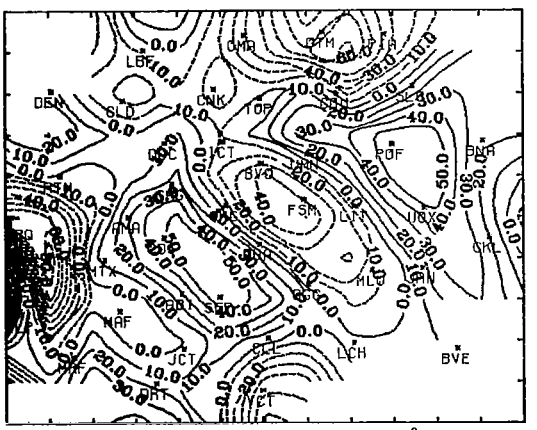

Fig. 40. Fields of terms in the vorticity equation at 300 mb for 1800 GMT 10 April 1979.

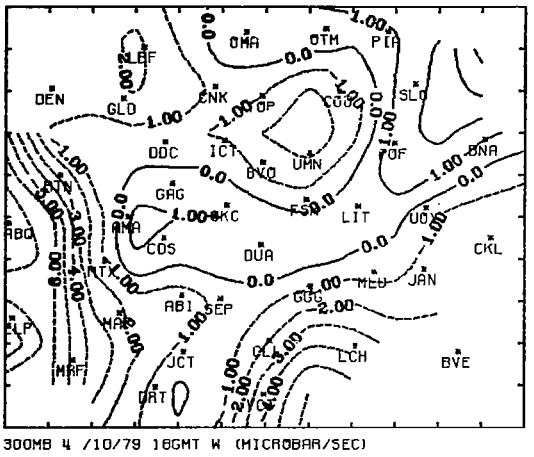

Fig. 41. Vertical motion, ω (μbars s^{-1}), at 300 mb for 1800 GMT 10 April 1979.

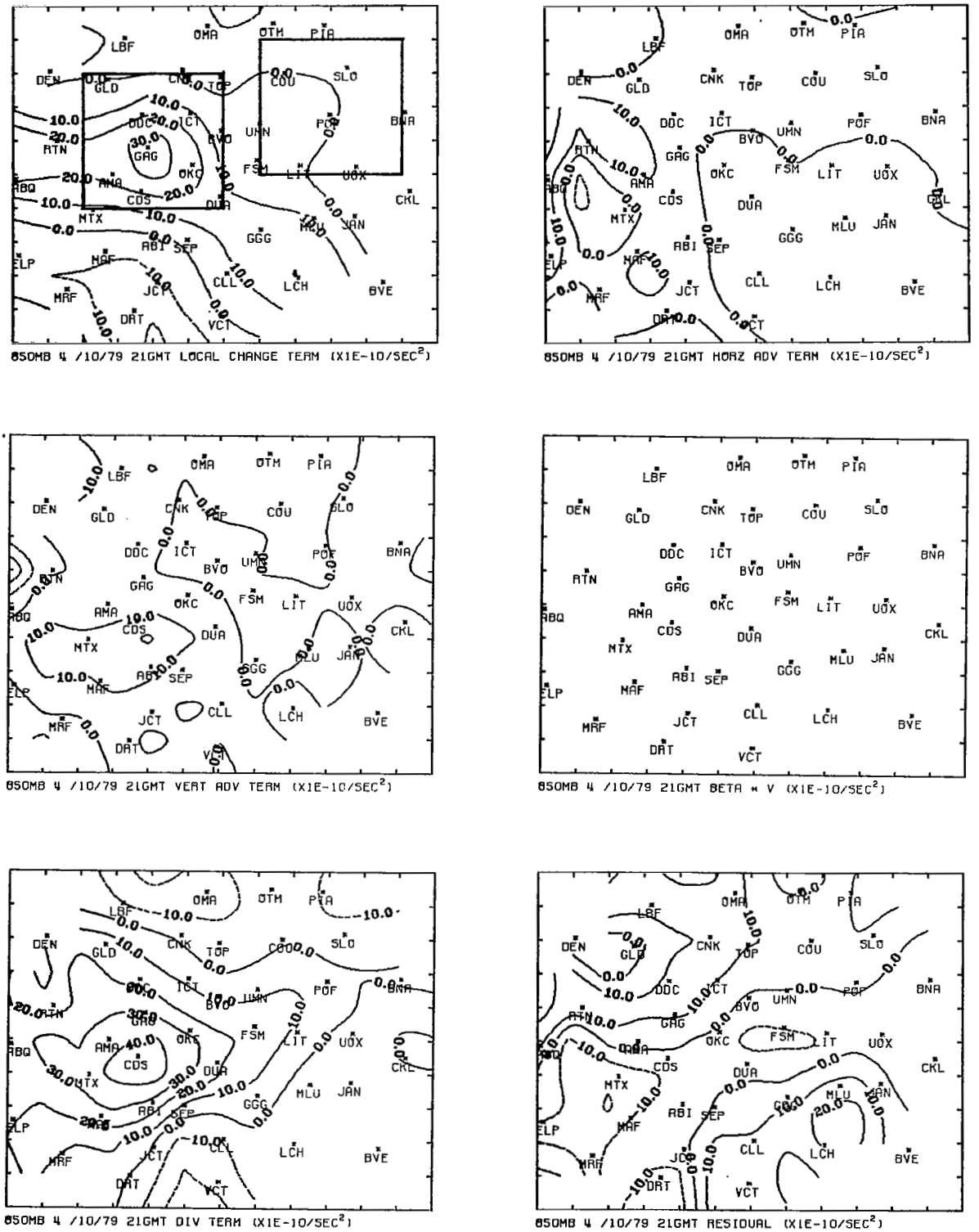

Fig. 42. Fields of terms in the vorticity equation at 850 mb for 2100 GMT 10 April 1979.

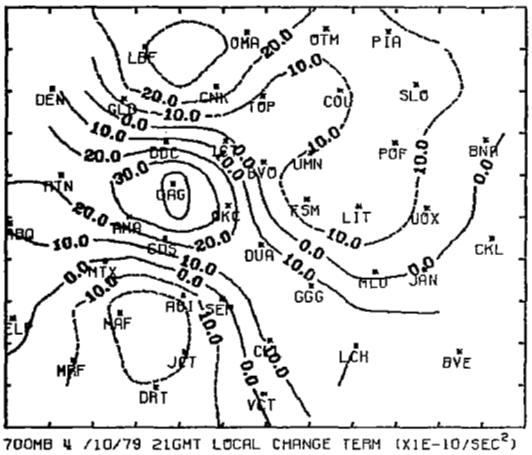

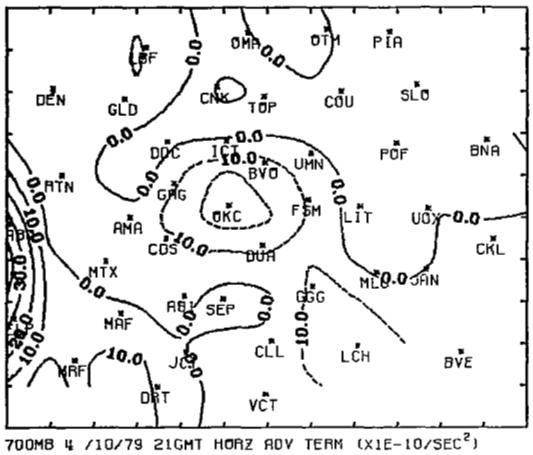

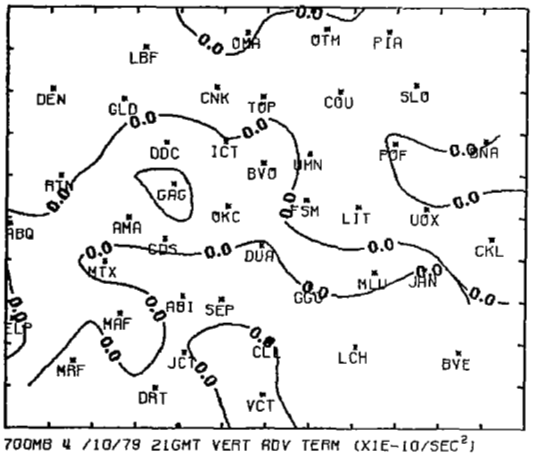

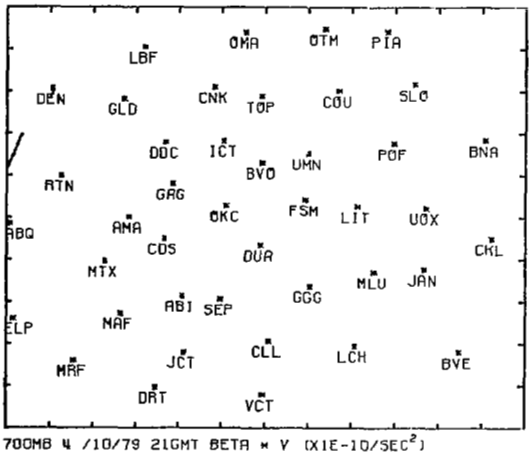

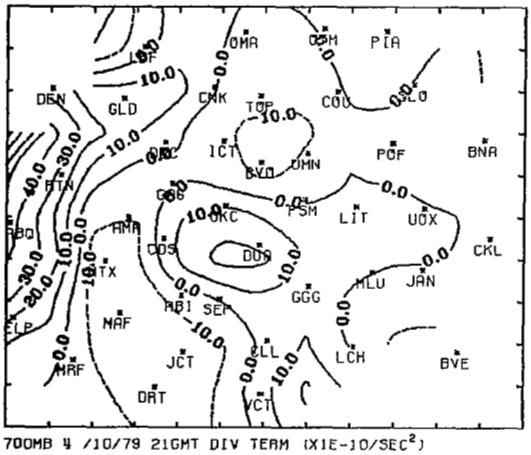

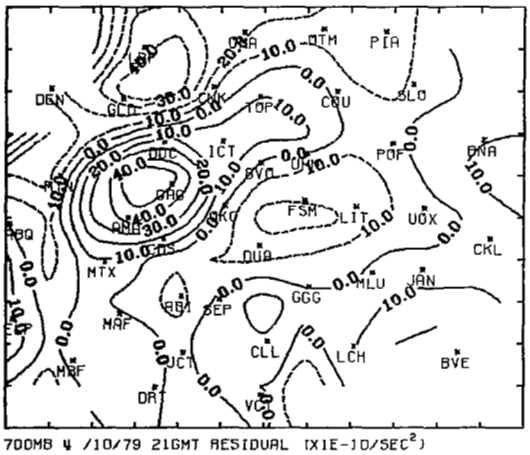

Fig. 43. Fields of terms in the vorticity equation at 700 mb for 2100 GMT 10 April 1979.

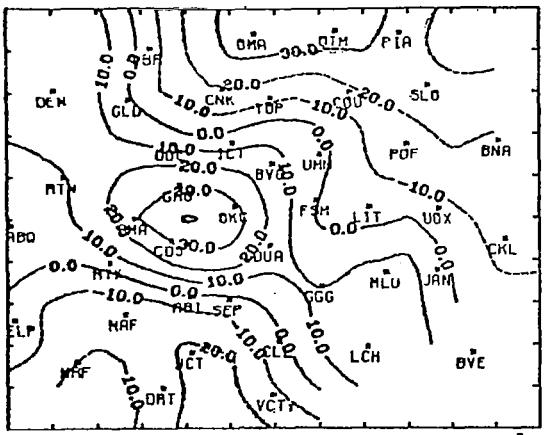

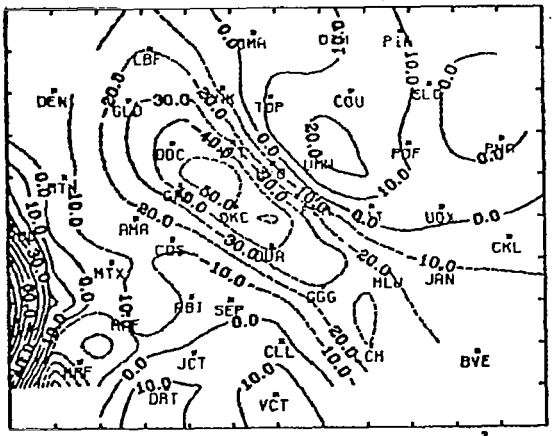

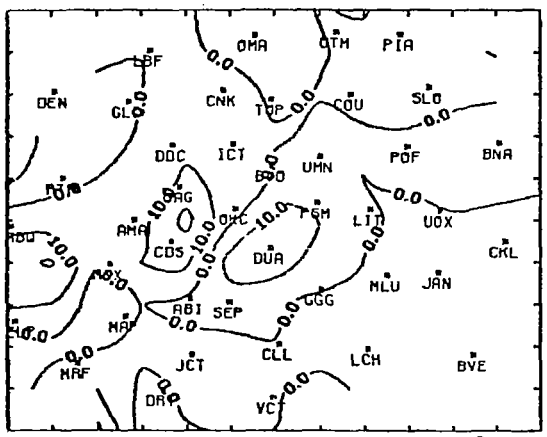

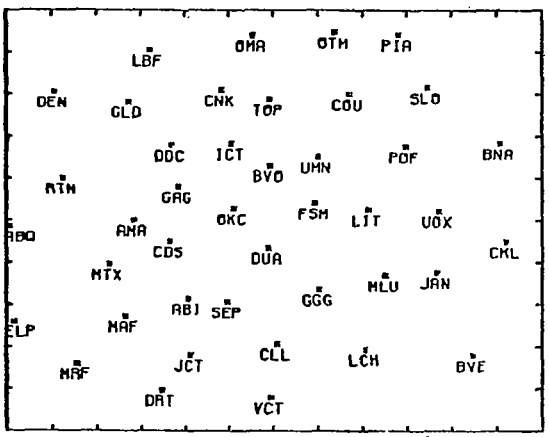

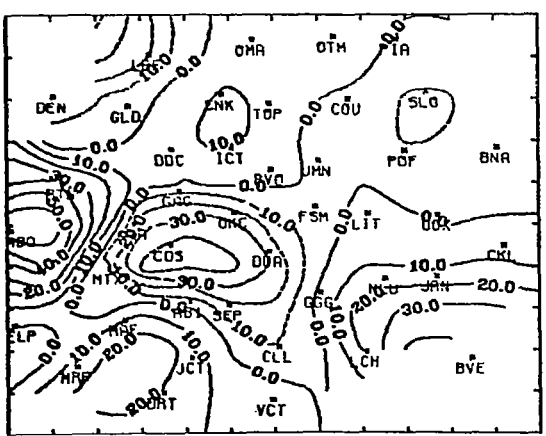

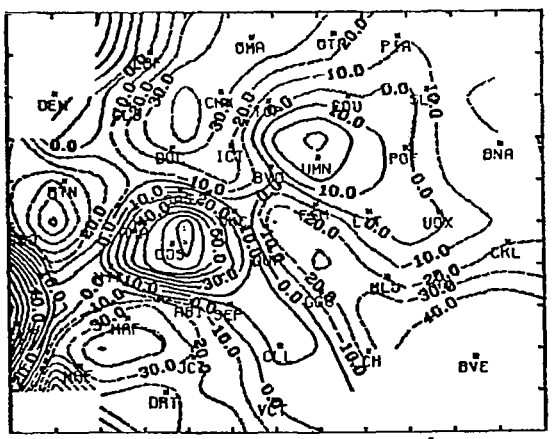

Fig. 44. Fields of terms in the vorticity equation at 500 mb for 2100 GMT 10 April 1979.

Such positive vertical motion resulted in negative vorticity being advected upward which shows up as a positive center of $\omega\frac{\partial\zeta}{\partial p}$ near GAG. The residual term was the largest in magnitude with two positive centers, one near CDS and one near UMN. Figure 45 shows a similar situation at 300 mb. The few exceptions included a position change for the center of negative vertical advection of relative vorticity (positive values) to FSM. The horizontal advection, divergence, and residual terms were all of very large magnitude, greater than at any of the other three levels.

0000 GMT 11 April 1979

At 850 mb, Fig. 46, the vertical advection and βv terms were negligibly small, as they were during the prior observation. In fact, the budget of vorticity here is very similar to that of 2100 GMT. The only difference in the contoured fields of terms in the vorticity equation was in location of maxima and minima which changed positions with the developing convective activity. Figures 47, 48, and 49 show the fields of terms in the vorticity equation at 700, 500, and 300 mb, respectively.

5.2. Vorticity Budget of Convective and Nonconvective Areas

Using NWS radar summaries, convective and nonconvective areas were selected for each time in both the AVE VII and AVE-SESAME I experiments. Each of these areas includes twenty-five grid points and is approximately 632 km on a side. The areas change position with time to follow the convective activity as it migrates across the area. These areas are outlined in the previously presented plot of the local change term corresponding to each observation time. The convective and nonconvective areas are labeled 1 and 2, respectively.

Each term in the vorticity equation was averaged arithmetically over these convective and nonconvective areas. Upon examination of these averages some similarities between the respective areas of the two experiments can be recognized.

5.2.1. AVE VII. The results for AVE VII are presented in Table 3. The 850-mb local time rate-of-change underwent steady increase over the six-hour period examined and the increase was coincident with the increase in convective activity in the area. At this level the horizontal advection and divergence terms had the greatest magnitude and the sign of the

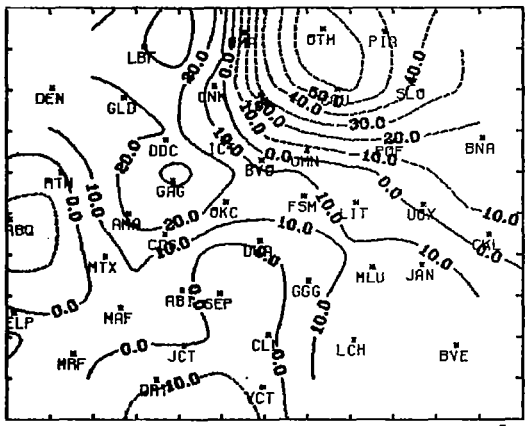

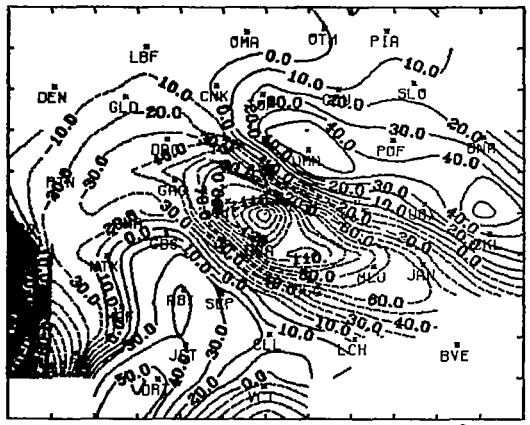

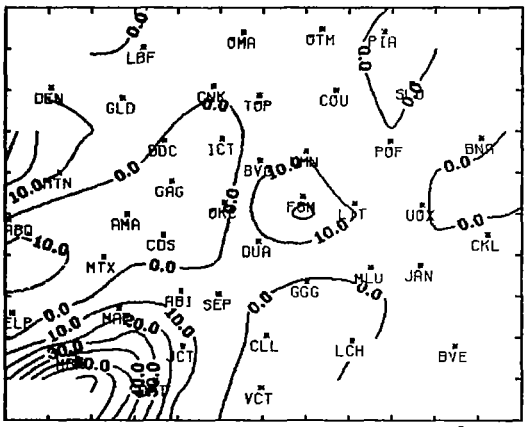

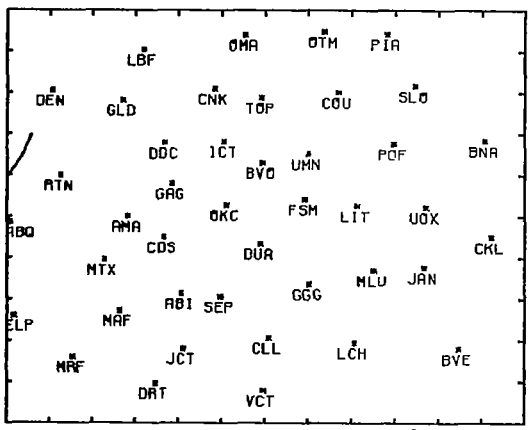

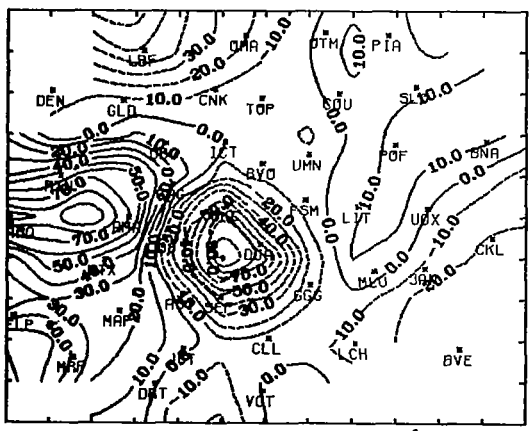

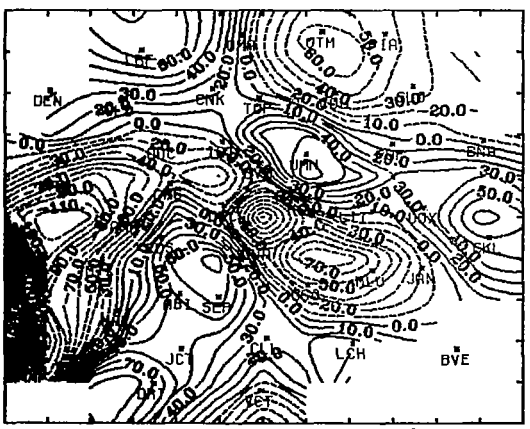

Fig. 45. Fields of terms in the vorticity equation at 300 mb for 2100 GMT 10 April 1979.

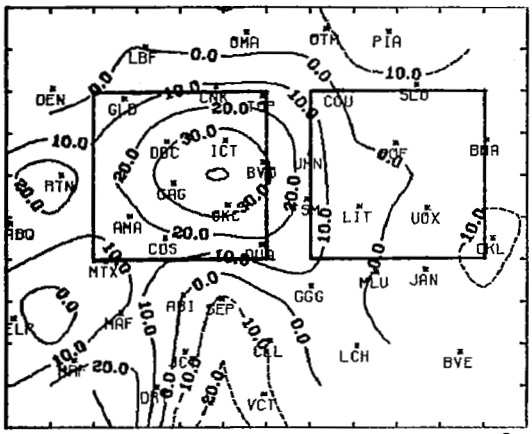

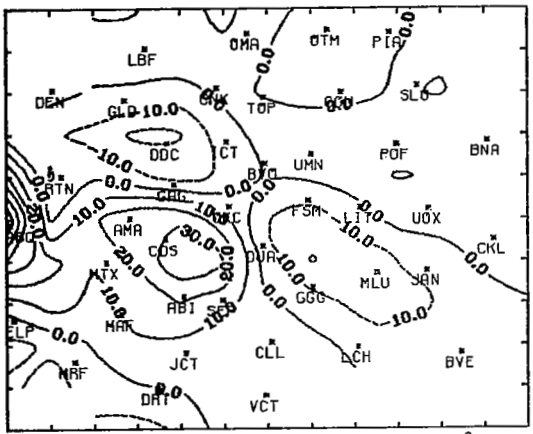

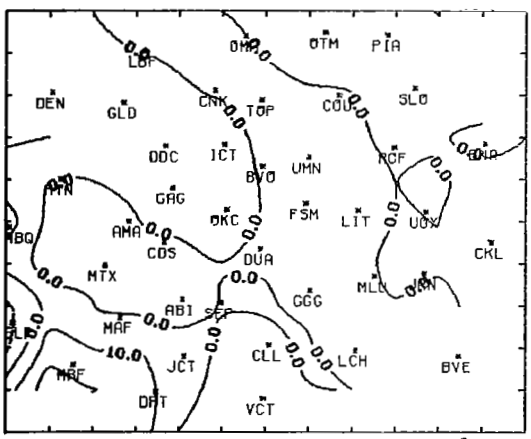

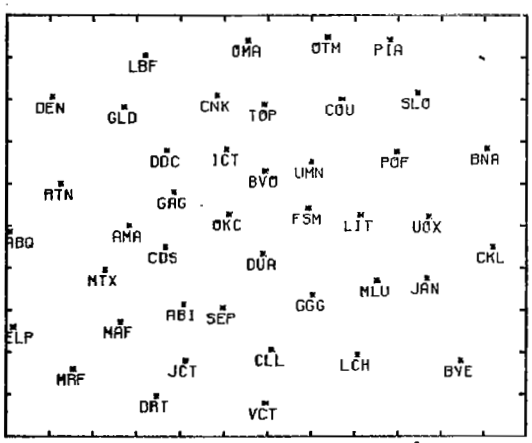

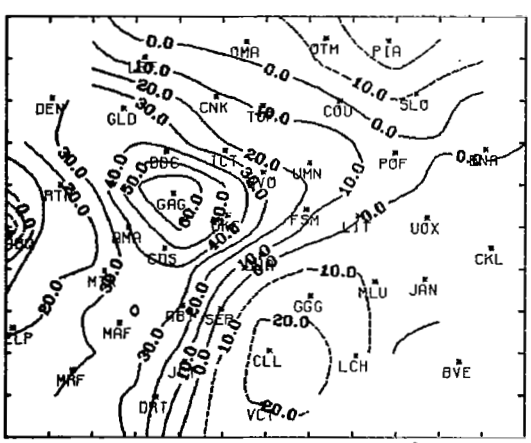

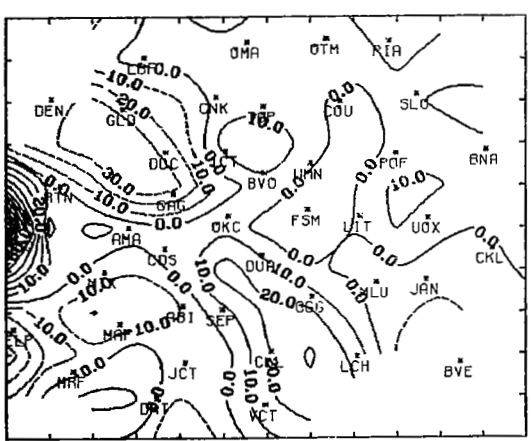

Fig. 46. Fields of terms in the vorticity equation at 850 mb for 0000 GMT 11 April 1979.

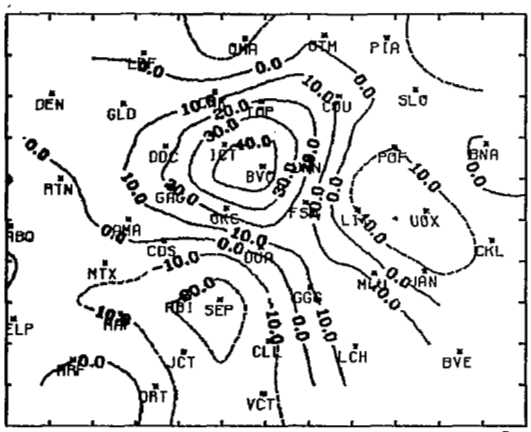

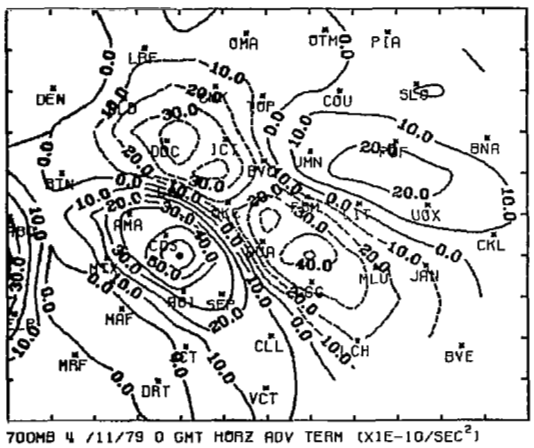

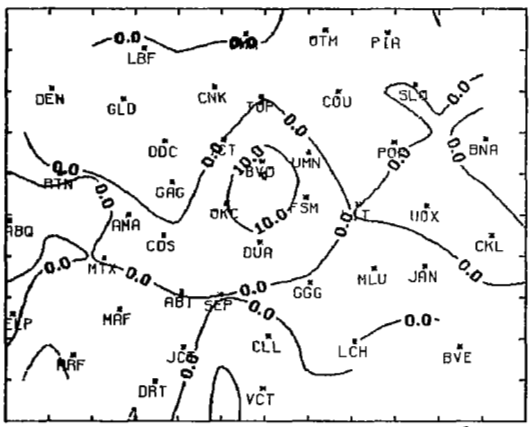

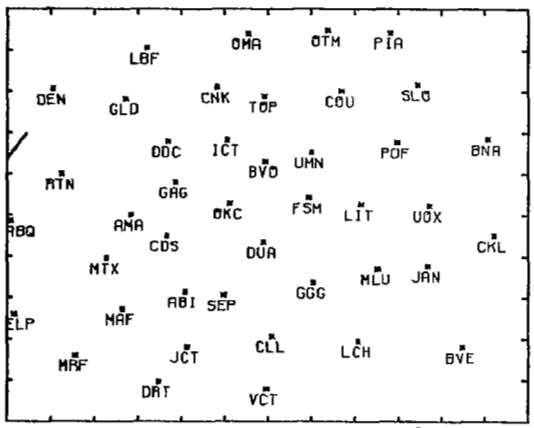

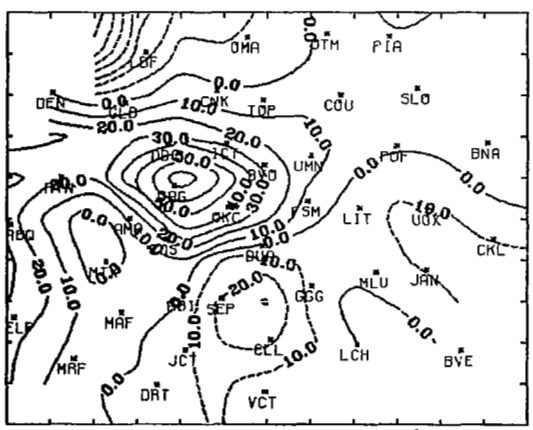

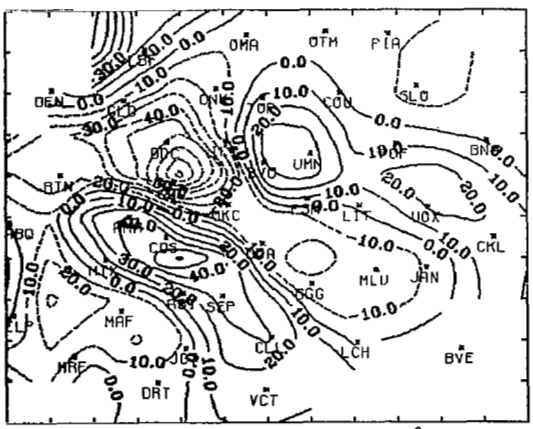

Fig. 47. Fields of terms in the vorticity equation at 700 mb for 0000 GMT 11 April 1979.

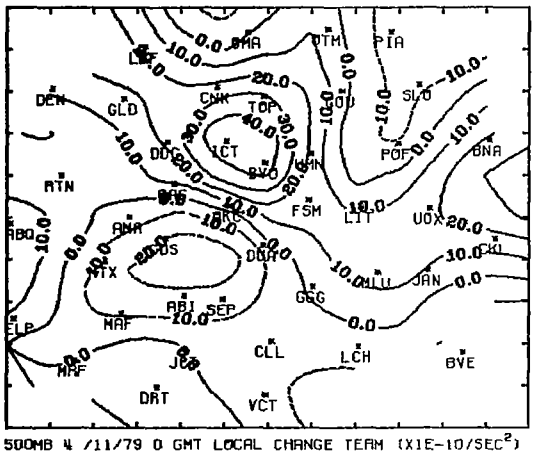

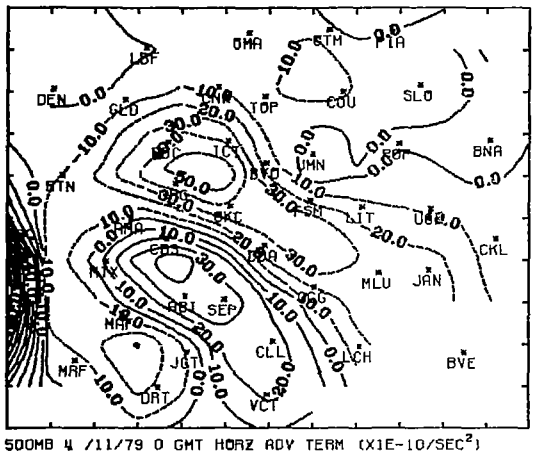

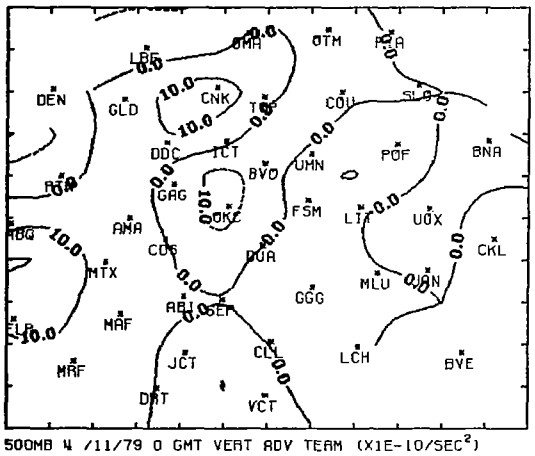

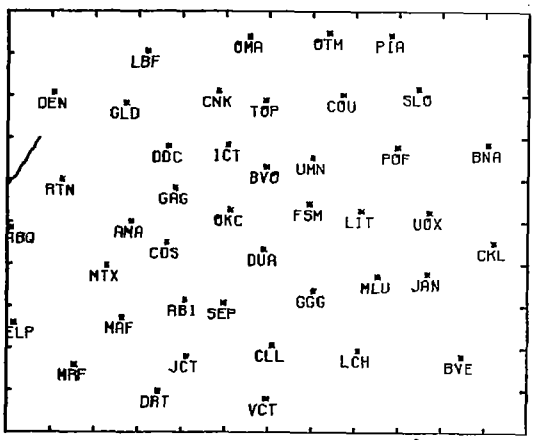

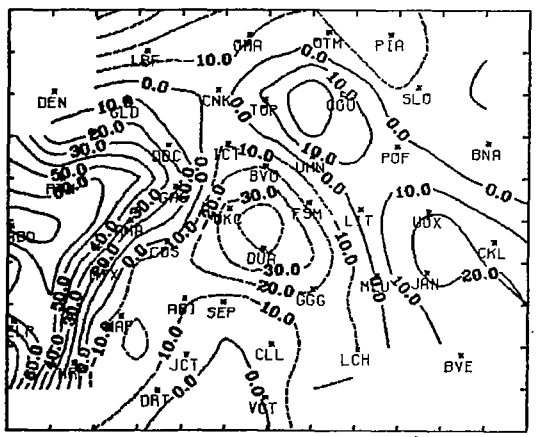

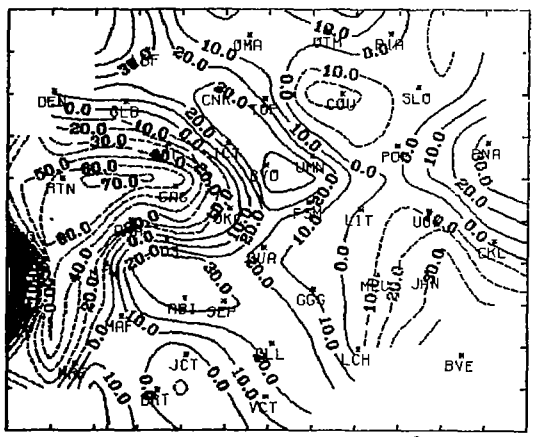

Fig. 48. Fields of terms in the vorticity equation at 500 mb for 0000 GMT 11 April 1979.

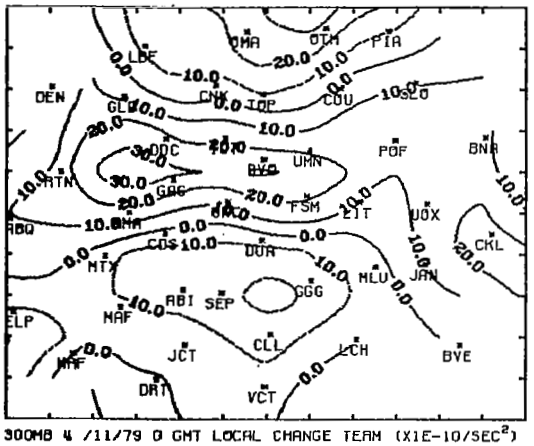

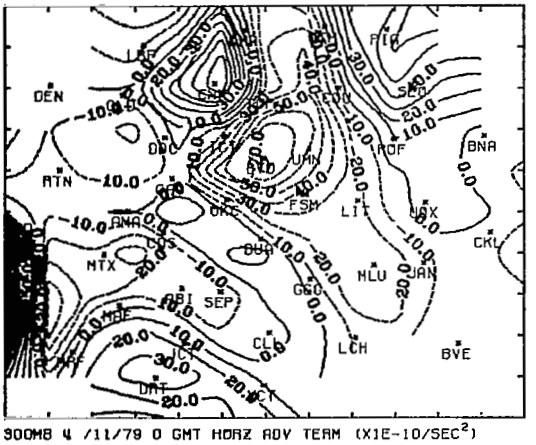

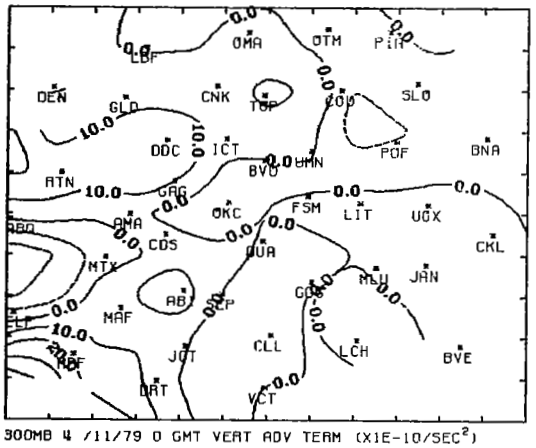

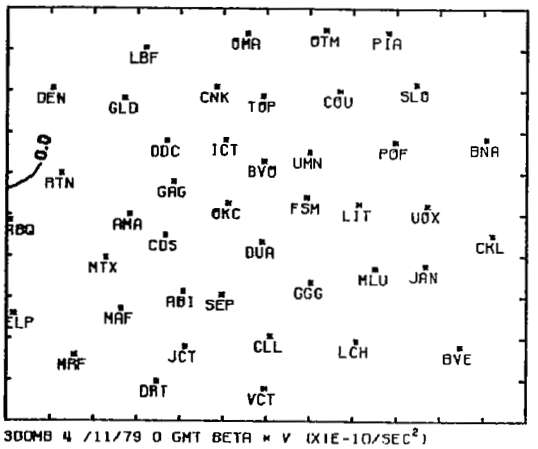

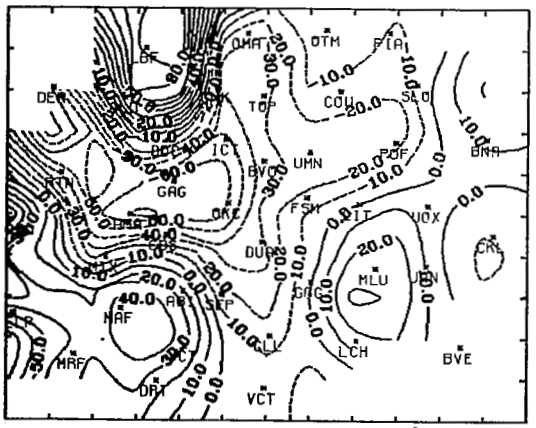

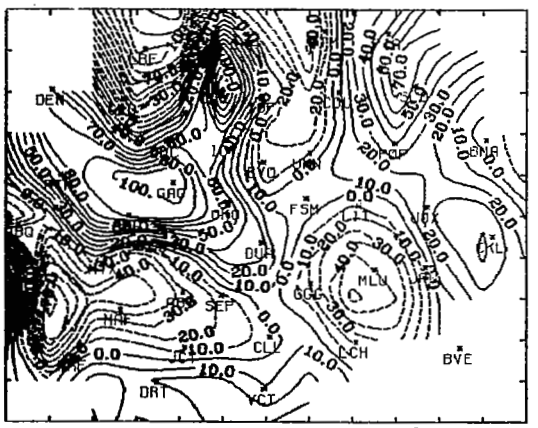

Fig. 49. Fields of terms in the vorticity equation at 300 mb for 0000 GMT 11 April 1979.

Table 3. Average values of terms in the vorticity equation for a convective (Area 1) and a nonconvective (Area 2) area during AVE VII. Units of 10^{-10} s^{-2}.

	Pressure (mb)	$\frac{\partial \zeta}{\partial t}$	$\vec{\nabla}_p \cdot \vec{\nabla}_p \zeta$	$\omega \frac{\partial \zeta}{\partial p}$	βv	$-(\zeta+f)\vec{\nabla}_p \cdot \vec{\nabla}_p$	R
			2100 GMT				
Area 1	850	5	8	1	1	9	5
	700	2	-5	-6	2	8	-14
	500	19	-4	5	3	16	6
	300	13	-28	4	4	-25	18
Area 2	850	-1	-0	-1	-1	-1	-2
	700	-2	1	-1	-0	-0	-2
	500	-3	-3	2	-0	-7	1
	300	-2	-1	-3	-0	-1	-5
			0000 GMT				
Area 1	850	14	9	1	0	23	1
	700	8	-2	2	2	12	-2
	500	14	-6	-5	3	8	-1
	300	2	-16	10	3	-19	18
Area 2	850	1	0	-1	-1	-3	3
	700	-2	1	-1	-1	-2	-1
	500	-1	3	1	-1	2	1
	300	1	22	3	-1	6	19
			0300 GMT				
Area 1	850	17	6	0	1	13	11
	700	9	-3	-6	1	6	-3
	500	4	-6	5	2	0	5
	300	6	-8	1	1	-13	14
Area 2	850	2	-0	-1	-1	1	-1
	700	-6	-0	-0	-1	-8	2
	500	-12	-2	1	-1	-0	-13
	300	-37	10	7	-1	21	-43

divergence term gave the sign of horizontal relative vorticity advection. This sign being positive, negative vorticity advection was occurring thereby implying upward vertical motion in the mid-troposphere. This could also have been deduced from the positive vorticity advection at 300 mb by Dine's compensation principle since PVA indicates that divergence was present. At the 300-mb level, the local change and residual terms were not negligibly small so Eq. (3) would not have been a good approximation of the vorticity budget. The horizontal advection and divergence terms were, however, approximately equal and use of Eq. (3), in the convective area (Area 1), would have resulted in the proper conclusion regarding the direction of vertical motion. That is, provided it was applied above the LND, which in this case was above 500 mb, not below, as per the usual assumption. Since the LND was above 500 mb it appears the usual application of the approximate vorticity equation at this level would not have been appropriate since PVA did not indicate convergence, as the table shows. Merely determining the sign of the horizontal advection term would indicate the sign of the mid-tropospheric vertical motion, but the magnitude of this term is small at this level compared to the divergence term as well as the local time rate-of-change. The poor relationship between the two terms of the approximate vorticity equation implies that a good estimation of the vertical motion might not have been reached.

In the nonconvective areas at 2100 GMT, the first noticeable feature was that the magnitude of all terms was small compared to those in the convective area indicating little or no development. Also, all terms were of the same order of magnitude with no one or two terms being dominant. At 300 mb, which was above the LND, the PVA was nearly thirty times smaller than that in the convective area and the vertical motion in this area was very small with no activity occurring.

At 0000 GMT, the divergence term was the largest and its sign indicates that convergence was occurring at 850 mb since ζ_a is nearly always positive. This large production of vorticity was manifested in the local change term which at this level indicates that development was occurring. Aloft, at 300 mb, PVA indicated positive vertical motion in the mid-troposphere, which was leading to this intensification of convective activity. Again, at this level, use of the approximate vorticity equation is applicable, but the residual term was the same order of magnitude as

$\frac{\partial \zeta}{\partial t}$ and $-\zeta_a \vec{\nabla}_p \cdot \vec{V}_p$ and its contribution to vorticity production could not have been neglected. The proper equation of vorticity for the middle layers would have a different form altogether. Here the local change term was large, not negligible by any means, compared to the others and the 700-mb divergence term indicated convergence at that level as it did at 500 mb. The residual term was small in the low and middle layers. The 0300 GMT convective area situation was very similar to that at 0000 GMT (Table 3).

The situation in the 0000 GMT nonconvective area was similar to that at 2100 GMT, except that strong NVA (negative vorticity advection) occurred above the LND at 300 mb. The conditions in the corresponding area at 0300 GMT were similar to 0000 GMT with NVA and convergence (determined by the sign of the divergence term) above the LND, which in the usual application of Eq. (3), indicates development would not have occurred in this area. Also, destruction of vorticity by the residual term was indicated by large negative values of $\frac{\partial \zeta}{\partial t}$ which, in turn, indicates that system development was not occurring but rather the opposite.

5.2.2 AVE-SESAME I. The results for AVE-SESAME I are presented in Table 4. In the convectively active areas (at all three observation times) the local change and horizontal advection terms are the most important. Both are similar in each case, with the $\frac{\partial \zeta}{\partial t}$ term at 850 mb increasing with time. Using the corresponding NWS radar summaries, more intense convective activity was indeed observed at 0000 GMT than at either of the earlier times.

The divergence term also was similar in each case for the convective area, with convergence indicated in the lower levels and divergence indicated aloft. Above the LND the PVA indicated divergence aloft. This was verified by a negative divergence term. Also, the divergence term underwent a large increase in magnitude from 1800 to 0000 GMT. This was accompanied by an increase in both the low level convergence and intensity of convective activity.

In the areas with no activity the sign of the local change term was negative (opposite that of the area of convection), but in the 0000 GMT case the sign had changed aloft and was becoming more positive at each level. This signifies development in or near this area. Also, the

Table 4. Average values of terms in the vorticity equation for a convective (Area 1) and a nonconvective (Area 2) area during AVE-SESAME I. Units of 10^{-10} s^{-2}.

	Pressure (mb)	$\frac{\partial \zeta}{\partial t}$	$\vec{V}_p \cdot \vec{\nabla}_p \zeta$	$\omega \frac{\partial \zeta}{\partial p}$	βv	$-(\zeta+f)\vec{\nabla}_p \cdot \vec{V}_p$	R
				1800 GMT			
Area 1	850	5	-0	1	3	10	-1
	700	10	-5	0	3	1	7
	500	13	-23	2	4	-3	-1
	300	14	-20	0	5	-13	12
Area 2	850	1	2	0	1	1	3
	700	-4	2	-0	2	-11	11
	500	-12	12	1	2	-22	25
	300	-13	20	-0	3	9	1
				2100 GMT			
Area 1	850	13	4	4	2	21	2
	700	9	-5	1	3	3	5
	500	13	-23	2	4	-7	3
	300	11	-30	1	5	-2	-11
Area 2	850	-3	1	-0	1	-0	-0
	700	-10	3	-1	2	-2	-4
	500	-16	6	0	2	-4	-5
	300	-23	20	3	4	4	-1
				0000 GMT			
Area 1	850	19	3	1	3	32	-6
	700	12	-4	1	3	18	-6
	500	10	-14	2	4	4	-3
	300	9	-10	5	6	-29	39
Area 2	850	-0	-0	-1	2	1	1
	700	-2	3	0	3	-0	4
	500	9	-9	1	3	5	-0
	300	11	-9	-1	4	-4	9

horizontal advection term was positive at 1800 and 2100 GMT (negative vorticity advection), but PVA occurred by 0000 GMT, again signifying development in or near the area. The divergence term in these areas at 1800 and 2100 GMT indicates divergence in the middle levels which is not conducive to strong development. The nature of this term changed, however, by 0000 GMT when new activity may have been developing.

A more schematic view of the features of the vorticity budget as well as variation of the terms with height is presented by means of a vertical profile of the terms in the expanded vorticity equation. The profiles for each observation time in AVE VII are presented in Fig. 50, and Fig. 51 shows the profiles for AVE-SESAME I. These graphs support the assumption that the $\frac{\partial \zeta}{\partial p}$ and βv terms are negligibly small compared to the other terms. These terms exhibit little variation with decreasing pressure.

Perhaps the most striking aspect of these profiles is the magnitude of the residual term, R, especially in the upper levels. Certain patterns were noted in the $\frac{\partial \zeta}{\partial t}$ and $\vec{V}_p \cdot \vec{\nabla}_p \zeta$ profiles. The local change term remained positive in the convective areas (labeled 1) and negative in the non-convective areas (labeled 2), except at 0000 GMT during AVE-SESAME I where $\frac{\partial \zeta}{\partial t}$ was positive, but less than in the convective areas. A possible explanation for this is that convective development may have been in the initial stages. The horizontal advection term exhibits the expected pattern of PVA aloft in the convective areas and NVA in the nonconvective areas. The divergence term underwent the greatest vertical change with convergence in the lower and divergence in the upper layers in the convective areas and vice versa in the nonconvective areas. One additional feature to note is the change in sign at 500 mb in the horizontal advection and divergence terms.

Included with the profiles of $\vec{V} \cdot \vec{\nabla}\zeta$, $\omega\frac{\partial \zeta}{\partial p}$, and $-\zeta_a \vec{\nabla} \cdot \vec{V}$ in Figs. 50 and 51 are the profiles presented by Esbensen, Tollerud, and Chu (1982) for these same terms. They did not present a vertical profile of $\frac{\partial \zeta}{\partial t}$ and their horizontal vorticity advection is for absolute vorticity and, therefore, includes the βv term which is presented separately in this study. The βv term has been found to be relatively small and thereby contributes little to horizontal advection of absolute vorticity. Therefore, Esbensen, Tollerud, and Chu's (1982) horizontal vorticity advection may be interpreted in the

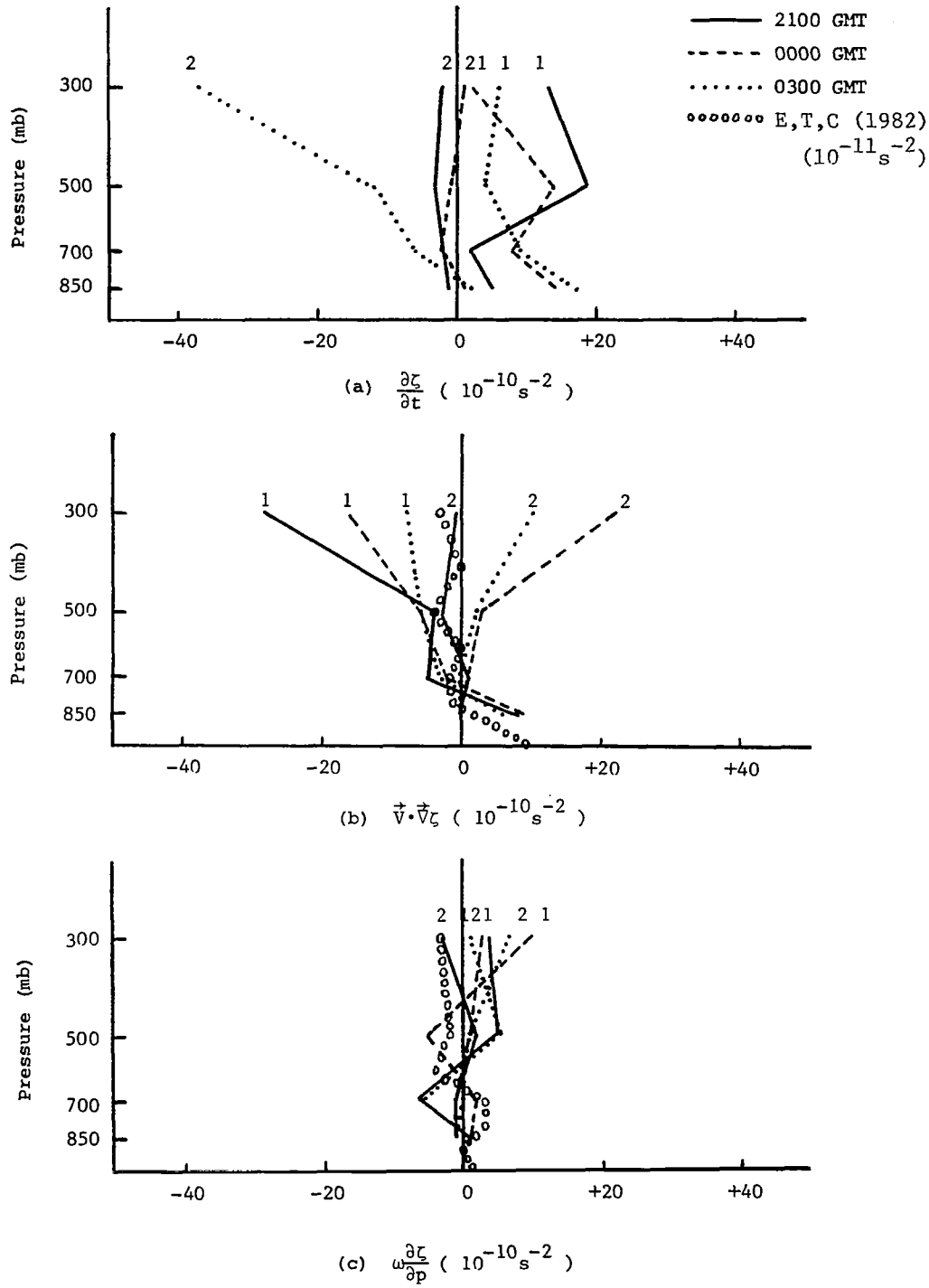

Fig. 50. Mean profiles of terms in the vorticity equation for the convective area (1) and nonconvective area (2) of AVE VII. Also, mean profiles of all categories of an easterly wave as determined by Esbensen, Tollerud, and Chu (1982), (E,T,C).

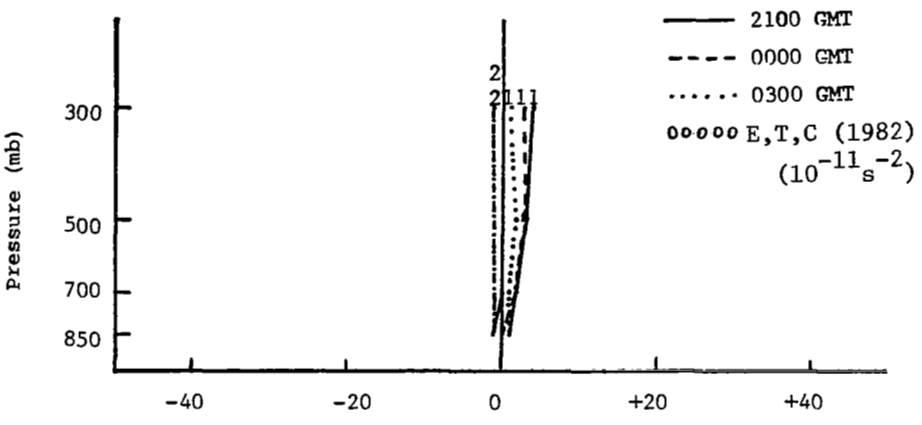

(d) βv ($10^{-10}s^{-2}$)

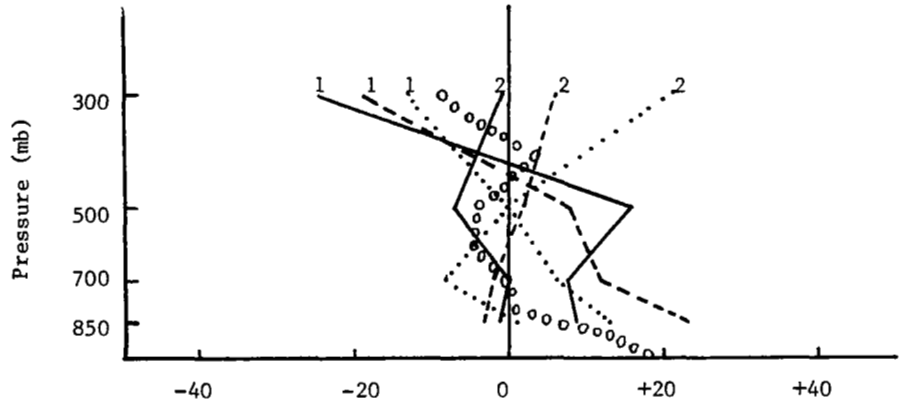

(e) $-\zeta_a \vec{\nabla} \cdot \vec{V}$ ($10^{-10}s^{-2}$)

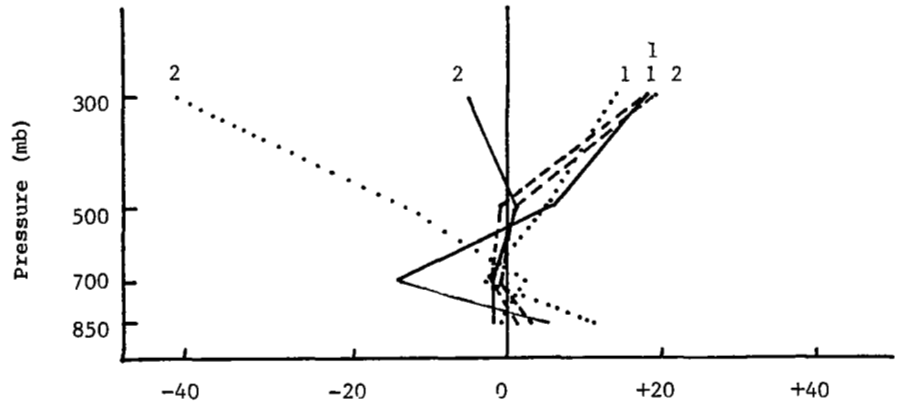

(f) R ($10^{-10}s^{-2}$)

Fig. 50. Continued.

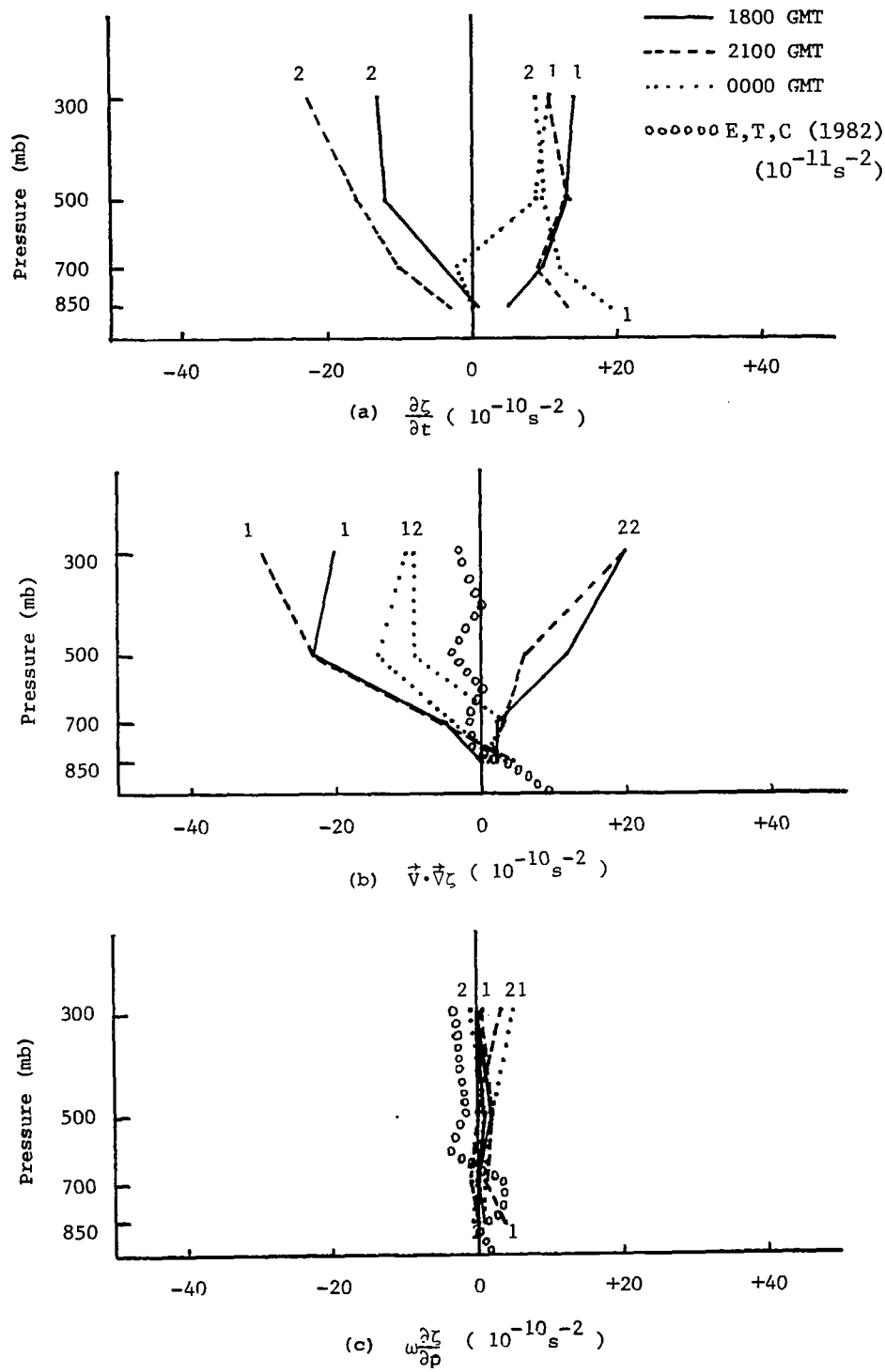

Fig. 51. Mean profiles of terms in the vorticity equation for the convective area (1) and nonconvective area (2) of AVE-SESAME I. Also, mean profiles of all categories of an easterly wave as determined by Esbensen, Tollerud, and Chu (1982), (E,T,C,).

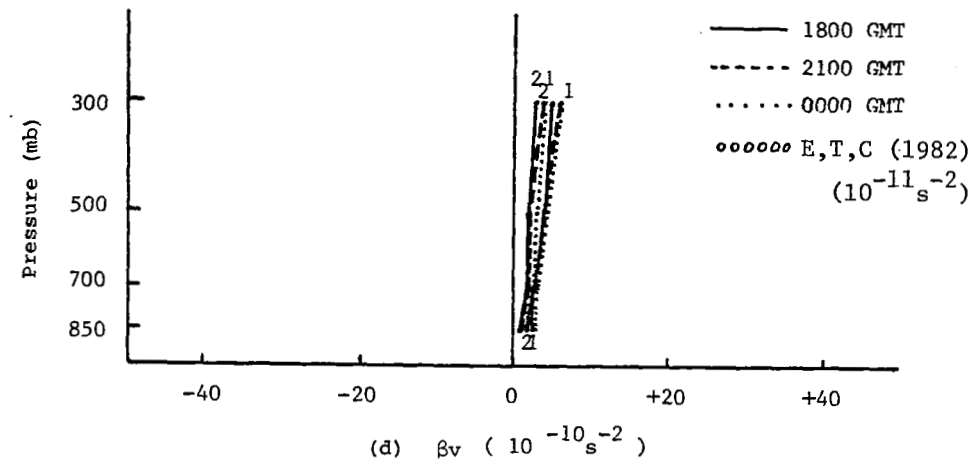

(d) βv ($10^{-10}s^{-2}$)

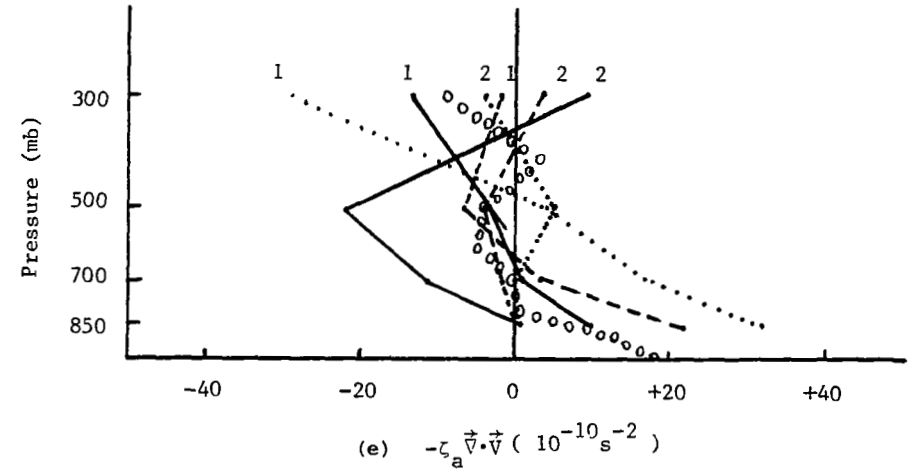

(e) $-\zeta_a \vec{\nabla}\cdot\vec{V}$ ($10^{-10}s^{-2}$)

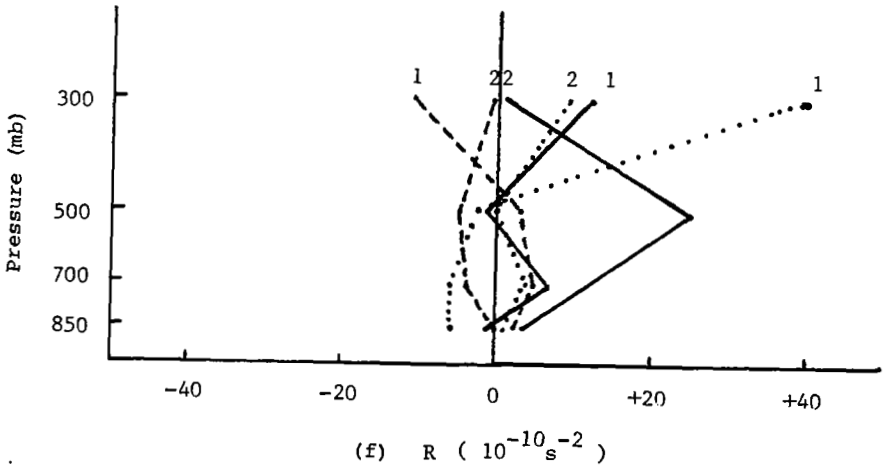

(f) R ($10^{-10}s^{-2}$)

Fig. 51. Continued.

same manner as the horizontal advection of relative vorticity presented in the present study. Although each profile is plotted on the same scale as that of the present study, the values obtained by Esbensen, Tollerud, and Chu (1982) are actually smaller by an order of magnitude.

The profiles taken from Esbensen, et al. and presented in Figs. 50 and 51 represent conditions averaged over a complete tropical wave and, therefore, represent neither convective nor nonconvective conditions. The comparison of their profiles with those for the present study is remarkable inasmuch as theirs tends to be intermediate to those representing convective and nonconvective conditions.

Profiles for the various terms in the vorticity budget presented above represent averages over 25 grid points (632 km on each side) for each convective and nonconvective area at each time for each data set. Large differences in the profiles are evident which apparently result from different effects from the convective activity and sampling variations. In order to reduce these effects, all the profiles of the residual for convective and nonconvective areas were each averaged and are presented for comparison in Fig. 52 along with profiles of the residual taken from Reed and Johnson (1974). Reed and Johnson's results are for trough and ridge conditions in a tropical wave while profiles for the present research represent conditions associated with and without convective activity (with and without radar echoes) at mid-latitudes. The magnitude of the residual differs by an order of magnitude (those in the present research are larger than those of Reed and Johnson), but the trend with altitude is consistent. In convective areas for both AVE VII and AVE-SESAME I, the residual is small in magnitude and tends to be negative (a sink for vorticity) in the lower troposphere, and positive in the upper troposphere (a source for vorticity). The same trend is shown in the Reed and Johnson profiles with the change from negative to positive occurring at about 300 mb rather than 500 mb as in our profiles. For the nonconvective areas, our profiles tend to show a greater tendency toward more positive (or less negative) values in the lower troposphere compared to the convective profiles, and more negative (or less positive) in the upper troposphere compared to the convective profiles. These same trends are present in the Reed and Johnson profiles. In the present study, the residual represents the sum of all terms on the right-hand side of Eq. 5, and it appears that the Reed and Johnson residual represents the same terms.

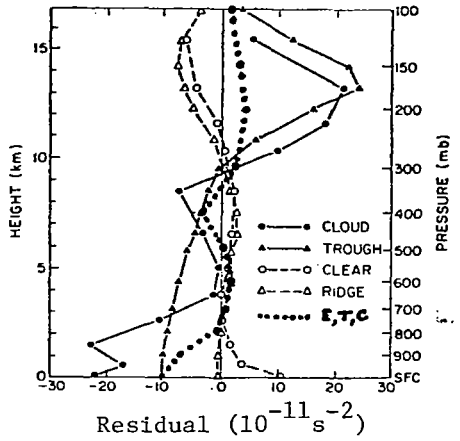

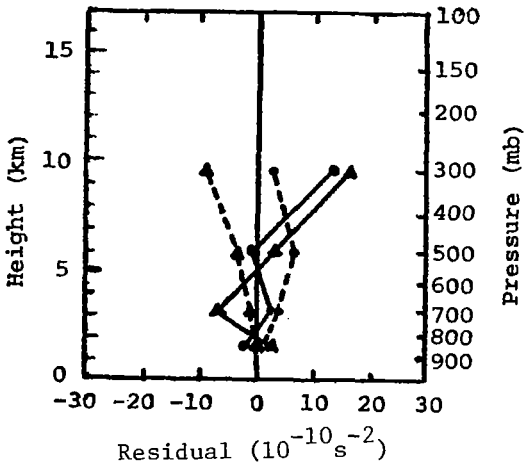

From Reed and Johnson, 1974

Reed and Johnson - Δ
Williams (1970) - o
Esbensen et al. (1982) - ···

Convective	AVE VII	▲—▲
	AVE-SESAME I	●—●
Non-Convective	AVE VII	▲---▲
	AVE-SESAME I	●---●

Fig. 52. Vertical profiles of the residual compared with similar profiles taken from Reed and Johnson (1974), and Esbensen, Tollerud, Chu (1982).

Figure 52 also shows the residual profile presented by Esbensen, Tollerud, and Chu (1982). Their result, which was also found using data for a tropical wave, is an arithmetic average over the eight wave phase categories for which they performed their vorticity budget analysis. As in the case of Reed and Johnson (1974), the values are an order of magnitude smaller than those of the present study, but the profile remains similar.

5.3. Interpretation of the Vorticity Budget

As previously discussed under Theoretical Considerations, the vorticity equation is not usually applied in its complete extended form. Instead, an approximate vorticity equation is used for forecasting purposes, in which most of the terms of the complete equation are neglected. Thus, the form of the equation normally used is

$$\vec{V}_p \cdot \vec{\nabla}_p \zeta \simeq -\zeta_a \vec{\nabla}_p \cdot \vec{V}_p ,$$

but in the cases examined here it was noted that those terms usually considered negligible were not consistently smaller by an order of magnitude or more than the predominant terms. Therefore, the question arose as to whether or not the above equation is universal on the synoptic scale. The answer appears to be no since in the cases considered here vorticity production by the residual term is the same order of magnitude as that by the divergence term. The sign of the divergence term does, however, give the sign of the horizontal vorticity advection when the above equation is applied above the LND (in these cases at 300 mb and not 500 mb). But vorticity production by the residual must still be accounted for. A new approximate vorticity equation might be suggested in the form

$$\vec{V}_p \cdot \vec{\nabla}_p \zeta \simeq -\zeta_a \vec{\nabla}_p \cdot \vec{V}_p + R ,$$

but vorticity production by R may not be manifested in the horizontal advection term. In fact the local time rate-of-change and vertical advection terms are sometimes important and the increased vorticity due to production by R may be found in these terms. The twisting/tilting terms in the vorticity equation are usually considered to be small, and thus are neglected when considering vorticity production on the synoptic scale. In this analysis, these terms were included in the residual term and it has been shown that R was not negligible but played a significant role in the vorticity budget, especially in the mid- and upper- levels of the convective areas. The contributors to R, other than the twisting/tilting terms, were the effects due to friction and computational error as a result of the finite differencing process. It was assumed that these effects would be negligible and that the R term would be a measure of the twisting/tilting effects. Therefore, whenever a large value of R (of the same magnitude as the largest term in the budget) was noted, it was assumed to be a result of large horizontal gradients in the vertical motion field which resulted in significant vorticity production due to twisting/tilting.

Therefore, in some cases, the vorticity budget above the LND would be better approximated by an equation other than Eq. (3). This approximation would include vorticity production by the residual term. Also, in the lower levels of convectively active areas the residual term contributed significantly to the vorticity budget. Specifically, it shows up in the local

time rate-of-change. In the areas with no convective activity, the residual also had large magnitude in the upper levels, but was negative in sign. Therefore, synoptic-scale vorticity destruction rather than production occurred. This was manifested by the significant negative local change term.

Petterssen (1956) and others have suggested using the local time rate-of-change of relative vorticity as a tool for measuring the development of synoptic-scale cyclones and anticyclones. This idea was tested in the upper levels here by comparing the contoured relative vorticity field with the 500-mb flow pattern and noting changes in the two with time.

Figure 53 shows the 500 mb contoured fields of relative vorticity for 2100, 0000, and 0300 GMT during AVE VII and the corresponding 500-mb contours are shown in Fig. 54. These fields were computed to ascertain the relationship of ζ to the flow pattern and the relationship between changes in the relative vorticity and trough development. It can be seen that maximum relative vorticity occurred where cyclonic curvature of the height contours was a maximum and where the curvature was anticyclonic the relative vorticity was a minimum. This was true for the three observation times shown. The interesting point, however, is as the maximum relative vorticity progressed downstream the magnitude of the local change term increased in the area of the new vorticity maximum. It was this increase in relative vorticity, or large $\frac{\partial \zeta}{\partial t}$, that delineated the area of trough or cyclonic development. In this case the downstream progression of the 500-mb trough was preceeded by a maximum in the local change term.

a)

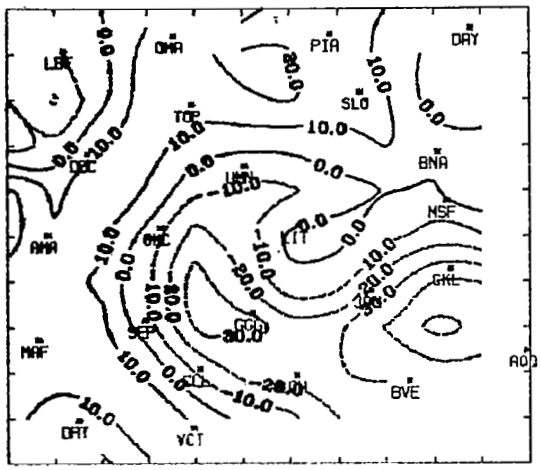

b)

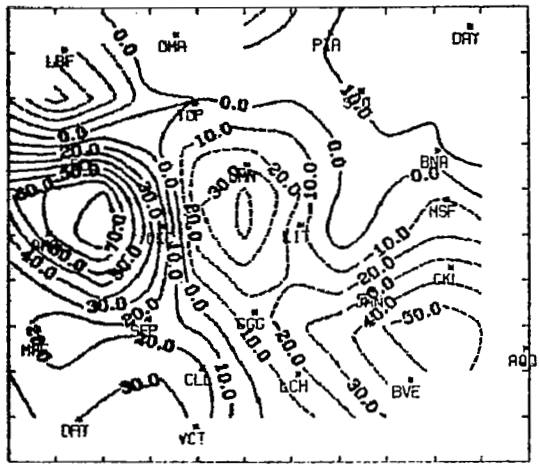

c)

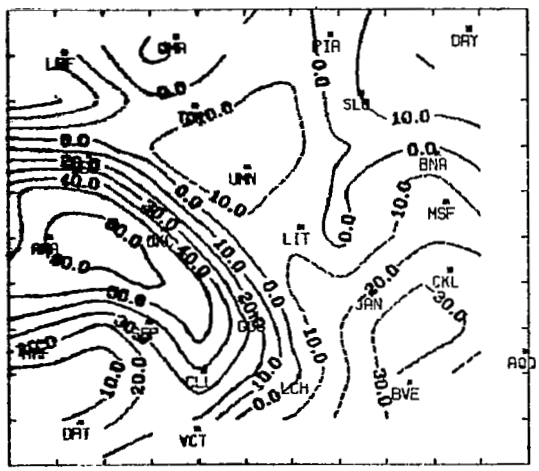

Fig. 53. Relative vorticity at 500 mb for a) 2100 GMT 2 May 1978, b) 0000 GMT 3 May 1978, and c) 0300 GMT 3 May 1978.

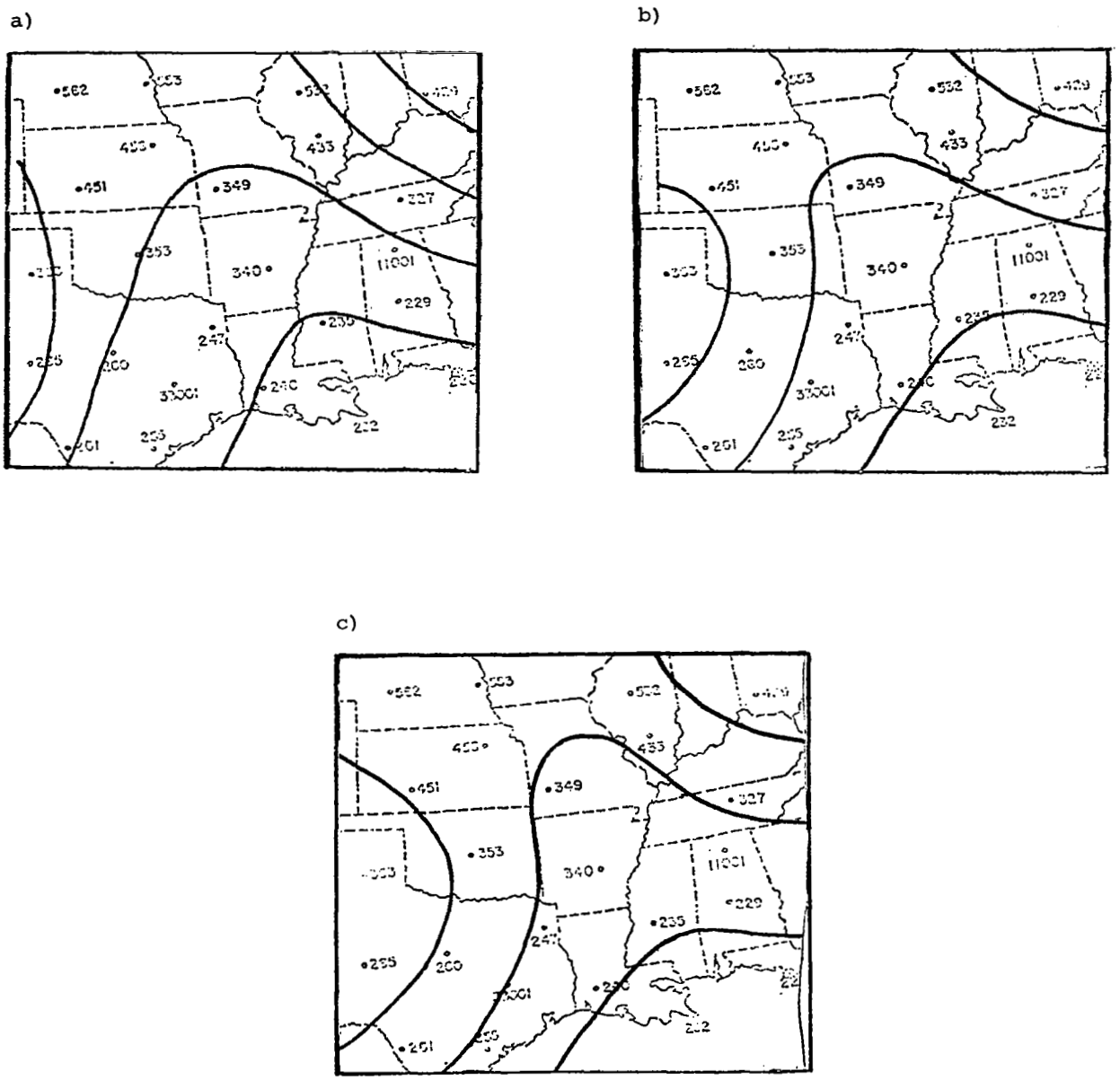

Fig. 54. Height contours at 500 mb for a) 2100 GMT 2 May 1978, b) 0000 GMT 3 May 1978, and c) 0300 GMT 3 May 1978.

6. CONCLUSIONS

The results of this research lead to several conclusions concerning the synoptic-scale vorticity budget in areas of convective activity. The first of these is that the synoptic-scale vorticity budget is influenced by convective activity. Usually only those terms in the vorticity equation which are significant on the synoptic scale are considered. The following conlusions tell how the synoptic-scale vorticity budget is influenced by convective activity.

First, the R term in both AVE VII and AVE-SESAME I was of comparable magnitude as the horizontal advection and divergence terms although it is usually assumed to be small. The results clearly demonstrate that this term cannot be neglected in vorticity budget analyses. The study included regions of developing and already developed convection. Thus, there were large horizontal gradients of vertical motion, ω, between the convection and surrounding areas. This led to large residuals in the budget of vorticity since R contains the twisting and tilting terms along with the frictional effects and computational error. These latter two sources of R are believed to be small in the present study.

The assumption that the simplified vorticity equation may be represented as a balance between the advection and divergence terms is not realistic, although the vorticity budget above the LND (above 500 mb in convective regions) suggests a close relationship between those terms. In convective areas, the residual term represented a sink for vorticity below 500 mb and a source above. In nonconvective areas, the residual term was either slightly negative or positive in the lower troposphere, and was near zero or negative (vorticity sink) at 300 mb where it was strongly positive (vorticity source) in convective areas.

The local time rate-of-change of vorticity over convective areas was positive with a tendency to be balanced by the production due to the residual term. The relationship did not hold in nonconvective areas where the local change was generally negligible. Over convective areas as well as in troughs and ridges the local change term appeared to be a good indicator of development.

The results of this study show that vorticity processes represented by the budget equation cannot be simplified and remain realistic especially in and near convective regions. Specifically, the residual and local change

terms, and occasionally other terms as well, must be considered.

Vertical profiles of the various terms in the vorticity budget were reasonably consistent with those presented for the tropics by other authors, but the magnitudes of the terms in the present study were an order of magnitude larger than those for the tropics.

REFERENCES

Barnes, S. L., 1964: A technique for maximizing details in numerical weather map analysis. J. Appl. Meteor., 3, 396-409.

Beebe, R. G., and F. C. Bates, 1955: A mechanism for assisting in the release of convective instability. Mon. Wea. Rev., 83, 1-10.

Cho, H. -R., L. Cheng and R. M. Bloxam, 1979: The Representation of Cumulus Cloud Effects in the Large-Scale Vorticity Equation. J. Atmos. Sci., 36(1), 127-139.

Chu, J. -H., M. Yanai and C. -H. Sui, 1981: Effects of Cumulus Convection on the Vorticity Field in the Tropics Part I: The Large-Scale Budget. J. Meteor. Soc. of Japan, 59(4), 535-546.

Davis, J. G., H. E. Fuelberg and R. E. Turner, 1978: NASA's AVE VII experiment: 25 mb sounding data. NASA TM-78197, NASA Marshall Space Flight Center, Alabama, 218 pp.

Endlick, R. M., and R. L. Mancuso, 1968: Objective analysis of environmental conditions associated with severe thunderstorms and tornadoes. Mon. Wea. Rev., 96(6), 342-350.

Esbensen, S. K., E. I. Tollerud and J. -H. Chu, 1982: Cloud-cluster-scale circulations and the vorticity budget of synoptic-scale waves over the eastern Atlantic intertropical convergence zone. Mon. Wea. Rev., 110, 1577-1692.

Fuelberg, H. E., 1974: Reductions and error analysis of the AVE II pilot experiment data. NASA Contractor Report CR-120496. Marshall Space Flight Center, Alabama, 218 pp.

Gerhard, M. L., H. E. Fuelberg, S. F. Williams and R. E. Turner, 1979: AVE-SESAME I: 25-mb sounding data. NASA TM-78256, NASA Marshall Space Flight Center, Alabama, 361 pp.

Hawkins, H., 1972: Development of a seven-level balanced, diagnostic model and its application to three disparate tropical disturbances. NOAA Tech. Memo. ERL NHRL-98, 207 pp. [NTIS COM-72-10330.]

Hodur, R. M., and J. S. Fein, 1977: A vorticity budget over the Marshall Islands during the spring and summer months. Mon. Wea. Rev., 10, 1521-1526.

Holton, J. R., and D. E. Colton, 1972: A diagnostic study of the vorticity balance at 200 mb in the tropics during the northern summer. J. Atmos. Sci., 29, 1124-1128.

Lateef, M. A., 1967: Vertical motion, divergence, and vorticity in the troposphere over the Caribbean, August 3-5, 1963. Mon. Wea. Rev., 95(11), 778-790.

McNulty, R. P., 1978: On upper tropospheric kinematics and severe weather occurrence, Mon. Wea. Rev., 106, 662-672.

O'Brien, J. J., 1970: Alternate solution to the classical vertical velocity problem. J. Appl. Meteor., 9, 197-203.

Palmén, E., and C. W. Newton, 1969: Atmospheric Circulation Systems. New York, Academic Press, 603 pp.

Panofsky, H. A., 1956: Introduction to Dynamic Meteorology. University Park, Pa., The Pennsylvania State University, 243 pp.

Read, W. L., and James R. Scoggins, 1977: Vorticity imbalance and stability in relation to convection. NASA Contractor Report CR-2819, Marshall Flight Center, Alabama, 111 pp.

Reed, R. J., and R. H. Johnson, 1974: The vorticity budget of synoptic-scale wave disturbances in the tropical western Pacific. J. Atmos. Sci., 31, 1784-1790.

Reed, R. J., P. Norquist and E. Recker, 1977: The structure and properties of African wave disturbances as observed during Phase III of GATE. Mon. Wea. Rev., 105, 317-333.

Reeves, R. W., C. F. Ropelewski and M. D. Hudlow, 1979: Relationships between large-scale motion and convective precipitation during GATE. Mon. Wea. Rev., 107(9), 1154-1168.

Riehl, H. and R. P. Pearce, 1968: Studies on the interaction between synoptic and mesoscale weather elements in the tropics. Rept. No. 126, Dept. of Atmospheric Science, Colorado State University, Ft. Collins.

Ruprecht, E. and W. M. Gray, 1976: Analysis of satellite-observed tropical cloud clusters I. Wind and Dynamic Fields. Tellus, 28(5), 391-413.

Shapiro, L. J., 1978: The vorticity budget of a composite African tropical wave disturbance. Mon. Wea. Rev., 106, 806-817.

Shapiro, L. J., and D. E. Stevens, 1980: Parameterization of convective effects on the momentum and vorticity budgets of synoptic-scale Atlantic tropical waves. Mon. Wea. Rev., 108(11), 1816-1826.

Stevens, D. E., 1979: Vorticity, momentum and divergence budgets of synoptic-scale wave disturbances in the tropical eastern Atlantic. Mon. Wea. Rev., 107, 535-550.

Stevens, D. E. , R. S. Lindzen and L. J. Shapiro, 1977: A new model of tropical waves incorporating momentum mixing by cumulus convection. Dyn. Atmos. Oceans, 1, 365-425.

Thompson, R. M. Jr., S. W. Payne, E. E. Recker and R. J. Reed, 1979: Structure and properties of synoptic-scale wave disturbances in the intertropical convergence zone of the eastern Atlantic. J. Atmos. Sci., 36, 53-72.

Williams, K. T., 1970: A statistical analysis of satellite-observed trade wind clusters in the western North Pacific. Rept. No. 161, Dept. Atmospheric Science, Colorado State University, Ft. Collins, 1-80.

Williams, K., and W. Gray, 1973: Statistical analysis of satellite-observed trade wind clusters in the western North Pacific. Tellus, 25, 313-336.

Williams, S. F., J. R. Scoggins, N. Howath and K. Hill, 1980: A preliminary look at AVE-SESAME I conducted on April 10-11, 1979. NASA TM-78262, NASA Marshall Space Flight Center, Alabama, 56 pp.

Yanai, M., and T. Nitta, 1967: Computation of vertical motion and vorticity budget in a Caribbean easterly wave. J. Meteor. Soc. of Japan, 45, 444-446.

Yanai, T., S. Esbensen and J.-H. Chu, 1973: Determination of bulk properties of tropical cloud clusters from large-scale heat and moisture budgets. J. Atmos. Sci., 30, 611-627.

1. REPORT NO.	2. GOVERNMENT ACCESSION NO.	3. RECIPIENT'S CATALOG NO.
NASA CR-3752		

4. TITLE AND SUBTITLE	5. REPORT DATE
The Influence of Convective Activity on the Vorticity Budget	December 1983
	6. PERFORMING ORGANIZATION CODE

7. AUTHOR(S)	8. PERFORMING ORGANIZATION REPORT #
Tamara L. Townsend and James R. Scoggins	

9. PERFORMING ORGANIZATION NAME AND ADDRESS	10. WORK UNIT NO.
Department of Meteorology Texas A&M University College Station, Texas 77843	M-431
	11. CONTRACT OR GRANT NO. NAS8-33776
	13. TYPE OF REPORT & PERIOD COVERED
12. SPONSORING AGENCY NAME AND ADDRESS	Contractor Report
National Aeronautics and Space Administration Washington, D. C. 20546	14. SPONSORING AGENCY CODE

15. SUPPLEMENTARY NOTES

Technical Monitor: Robert E. Turner, Marshall Space Flight Center, Alabama.
Final Report

16. ABSTRACT

The influence of convective activity on the vorticity budget was determined during the AVE VII and AVE-SESAME I periods. This was accomplished by evaluating each term in the expanded vorticity equation with twisting and tilting and friction representing the residual of all other terms. Convective areas were delineated by use of radar summary charts. The influence of convective activity was established by analyzing contoured fields of each term as well as numerical values and profiles of the various terms in convective and nonconvective areas. Vertical motion was computed by the kinematic method, and all computations were performed over the central United States using a grid spacing of 158 km.

The results show that, in convective areas in particular, the residual is of comparable magnitude to the horizontal advection and divergence terms, and therefore, cannot be neglected. In convective areas, the residual term represents a sink of vorticity below 500 mb and a strong source near 300 mb. In nonconvective areas, the residual was small in magnitude at all levels, but tended to be negative (vorticity sink) at 300 mb. The local change term, over convective areas, tended to be balanced by the residual term, and appeared to be a good indicator of development (vorticity becoming more cyclonic). Finally, the shape of the vertical profiles of the term in the budget equation agreed with those found by other investigators for easterly waves, but the terms were one order of magnitude larger than those for easterly waves.

17. KEY WORDS	18. DISTRIBUTION STATEMENT
Vorticity budget Convective activity development Vorticity Vorticity residual Vorticity equation	Unclassified-Unlimited STAR Category: 47

19. SECURITY CLASSIF. (of this report)	20. SECURITY CLASSIF. (of this page)	21. NO. OF PAGES	22. PRICE
Unclassified	Unclassified	112	A06

For sale by National Technical Information Service, Springfield, Virginia 22161

NASA-Langley, 1983